

# **Physical Layer Forward Error Correction in DVB-S2 Networks**

By

**Theran Naidoo**



**University of KwaZulu-Natal**

February 2012

Submitted in fulfillment of the academic requirements for the degree of Master of Science in Engineering in Electronic Engineering in the School of Electrical, Electronic and Computer Engineering, University of KwaZulu-Natal, Durban, South Africa

Supervised by

Professor F Takawira

Co-supervised by

Professor HJ Xu

CORRECTED VERSION

.....  
As the candidate's supervisor I have approved this dissertation for submission.

Signed: \_\_\_\_\_

Name: Prof. F Takawira  
Date: 10 October 2012

## DECLARATION

I Theran Naidoo declare that

- (i) The research reported in this dissertation/thesis, except where otherwise indicated, is my original work.
- (ii) This dissertation/thesis has not been submitted for any degree or examination at any other university.
- (iii) This dissertation/thesis does not contain other persons' data, pictures, graphs or other information, unless specifically acknowledged as being sourced from other persons.
- (iv) This dissertation/thesis does not contain other persons' writing, unless specifically acknowledged as being sourced from other researchers. Where other written sources have been quoted, then:
  - a) their words have been re-written but the general information attributed to them has been referenced;
  - b) where their exact words have been used, their writing has been placed inside quotation marks, and referenced.
- (v) Where I have reproduced a publication of which I am an author, co-author or editor, I have indicated in detail which part of the publication was actually written by myself alone and have fully referenced such publications.
- (vi) This dissertation/thesis does not contain text, graphics or tables copied and pasted from the Internet, unless specifically acknowledged, and the source being detailed in the dissertation/thesis and in the References sections.

Signed: Theran Naidoo

## **ACKNOWLEDGEMENTS**

I would like to acknowledge my supervisor and co-supervisor; Professor Takawira for his knowledge and effort which have made this dissertation possible and Professor Xu for his keen attention which ensured the smooth progress of research. To everyone who has contributed to the research and formation of the dissertation, thank you.

## ABSTRACT

The rapid growth of wireless systems has shown little sign of ceasing, due to increased consumer demand for reliable interactive services. A key component of the development has centered on satellite networks, which allows provision of services in scenarios where terrestrial systems are not viable. The Digital Video Broadcasting-Satellite Second Generation (DVB-S2) standard was developed for use in satellite broadcast applications, the foremost being video broadcasting. Inherent to DVB-S2 is a powerful forward error correction (FEC) module, present in both the Physical and Data Link Layer. Improving the error correcting capability of the FEC is a natural advent in improving the quality of service of the protocol. This is more crucial in real time satellite video broadcast where retransmission of data is not viable, due to high latency.

The Physical Layer error correcting capability is implemented in the form of a concatenated BCH-LDPC code. The DVB-S2 standard does not define the decoding structure for the receiver system however many powerful decoding systems have been presented in the literature; the Belief Propagation-Chase concatenated decoder being chief amongst them. The decoder utilizes the concept of soft information transfer between the Chase and Belief Propagation (BP) decoders to provide improved error correcting capability above that of the component decoders.

The following dissertation is motivated by the physical layer (PL) FEC scheme, focused on the concatenated Chase-BP decoder. The aim is to generate results based on the BP-Chase decoder in a satellite channel as well as improve the error correcting capability.

The BP-Chase decoder has shown to be very powerful however the current literature provides performance results only in AWGN channels. The AWGN channel however is not an accurate representation of a land-mobile satellite (LMS) channel; it does not consider the effect of shadowing, which is prevalent in satellite systems. The development of Markov chain models have allowed for better description of the characteristics of the LMS channel. The outcome being the selection of a Ku band LMS channel model. The selected LMS channel model is composed of 3 states, each generating a different degree of shadowing. The PL system has been simulated using the LMS channel and BP-Chase receiver to provide a more accurate representation of performance of a DVB-S2 network. The effect of shadowing has shown to reduce coding performance by approximately 4dB, measured over several code lengths and decoders, when compared with AWGN performance results.

The second body of work aims to improve the error correcting capability of the BP-Chase decoder, concentrating on improving the LDPC decoding module performance. The LDPC

system is the basis for the powerful error correcting ability of the concatenated scheme. In attempting to improve the LDPC decoder a reciprocal improvement is expected in the overall decoding performance of the concatenated decoder. There have been several schemes presented which improve BP performance. The BP-Ordered statistics decoder (OSD) was selected through a process of literary review; a novel decoding structure is presented incorporating the BP-OSD decoder into the BP-Chase structure. The result of which is the BP-OSD-Chase decoder. The decoder contains two stages of concatenation; the first stage implements the BP-OSD algorithm which decodes the LDPC code and the second stage decodes the BCH code using the Chase algorithm. Simulation results of the novel decoder implementation in the DVB-S2 PL show a coding gain of 0.45dB and 0.15dB versus the BP and BP-Chase decoders respectively, across both the AWGN and LMS channel.

# CONTENTS

DECLARATION	iii
ACKNOWLEDGEMENTS	iv
ABSTRACT	v
CONTENTS	vii
LIST OF FIGURES	x
LIST OF TABLES	xii
LIST OF ACRONYMS	xiii
LIST OF SYMBOLS	xvi
INTRODUCTION	1
1.1    Satellite communications	1
1.2    Satellite digital video broadcasting	2
1.2.1    DVB-S	3
1.2.2    DVB-S2	4
1.3    Motivation for research	6
1.4    Dissertation overview	8
1.5    Original contributions	9
2    LITERATURE SURVEY OF DVB-S2 FEC	10
2.1    Introduction	10
2.2    DVB-S2 transmission model	10
2.2.1    Mode and Stream Adaptation	11
2.2.2    FEC Encoding	12
2.2.3    Mapping	13
2.2.4    PL Framing	14
2.2.5    Modulation	15
2.3    BCH	16
2.4    LDPC	18
2.5    Literature survey of FEC decoders	23

2.5.1	LDPC decoding	24
2.5.2	BCH decoding	29
2.5.3	Concatenated decoding	34
2.6	Conclusion	35
3	PHYSICAL LAYER IMPLEMENTATION	36
3.1	Introduction	36
3.2	Transmission model	37
3.3	Channel model	38
3.3.1	Satellite channel modeling	39
3.3.2	Literature survey of LMS channel models	41
3.3.3	Implementation	44
3.3.4	Link budget	46
3.4	Receiver model	48
3.4.1	Belief propagation	49
3.4.2	Chase decoder	52
3.4.3	BP-Chase decoder	57
3.5	Simulation results	59
3.6	Conclusion	65
4	ADVANCED CONCATENATED DECODER	66
4.1	Introduction	66
4.2	Constituent decoder development	67
4.2.1	Literature review of improved BP decoders	68
4.3	BP-OSD	73
4.4	Novel BP-OSD-Chase decoder	74
4.5	Simulation results	79
4.6	Conclusion	83
5	CONCLUSION AND FUTURE WORK	84
5.1	Conclusion	84
5.2	Future work	86





## LIST OF FIGURES

<i>Figure 1.1-DVB-S Functional block diagram [9] .....</i>	<i>4</i>
<i>Figure 1.2-DVB-S2 system model [11].....</i>	<i>6</i>
<i>Figure 1.3-Iterative concatenated decoder model.....</i>	<i>7</i>
<i>Figure 2.1-DVB-S2 physical layer transmission system [12].....</i>	<i>11</i>
<i>Figure 2.2-Mode &amp; Stream Adaptation module [12] .....</i>	<i>11</i>
<i>Figure 2.3-Structure of a BBFRAME [11].....</i>	<i>12</i>
<i>Figure 2.4- FEC module [12].....</i>	<i>13</i>
<i>Figure 2.5-FECFrame structure [11].....</i>	<i>13</i>
<i>Figure 2.6- Mapping module [12] .....</i>	<i>14</i>
<i>Figure 2.7-16APSK symbol mapping [11].....</i>	<i>14</i>
<i>Figure 2.8- PL framing module [12] .....</i>	<i>15</i>
<i>Figure 2.9- Modulation module [12].....</i>	<i>15</i>
<i>Figure 2.10-Bipartite graph.....</i>	<i>19</i>
<i>Figure 2.11-BCH decoding process [52] .....</i>	<i>30</i>
<i>Figure 2.12-GMD decoder structure [84].....</i>	<i>32</i>
<i>Figure 3.1-FEC system model .....</i>	<i>37</i>
<i>Figure 3.2-Transmission model.....</i>	<i>38</i>
<i>Figure 3.3-Two state Markov chain .....</i>	<i>41</i>
<i>Figure 3.4-Three state channel model .....</i>	<i>43</i>
<i>Figure 3.5-Ku band LMS channel model [109] .....</i>	<i>45</i>
<i>Figure 3.6-Receiver model .....</i>	<i>49</i>
<i>Figure 3.7-Process of updating the check nodes [122] .....</i>	<i>51</i>
<i>Figure 3.8-Process of update in bit nodes [122].....</i>	<i>52</i>
<i>Figure 3.9-Depiction of channel measurement decoding technique.....</i>	<i>54</i>
<i>Figure 3.10-Chase decoder structure .....</i>	<i>55</i>
<i>Figure 3.11- BER performance of PL decoding system over AWGN channel.....</i>	<i>61</i>
<i>Figure 3.12-BER performance of half rate codes in PL decoding system over AWGN .....</i>	<i>62</i>
<i>Figure 3.13-PL system BER results over AWGN and satellite channel .....</i>	<i>63</i>
<i>Figure 3.14-PL system BER results for large code lengths over AWGN and satellite channel.....</i>	<i>64</i>
<i>Figure 4.1-Construction of improved system model .....</i>	<i>67</i>
<i>Figure 4.2-BP-OSD decoder.....</i>	<i>71</i>
<i>Figure 4.3- Yang BP-OSD mode [14]  .....</i>	<i>73</i>
<i>Figure 4.4-Novel BP-OSD-Chase decoder .....</i>	<i>75</i>
<i>Figure 4.5-Integrated Yang BP-OSD decoder .....</i>	<i>75</i>
<i>Figure 4.6-PER curves for validation of decoding system .....</i>	<i>79</i>

*Figure 4.7-Comparison of PER of BP-OSD-Chase for varying decoding parameters for length(210,105).. 81*  
*Figure 4.8-Comparison of PER of BP-OSD-Chase for varying decoding parameters for length(496,248).. 82*  
*Figure 4.9-Comparison of PER performance of PL system in satellite and AWGN channels..... 82*  
*Figure 5.1-Structure of LL-FEC frame [140]..... 87*

## LIST OF TABLES

<i>Table 2.1-Table of DVB-S2 modes [11].....</i>	<i>17</i>
<i>Table 2.2-Generator polynomials [11].....</i>	<i>18</i>
<i>Table 2.3-Table of values of q [6].....</i>	<i>21</i>
<i>Table 2.4-Look up table for code rate ¼ copied from [11].....</i>	<i>23</i>
<i>Table 3.1 Ka band LMS channel parameters [109].....</i>	<i>45</i>
<i>Table 3.2-Link budget values [109].....</i>	<i>47</i>
<i>Table 4.1 Decoding complexity of a single iteration of BP [37] [42].....</i>	<i>77</i>
<i>Table 4.2-Decoding complexity for OSD order-i reprocessing [128].....</i>	<i>77</i>
<i>Table 4.3-Decoding complexity of Chase algorithm [139].....</i>	<i>78</i>
<i>Table 4.4-Decoding complexity of BP-OSD-Chase algorithm.....</i>	<i>78</i>

## LIST OF ACRONYMS

1G	First Generation
4G-LTE	Fourth Generation Long Term Evolution
ABP	Adaptive BP
ACM	Adaptive Coding and Modulation
APSK	Amplitude PSK
AWGN	Additive White Gaussian Noise
BB	Base Band
BCH	Bose-Chaudhuri-Hocquenghem
BER	Bit Error Rate
BF	Bit Flipping
BMA	Berlekamp Massey Algorithm
BP	Belief Propagation
BSC	Binary Symmetric Channel
BSS	Broadcast Satellite Service
CBBF	Candidate Based BF
DE	Density Evolution
DTH	Direct To Home
DVB	Digital Video Broadcasting
DVB-C	Digital Video Broadcasting-Cable
DVB-DSNG	DVB-Data Services and News Gathering
DVB-S	Digital Video Broadcasting-Satellite
DVB-S2	Digital Video Broadcasting Satellite Second Generation
DVB-T	Digital Video Broadcasting-Terrestrial
EPCM	Extended Parity Check Matrix
ESA	European Space Agency
ETSI	European Telecommunications Standards Institute
EXIT	Extrinsic Information Transfer
FC	Forced Convergence
FEC	Forward Error Correction
FFT	Fast Fourier Transform
FOMS	Fixed Offset MS
FSS	Fixed Satellite Service
GEO	Geostationary Earth Orbit

GMD	Generalized Minimum Distance
GOP	Giga Operations per Second
HDTV	High Definition Television
HEO	Highly Elliptical Orbit
IERRWBF	Implementation Efficient RRWBF
ISDB-S	Integrated Services Digital Broadcasting-Satellite
KV	Koetter-Vardy
LDPC	Low Density Parity Check
LEO	Low Earth Orbit
LL-FEC	Link Layer FEC
LLR	Log Likelihood Ratios
LMS	Land-Mobile satellite
LOS	Line of Sight
LRB	Least Reliable Bit
LUT	Look Up Table
MEO	Medium Earth Orbit
ML	Most Likely
MLG	Majority Logic
MPEG-2	Moving Pictures Experts Group-2
MRB	Most Reliable Basis
MRIP	Most Reliable Independent Positions
MS	Min-Sum
MWBF	Modified WBF
OMS	Offset MS
OSD	Ordered Statistics Decoder
PL	Physical Layer
PSK	Phase Shift Keying
QoS	Quality of Service
RiBMA	Inversion-less BMA
RRWBF	Reliability Ratio WBF
RS	Reed Solomon
RSDT	RS Data Table
S-DMB	Satellite-Digital Multimedia Broadcasting
SDTV	Standard Definition Television
SEW	Sliding Encoding Window
SiBMA	Simplified Inversion-less BMA
SPA	Sum Product Algorithm

TP .....	Test Patterns
UMP .....	Uniformly Most Powerful
WBF .....	Weighted BF
WLAN .....	Wireless LAN

## LIST OF SYMBOLS

$B(x)$	.....	BCH codeword
BBFRAME	.....	Baseband frame
BBHEADER	.....	Baseband header
$c$	.....	Ratio between direct signal and multipath power
$c(x)$	.....	BCH codeword of length defined by $k_{ldpc}$
$C_{BP-OSD}$	.....	Output codeword of BP-OSD
$C'_c$	.....	Set of corrected candidate codewords
$c''$	.....	Output of Reorder Re-encode block
$c_k''$	.....	Candidate codeword $k$ in candidate set $c''$
$d$	.....	Input to channel model either $\pm 1$
$d(x)$	.....	Remainder polynomial with defined length $n_{bch}-k_{bch}$
$d_h$	.....	Hamming distance
$D_{y,c}$	.....	Discrepancy function, determines the discrepancy between $y$ and $c$
DATA FIELD	.....	Fixed segment from input stream
$E_b$	.....	Energy per bit
$Env_j$	.....	Environment for channel simulation
FECFRAME	.....	Output of FEC module
$g(x)$	.....	Generator polynomial
$G$	.....	Generator matrix of LDPC
$G_R$	.....	Receiver gain
$G_T$	.....	Transmitter gain
$H$	.....	LDPC parity check matrix
$H_{mn}$	.....	LDPC parity check matrix consisting of $m$ rows and $n$ columns
$i$	.....	Information bit array of length $k_{ldpc}$
$i_c$	.....	Number of concatenated iterations
$I_0$	.....	Modified Bessel function of order zero
$I_{cMax}$	.....	Maximum number of iterations allowed of BP-Chase decoder
$I_{Max}$	.....	Maximum number of iterations allowed for BP
$K_{bch}$	.....	Length of BCH input
$L_A$	.....	Summation of losses
$L_0$	.....	Losses due to shadowing
$L_S$	.....	Free space loss



$L'_{y_j}$	Soft information transferred from Chase to BP decoders
$m$	Analog weight
$m(x)$	Message polynomial of length defined by $k_{bch}$
$M(n)$	Checks which bit $n$ participates in
$M_i$	Total number of state frames
$M_{i,j}$	Number of transitions between state $i$ and $j$
$N_0$	Noise power density
$N_{bch}$	Length of FECFRAME
$N_f$	Total number of samples in an environment
$N_k$	Ratio of the number of samples in state $k$
$N_m$	Bits which participate in check $m$
$\eta_{MOD}$	Modulation efficiency
$p$	Parity bit array of length $n_{ldpc}-k_{ldpc}$
$P_k$	State probability
$P_r$	Received signal power
$P_R$	Rician random variable
$P_T$	Transmitter power
PER	Packet error rate
PLFRAME	Physical Layer FRAME
PLHEADER	Physical Layer FRAME header
$q$	Constant value defined by the standard
$r$	Output of the Channel model
$r_n$	Reliability input to OSD
$R$	Transmission Rate
$R(x)$	Input Binary BCH Codeword
$S$	Instantaneous received power
$S_T$	Set of test patterns generated by Chase algorithm
$t$	Error Correction Capability of BCH Code
$v$	Velocity
XFECFRAME	Complex FECFRAME
$y$	Hard decision of $y_{OSD}$
$Y_{BP-OSD}$	Input into BP-OSD decoder
$Y_{OSD}$	Input into OSD
$Y$	Cross correlation function
$\lambda$	OSD permutation



# Chapter 1

## INTRODUCTION

The proliferation of wireless networks worldwide has experienced rapid progression in the past decade. The increase in development and deployment of wireless networks is due mainly to its inherent advantages over wired networks. It allows services to be available in scenarios where wired infrastructure is absent.

The Internet has also played a defining role in the adaptation to wireless networks, in its physical implementation and more importantly in the services it provides. The main drive in wireless development has been to replicate Internet services in a mobile scenario. Mobile services play an important role in society, whether in communication, entertainment or commerce [1], restriction of which would reduce the quality of life. The recent hardware innovations in the form of smart phones allow access to these services to a wider audience. It also increases the spectrum of requirements necessary to provide them.

This has required the evolution of the wireless network from voice only first generation networks (1G) to the current fourth generation long term evolution networks (4G-LTE). The emphasis of development has been aimed at increasing the data rate, improving the spectral efficiency as well as providing QoS requirements for several classes of services over varying types of networks, cellular and WLAN [2]. This will allow for more dynamic and reliable services to be rendered. Satellite systems play a pivotal role in achieving these targets as they provide high data rates and allow wireless connectivity over a broad region. This has led to the integration of satellite systems into the backbone of wireless provision systems.

Satellite systems will be expanded upon in Section 1.1, focus will then be placed on its application in digital video broadcasting in Section 1.2. A motivation for the research will also be provided together with an overview of the dissertation in Section 1.3 and 1.4 respectively, to conclude the chapter the original contributions derived from the research are presented.

### 1.1 Satellite communications

Satellite systems form an integral component in global wireless networks. They have undergone significant improvement in order to increase the range of services which they can provide. They utilize a transponder which orbits the earth, known as a satellite [3]. Information is transmitted to the satellite from a terrestrial station; the satellite then retransmits the message to a single or multiple terrestrial stations [3]. This allows satellite systems to cover large geographical ranges, the area of which is called the satellite's footprint [3]. The footprint is an important concept as it is proportional to the distance of the satellite from the earth. Satellites can be categorized into 4 types, given in increasing length of orbit, low earth orbits(LEO), medium earth orbits(MEO), highly elliptical orbits(HEO) and geostationary orbits(GEO) [2]. The relationship is the greater the distance from the earth, the larger the satellite footprint. The GEO system has the largest footprint requiring potentially fewer satellites to cover a designated area. The issue inherent with being further away is that the transmission is required to propagate over larger distances. The transmission signal strength is reduced, increasing the amount of errors and the latency of the transmission [2]. The type of service required generally determines the type of orbit implemented, considering the conditions stated above.

In the past satellite systems have been used mainly by national entities such as military organizations and scientific bodies [4], for information transfer and meteorological analysis respectively. This is due mainly to the high cost of launching satellites into orbit. Advancement in technology as well as the drive to improve consumer related services, has forced industry to implement and utilize satellite networks. Satellite systems are generally used as the backbone for communications networks both mobile and fixed. They are important in managing the handover between terrestrial networks, providing roaming capability, which is a key component in the evolution of mobile networks [2]. They are also used to provide multimedia and data transfer in point-to-point and broadcast applications. The most common consumer applications are satellite television, GPS navigation and Internet access. Satellite television plays an important role in disseminating information to a large audience; the principal element of a satellite television service is digital video broadcasting, the evolution of which will be expanded upon subsequently.

## **1.2 Satellite digital video broadcasting**

Digital video broadcasting is the process of transmitting digital video from a single transmitter to more than one receiver. This can be achieved using terrestrial means for which several protocols have been developed such as Digital Video Broadcasting-Cable(DVB-C) and Digital Video

Broadcasting-Terrestrial(DVB-T) [5]. This dissertation however will consider digital video broadcasting only from a satellite perspective.

There are several significant problems to consider when implementing a digital video broadcasting system; the first is the high cost of satellite infrastructure. There are also several issues inherent in satellite communication which must be addressed. Long propagation delays, which are dependent on the satellites orbit, affect the quality of the video transmission as it is sensitive to time delay. A second concern is atmospheric effects and channel losses both of which degrade the quality of the signal [2], increasing the possibility of bit errors in the transmission.

There have been several mechanisms put forward in order to rectify these issues. These have been accepted and standardized by the relevant technical bodies. The protocols define a set of rules for transmission and reception of data which aid in counteracting the issues discussed above. This allows for the provision of a predetermined level of performance. The standards effectively define the technology required at both the transmitter and receiver in order to provide a reliable service.

There have been many digital video broadcasting standards presented, such as Satellite Digital Multimedia Broadcasting(S-DMB) and Integrated Services Digital Broadcasting Satellite(ISDB-S) standardized and implemented in South Korea and South America respectively [6] [7]. The standard developed by the digital video broadcasting (DVB) workgroup has become the most popular. The DVB workgroup is an industry led association consisting of satellite broadcasters and regulatory bodies [8]. They have defined two protocols dealing with satellite broadcasting, digital video broadcasting satellite (DVB-S) and DVB-S2. The protocols define the physical layer transmission systems required for satellite communication. The receiver structure is not strictly described to allow for a flexible definition as per the requirements of the application. In terms of industry viability it is important to select a transmitter structure for which a suitably complex receiver can be constructed. This is considered in the process of defining the protocol. The protocols have both been standardized by the European Telecommunications Standards Institute (ETSI), and are discussed in greater detail below.

### 1.2.1 **DVB-S**

DVB-S is a protocol developed by the DVB workgroup and standardized in 1994. The protocol aims to provide a variety of services, the core function being the provision of digital multi-program television both standard (SDTV) and high definition (HDTV) in both Fixed Satellite

(FSS) and Broadcast Satellite service bands (BSS). It is also suitable for providing Direct-To-Home (DTH) services. [9].

The main objective of the protocol is to achieve resistance to noise and atmospheric affects hence two mechanisms are specified, the first is the addition of QPSK modulation; which was selected as a compromise between power and spectrum efficiency. The second was a concatenated Reed-Solomon (RS) and convolutional channel code, which uses redundancy to detect and correct errors in the transmission. The channel code is defined with enough flexibility to cater for a range of transponders [9]. The functional block diagram of DVB-S is given in Figure 1.1, where the system is shown to be compatible with only the Moving Pictures Experts Group-2(MPEG-2) audio visual format.

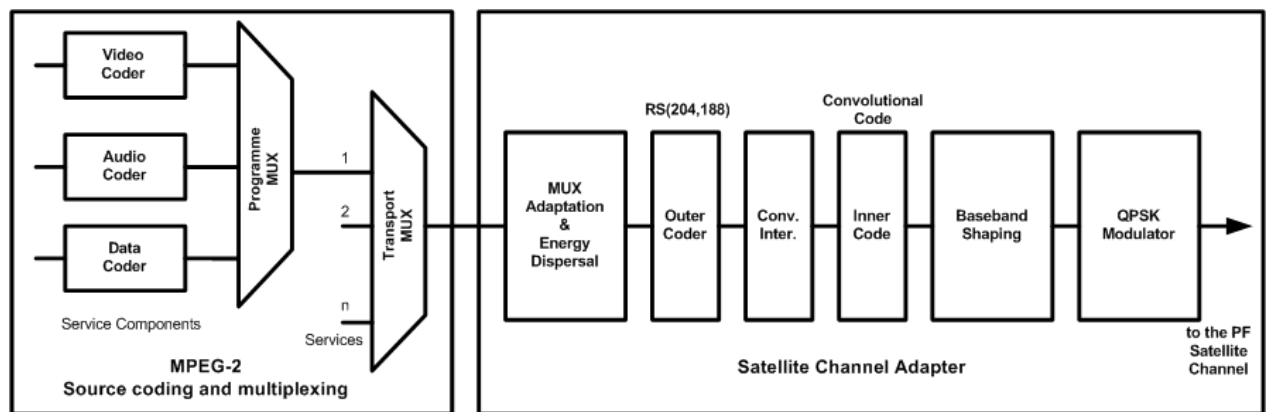


Figure 0.1-DVB-S Functional block diagram [9]

In 1997 DVB introduced DVB-Data Services and News Gathering (DVB-DSNG) protocol building on the success of DVB-S, in order to incorporate the news gathering into its services. The only significant change was the addition of the 8PSK and 16QAM modulation schemes to improve the spectral efficiency of transmission [10]

The need for further development of the DVB-S protocol became apparent as more powerful coding schemes were discovered. DVB-S2 was developed to take advantage of the improved coding as well as provide a wider variety of services.

### 1.2.2 DVB-S2

The Digital Video Broadcasting-Satellite Second Generation (DVB-S2) was defined in 2003 and standardized by ETSI in 2005 [11], it is the successor to DVB-S and DVB-DSNG .The push for

the second generation protocol was based on calls by consumers for improved services and greater capacity.

DVB-S2 was defined with a great degree of adaptability in order to provide a variety of satellite services. The fundamental service mentioned previously is digital broadcasting both SDTV and HDTV in FSS and BSS bands. Additionally it can be used to provide interactive services such as satellite Internet access. The protocol is a successor to DSNG and thus can also be used for news gathering. Point-to-point and multicast applications are also catered for [11].

In the process of development the DVB group focused on three targets, achieving the best transmission performance while maintaining flexibility and reasonable receiver complexity. In order to achieve this DVB-S2 was designed as a toolkit, where the appropriate modules can be selected according to the application requirements. The resultant standard has achieved a gain in capacity and performance while catering for a wide range of applications.

This was achieved by making several additions to the DVB-S system, the first being an input stream adapter which is capable of handling single and multiple input streams. The adaptor is also compatible with a range of formats, unlike DVB-S which could only handle the MPEG-2 format. The main reason for the gain in capacity is due to the revision of the forward error correction (FEC) structure. The main addition is a concatenated Bose-Chaudhuri-Hocquenghem (BCH)-Low Density Parity Check (LDPC) channel code. LDPC codes offer the minimum distance to the Shannon limit when operating on large block lengths, the standard defines frames of large length, producing improved transmission performance [12]. The system was also developed to handle a greater number of code rates, increasing the range of spectrum efficiency.

The second notable improvement was the addition of adaptive coding and modulation (ACM). This allows optimization of the transmission parameters to suit individual channels, in the case of multicasting on a frame by frame basis. The ACM selects the mode appropriate to the current channel condition; each mode has a different combination of code rate and modulation type.

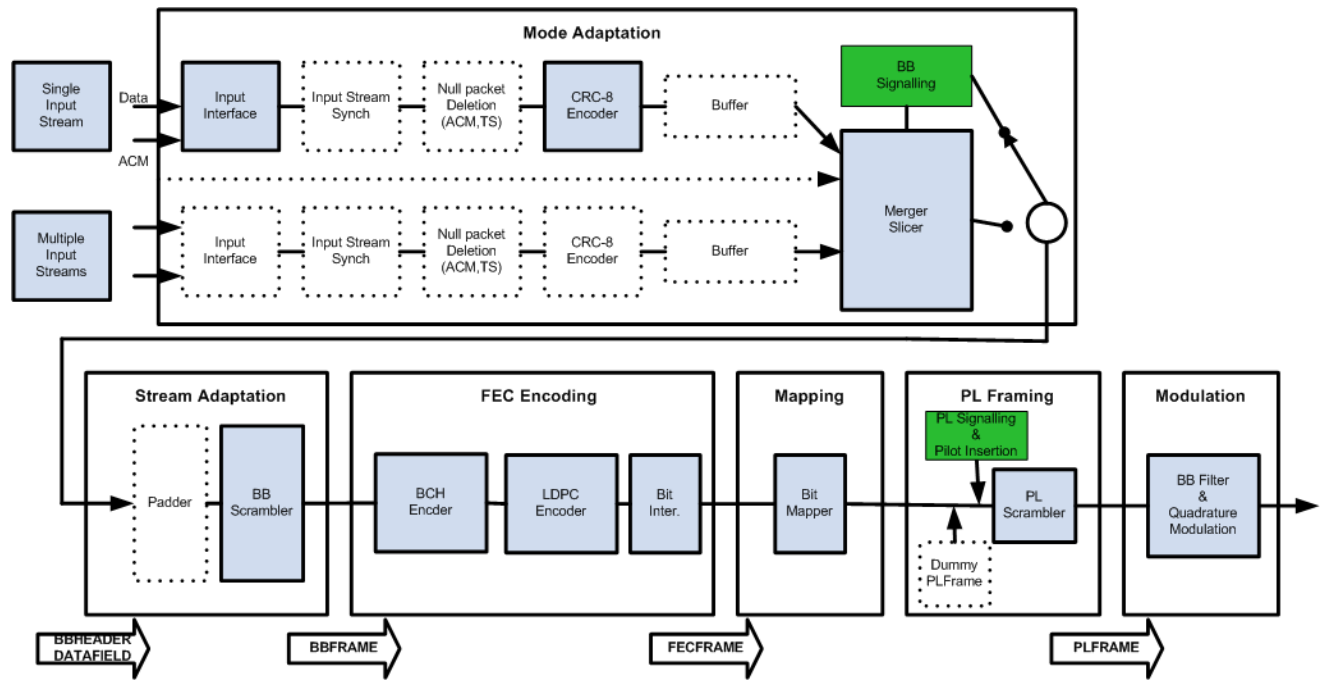


Figure 0.2-DVB-S2 system model [11]

Each of the modules defined in Figure 1.2 above have been specialized to handle transmission over a satellite medium. The large scale adoption of DVB-2 by broadcasters is testament to the improvements made by the DVB group. The standard allows both DVB-S2 transmitters and receivers to be incorporated into existing systems, achieving the goal of flexibility while still allowing it to operate in environments of high distortion.

### 1.3 Motivation for research

The DVB-S2 standard, mentioned above, aims to provide best possible transmission performance; in order to achieve this a BCH-LDPC concatenated channel code is defined in the FEC module. Transmission performance is generally measured by the number of errors experienced during transmission, the lower the number of errors the better the quality of the service.

An aspect of the DVB protocols touched on previously is the open receiver structure. It allows for flexibility in the design of decoders based on their application environment. There have been many decoding structures proposed and implemented in industry for use in DVB-S2 applications. These however are constrained by the cost versus complexity tradeoff. In general increasing the complexity of the receiver structure increases the cost of the implementation. High complexity



receivers can be impractical in terms of developing units for general sale. The issue of complexity however will not be the focus of the dissertation. The main aim is to develop and implement a receiver structure in order to improve the transmission performance of the DVB-S2 physical layer (PL).

There have been several decoding structures presented in the literature such as belief propagation and Chase decoding [13] in order to individually decode the components of the concatenated BCH-LDPC code. The basis for improving the system is an iterative concatenated BP-Chase soft decision decoder presented in [13]. The iterative decoder produces better performance than the constituent algorithms used to independently decode the BCH and LDPC, as seen in Figure 1.3.

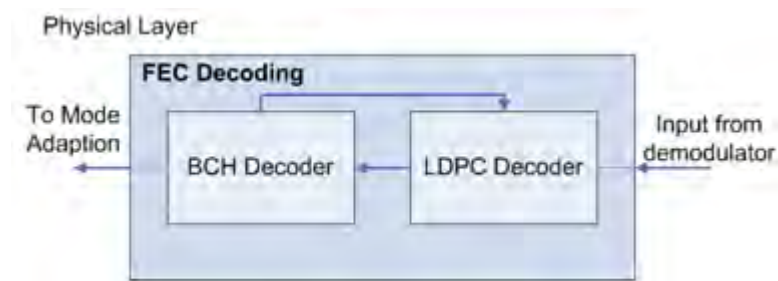


Figure 0.3-Iterative concatenated decoder model

The iterative concatenated decoder uses the Chase and Belief Propagation (BP) algorithms to decode the BCH and LDPC code respectively. The implementation makes use of the transfer of soft information between the Chase and BP decoders in order to provide coding gain. The performance results of the BP-Chase decoder have been provided using an additive white Gaussian noise (AWGN) channel in [13], under the assumption that AWGN is a suitable representation for satellite communications.

### Focus

In recent years there have been advancements in the production of a more accurate representation of the land-mobile satellite (LMS) channel; based on Markov representations. The initial aim of the dissertation is to produce more accurate performance results of the DVB-S2 PL system using the LMS channel and BP-Chase decoder in order to expand upon the literature.

The BP-Chase decoder discussed previously implements the Chase and BP soft decision algorithms to decode BCH and LDPC codes respectively. A logical step in targeting an improvement in the error correcting performance is to improve the performance of the constituent decoders. The Chase decoder operating on the BCH component of the FEC performs

an integral role in the decoding system by controlling the error floor problem inherent with BP [13]. The main decoding power of the FEC system however is provided by the LDPC code.

There have been several soft decision LDPC decoding algorithms presented in the literature. These focus on reducing the complexity of BP decoding while maintaining a similar standard of decoding performance. The concatenated BP-OSD iterative decoder, given in [14] differs it provides coding gain over the traditional BP algorithm. It will be examined and implemented as a part of the BP-Chase structure given in Figure 1.3, in order to achieve the aim of improving the error correcting performance of the PL system.

#### **1.4 Dissertation overview**

The dissertation is made up of five chapters. In Chapter 1 a brief overview of digital video satellite broadcasting and its importance in providing wireless communication services are discussed. The motivation for the research undertaken and a list of the original contributions are also produced.

Chapter 2 presents the DVB-S2 transmission system as well as undertaking a review of the literature of DVB-S2 FEC decoding systems. The focus is to select an algorithm suitable for decoding the concatenated BCH-LDPC channel code.

In Chapter 3 the PL system model is constructed and implemented. The focus is placed on the definition and implementation of the transmission system, channel model and the receiver system. A more accurate model of the LMS channel is selected and implemented after a process of literary review. The BP and Chase decoders constituting the concatenated decoder are defined independently as well as in their concatenated form. The simulation results for which are presented for both the AWGN and LMS channel.

Chapter 4 discusses possible improvements to the BP-Chase decoder described in Chapter 3. The concatenated OSD decoder is presented as an improvement to the BP decoding module. A novel BP-OSD-Chase algorithm is presented. Simulation results of the novel decoder incorporated into the PL system is provided for both the AWGN and the LMS channel.

Chapter 5 provides the conclusions that can be derived from the research presented in this dissertation as well as future research work.

## **1.5 Original contributions**

The original contributions derived from this research are as follows:

- 1) The BP-Chase decoder and LMS channel model are implemented in a DVB-S2 PL system. The simulation of the implemented system will generate an original set of results which will provide a more accurate representation of DVB-S2 decoding performance.
- 2) Improve the decoding performance achieved by the PL system by constructing a novel decoding structure, called the BP-OSD-Chase decoder. The BP-OSD-Chase decoder together with the performance results are presented in both an AWGN and LMS channel.

# Chapter 2

## LITERATURE SURVEY OF DVB-S2 FEC

### 2.1 Introduction

This chapter is a literature review of the DVB-S2 protocol with emphasis placed on the FEC encoding and decoding structure. The DVB-S2 protocol, briefly examined in Chapter 1, has experienced widespread adoption, due mainly to the flexibility and enhanced transmission performance of the protocol over its predecessors; which is in the main due to improvements made to the FEC module. The aim of the chapter is to firstly gain familiarisation with the inner workings of the transmission protocol, in order to grasp the requirements for selecting an appropriate receiver structure from those presented in the literature. The outcome of which will be the selection of an algorithm to be used as the basis for the decoding module which is a key component of the dissertation.

In Section 2.2 the DVB-S2 transmission model is defined with regard to the standard. The focus is then placed on the FEC module, firstly the FEC encoding algorithms are detailed in Section 2.3 and 2.4, after which the literature is reviewed with respect to LDPC, BCH and concatenated decoders in Section 2.5. Finally a summary of the outcomes of the chapter is given in Section 2.6.

### 2.2 DVB-S2 transmission model

The DVB-S2 protocol defines the PL transmission characteristics as presented in [11] and reviewed in [12], the modules comprising the transmission system are depicted in Figure 2.1. The DVB-S2 physical layer communication model is made up of a transmission and reception system, the transmission system for the standard is provided in detail by the DVB group. The receiver structure of the protocol however is not specified in order to maintain flexibility. The following section details the transmission layer modules which constitute the standard.

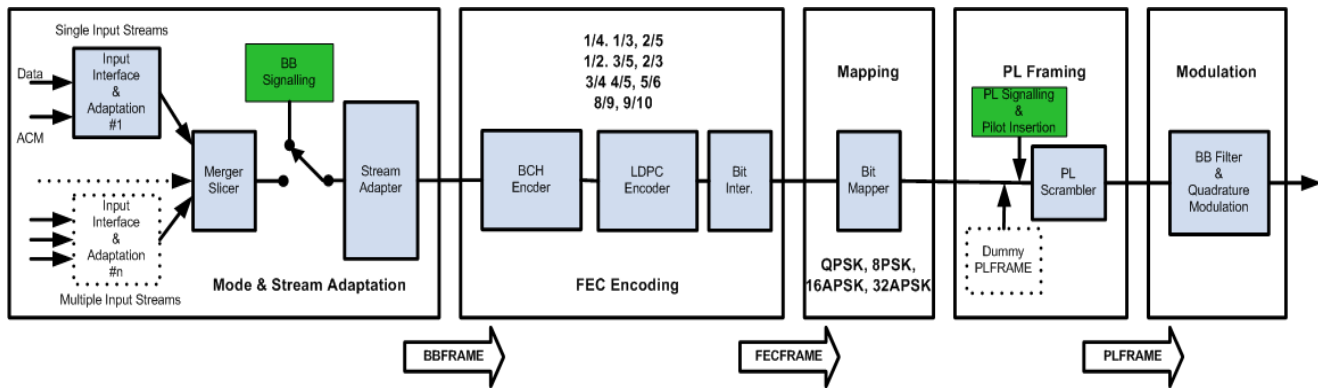


Figure 2.1-DVB-S2 physical layer transmission system [12]

The DVB-S2 protocol is made up of the following modules:

- Mode and Stream Adaptation
- FEC Encoding
- Mapping
- PL Framing
- Modulation

Each of which will be discussed subsequently.

### 2.2.1 Mode and Stream Adaptation

The mode and stream adaptation module pictured in Figure 2.2 below acts as the interface between the link and physical layers. The purpose of the module is to provide a generic output given a variety of inputs into the DVB-S2 transmitter. The module was developed in accordance with the DVB group design goal of improving flexibility. DVB-S2 is thus compatible with several forms of input such as MPEG-4 and IP packets [11], in both single and multiple streams.

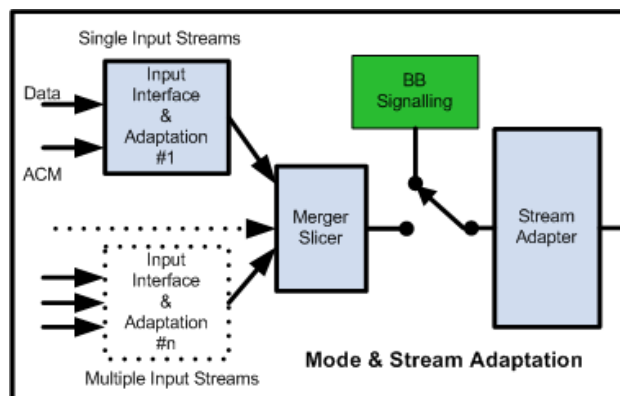


Figure 2.2-Mode & Stream Adaptation module [12]

The block contains several sub-modules such as Input Stream Synchronization, CRC-8 Encoder, Merger Slicer and baseband (BB) Signaling. The Merger Slicer module slices the input from one of several input streams into fixed segments, known as DATA FIELD's, which are merged to form a single stream. The BB signaling added to the stream is used to inform the receiver of the correct manner of stream reconstruction. The Stream Adaptation module is further responsible for ensuring that the BBFRAME, which is the output of the module, is adequately padded to a specified length given by  $K_{bch}$ . The length is determined by the input ACM signal to the module which selects the transmission mode to be utilized. The ACM signal selects a row of Table 2.1 which defines the lengths of the transmission frames. In Figure 2.3 the BBFRAME is shown to contain the BBHEADER, the BB signaling, the stream input in the form of the DATA FIELD and any additional padding required to achieve a length of  $K_{bch}$ .

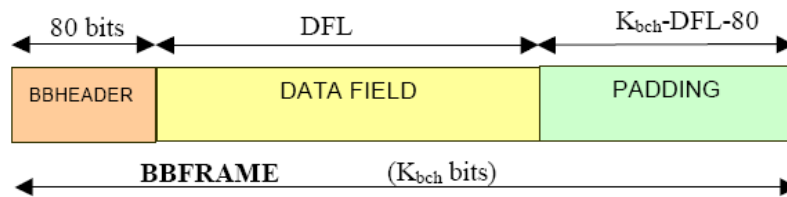


Figure 2.3-Structure of a BBFRAME [11]

### 2.2.2 FEC Encoding

The FEC encoding module is the chief reason for the gains in capacity achieved by DVB-S2 over its predecessors. Forward error correction also known as channel coding is a method of error correction and control over noisy channels, achieved by adding redundancy to the information stream in a given way. This allows the receiver to detect and correct a fixed amount of errors [15].

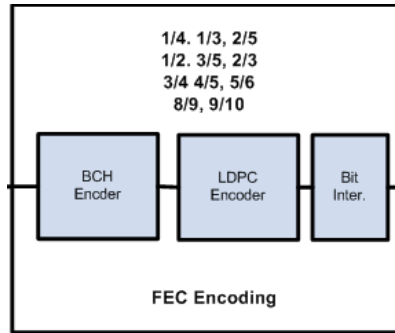


Figure 2.4- FEC module [12]

The FEC module consists of two types of error correcting codes; a BCH code (outer) and a LDPC code (inner) which are serially concatenated. The input BBFRAME's are initially encoded with the BCH encoder module, which adds a header to the end of the BBFRAME containing the BCH parity bit information. The LDPC encoder then proceeds to encode both the BBFRAME and BCH parity bit information such that the output FECFRAME has the structure given in Figure 2.5. The FEC encoder module can operate at various code rates as can be seen in Figure 2.4 above. The code rates are selected by the rate adaptive module and are chosen in accordance with channel conditions. Each code rate is assigned different values of  $K_{bch}$  and  $N_{bch}$  varying the amount of redundant bits comprising the FECFRAME.

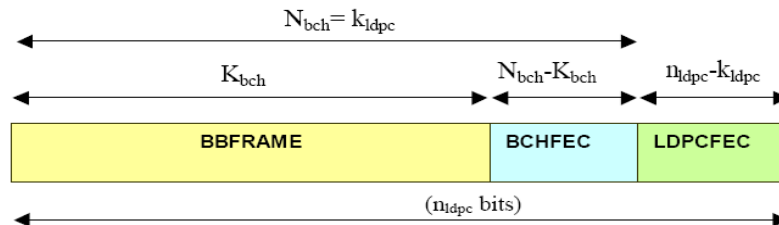


Figure 2.5-FECFrame structure [11]

### 2.2.3 Mapping

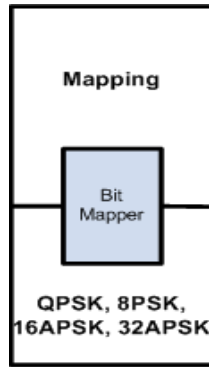


Figure 2.6- Mapping module [12]

The mapping module is responsible for mapping the FECFRAME into the appropriate modulation symbols required for transmission over a wireless channel. There are four different modulation schemes, quadrature and 8 phase shift keying (PSK) as well as 16 and 32 amplitude PSK (APSK), which can be selected by the adaptive modulation component; the schemes are also linked to a range of code rates. The input into the module is a FECFRAME and the output is a complex FECFRAME (XFECFRAME). The XFECFRAME is made up of  $64800/\eta_{MOD}$  symbols where  $\eta_{MOD}$  is the modulation efficiency. An example of bits mapped to the 16APSK modulation is depicted in Figure 2.7.

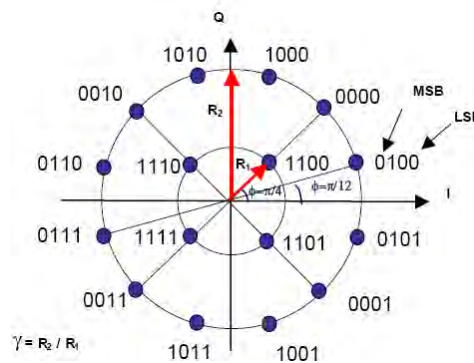


Figure 2.7-16APSK symbol mapping [11]

## 2.2.4 PL Framing

The PL Framing module is responsible for creating the physical layer frame (PLFRAME).The module receives the XFECFRAME as input however if no frame is available a dummy frame is inserted. The PL Signaling block is responsible for handling the administration of the PLFRAME, such that the receiver is capable of reconstructing the PLFRAME.



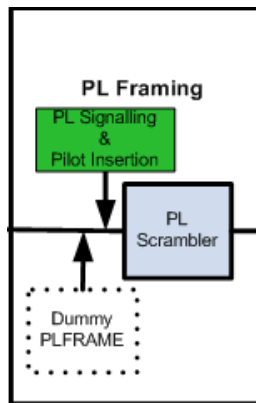


Figure 2.8- PL framing module [12]

This includes slicing the XFECFRAME into smaller blocks, adding a PLHEADER for receiver configuration and adding Pilot symbols which aid with receiver synchronization. The last function of the module is to scramble the frame in order to disperse the bit energy. It is implemented using a randomizing sequence added to the PLHEADER.

### 2.2.5 Modulation

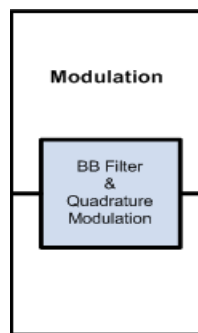


Figure 2.9- Modulation module [12]

The final block in the physical layer transmission system is the modulation subsystem. The output of the block is a modulated signal which is sent over the channel to the receiver. The process of modulation involves filtering the input signal which then undergoes quadrature modulation.

The modules discussed above make up the DVB-S2 physical layer transmission model, the focus of this dissertation is the FEC component of the protocol, which has been briefly mentioned

above. The contents of the FEC module, the BCH and LDPC channel codes will be discussed in greater detail as follows together with the presentation of their encoding algorithms.

### 2.3 BCH Codes

The following section discusses the characteristics and role of the BCH code in the physical layer FEC system as well as describing the encoding algorithm specified in the DVB-S2 standard. The BCH code was originally developed in 1959 by Hochquenghem and later expanded upon by Chaudhuri and Bose in 1960 [16], whose initials give name to the code.

A BCH code is a cyclic block code and is a generalization of Hamming codes [16] [17] which appends redundant data to the information allowing it to correct multiple bit errors. This has been observed in FEC module where the BCH encoder appends the BCHFEC header to the input data see Figure 2.5. BCH codes have gained popularity in communications due to the low level of hardware complexity required to implement the encoding and decoding modules [18]. The DVB-S2 standard employs a BCH code concatenated with a LDPC code to form the FEC mechanism at the physical layer. The concatenation negates the error floor problem experienced when using a message passing decoder to decode a LDPC code.

There are several different algorithms presented in the literature for the process of encoding BCH codes such as the look up table (LUT) based algorithms in [16] and [19]. The algorithms use LUTs to promote parallelization in the generation of the redundancy, improving the encoding efficiency. These algorithms however are variations of the polynomial division algorithm presented in the standard [16].

The algorithm uses polynomial representation to denote the codeword, input data and generator. The encoder utilizes polynomial division in order to generate the redundancy required to form the BCH codeword. The algorithm defined by the standard is as follows.

#### **Parameters**

$m(x)$ - The message polynomial of length defined by  $k_{bch}$ .

$g(x)$ - The generator polynomial

$d(x)$ -The remainder polynomial with defined length  $n_{bch} - k_{bch}$

$c(x)$ -The codeword of length defined by  $k_{ldpc}$

**BCH Encoder Algorithm** [20]

1. Multiply  $m(x)$  by  $x^{n_{bch}-k_{bch}}$
2. Divide  $m(x) \times x^{n_{bch}-k_{bch}}$  by  $g(x)$ , where the remainder is defined by  $d(x)$ .
3. Set the codeword polynomial  $c(x) = m(x) \times x^{n_{bch}-k_{bch}} + d(x)$ .

The three step process uses polynomial expression to describe the message, generator, remainder and codeword. The message polynomial is input into the module as a binary string of length  $k_{bch}$ , where  $k_{bch}$  together with several other bit length parameters are not statically defined due to the adaptive nature of the protocol. The variables in the above algorithm are defined for different transmission rates or modes given in Table 2.1. There are ten operational modes; each mode defines different lengths of data and redundancy. The DVB-S2 standard employs large block lengths however the standard also defines a set of operational modes which operate on lower block lengths to maintain flexibility in terms of application scenario [20]. The second aspect to consider is the number of errors which can be corrected; there are three modes of error correcting capability 8, 10 or 12 corrections.

**Table 2.1-Table of DVB-S2 modes [11]**

LDPC Code	BCH Uncoded Block $K_{bch}$	BCH coded block $N_{bch}$ LDPC Uncoded Block $k_{ldpc}$	BCH $t$ -error correction	LDPC Coded Block $n_{ldpc}$
1/4	16 008	16 200	12	64 800
1/3	21 408	21 600	12	64 800
2/5	25 728	25 920	12	64 800
1/2	32 208	32 400	12	64 800
3/5	38 688	38 880	12	64 800
2/3	43 040	43 200	12	64 800
3/4	48 408	48 600	12	64 800
4/5	51 648	51 840	12	64 800
5/6	53 840	54 000	10	64 800
8/9	57 472	57 600	8	64 800
9/10	58 192	58 320	8	64 800

The three modes require unique BCH generators; hence a table of generators is defined in Table 2.2. If 8 error corrections are required the first 8 generator polynomials are multiplied together, the pattern is maintained for both 10 and 12 error correction generators. An equivalent table of BCH generators is defined in [20] to be utilized in short length operational scenario.

**Table 2.2-Generator polynomials [11]**

$g_1(x)$	$1 + x^2 + x^3 + x^5 + x^{16}$
$g_2(x)$	$1 + x + x^4 + x^5 + x^6 + x^8 + x^{16}$
$g_3(x)$	$1 + x^2 + x^3 + x^4 + x^5 + x^7 + x^8 + x^9 + x^{10} + x^{11} + x^{16}$
$g_4(x)$	$1 + x^2 + x^4 + x^6 + x^9 + x^{11} + x^{12} + x^{14} + x^{16}$
$g_5(x)$	$1 + x + x^2 + x^3 + x^5 + x^8 + x^9 + x^{10} + x^{11} + x^{12} + x^{16}$
$g_6(x)$	$1 + x^2 + x^4 + x^5 + x^7 + x^8 + x^9 + x^{10} + x^{12} + x^{13} + x^{14} + x^{15} + x^{16}$
$g_7(x)$	$1 + x^2 + x^5 + x^6 + x^8 + x^9 + x^{10} + x^{11} + x^{13} + x^{15} + x^{16}$
$g_8(x)$	$1 + x^1 + x^2 + x^5 + x^6 + x^8 + x^9 + x^{12} + x^{13} + x^{14} + x^{16}$
$g_9(x)$	$1 + x^5 + x^7 + x^9 + x^{10} + x^{11} + x^{16}$
$g_{10}(x)$	$1 + x + x^2 + x^5 + x^7 + x^8 + x^{10} + x^{12} + x^{13} + x^{14} + x^{16}$
$g_{11}(x)$	$1 + x^2 + x^3 + x^5 + x^9 + x^{11} + x^{12} + x^{13} + x^{16}$
$g_{12}(x)$	$1 + x + x^5 + x^6 + x^7 + x^9 + x^{11} + x^{12} + x^{16}$

## 2.4 LDPC Codes

Low-density parity check codes are a class of linear block codes which were originally discovered by Robert Gallager in 1960 [21], as the name implies the characteristic feature of LDPC codes are their sparse parity check matrices. The following section discusses the characteristics of LDPC codes as well as their role in the DVB-S2 FEC; finally the LDPC encoding algorithm is presented.

The main benefit of LDPC codes is that it has shown both in theory and simulation to perform near the Shannon capacity in AWGN assuming large block lengths [13]. This property benefits the DVB-S2 standard which defines relatively large block lengths for transmission. LDPC codes also maintain a structure which lends itself to parallelism, which is beneficial for hardware implementation [22]. They are generally represented in the form of a sparse bipartite or Tanner graphs seen in Figure 2.10. The nodes on the left of Figure 2.10 represent the bits which form the parity check matrix, known as variable nodes. The nodes on the right represent the check nodes an edge between a variable and check node represents a binary '1' in the position given by the variable node in the parity check matrix. An important property which affects the performance of an LDPC code is the row and column weights given by  $d_c$  and  $d_v$ , respectively. The weight determines the performance of the code as it defines the structure of the bipartite graph which plays an important role in the decoding process.

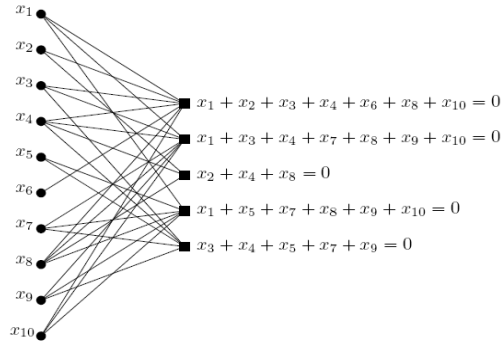


Figure 2.10-Bipartite graph

The LDPC Encoder presented in the DVB-S2 FEC is responsible for forming an LDPC codeword, of length  $n_{ldpc}$  which fixed at 64800 bits not considering the short length scenario, from the input BCH codeword of length  $k_{ldpc}$ .

The concatenation of the LDPC and BCH headers together with the input data forms the FECFRAME, see Figure 2.5. The advantage of which as has been previously mentioned is to solve the error floor problem inherent with LDPC decoding. The depiction of the performance results of iterative decoding algorithms are known as “waterfall” curves due to the shape of the curve. The bottom of the waterfall or the tapering off effect is known as the error floor region [23]. In LDPC codes the error floors are generally more prominent in high weight codes; the source of the problem are sets of variable nodes called stopping or trapping sets. These contribute to undetermined variable nodes during iterative decoding. Stopping sets dominate the performance of the code in the error floor region and the composition of the sets are determined by the method of construction of the LDPC code [23]

A LDPC code defines a sparse parity check matrix  $H$ , from which the associated generator matrix  $G$  can be derived. In order to generate an LDPC codeword the general technique multiplies the information  $I$  and the generator to produce the resultant codeword  $C$ ,  $C = I \times G$ . This algorithm is a basic encoding technique which can be applied to all linear block codes; it is simple however is computationally inefficient. Given that the parity check matrix  $H$  is sparse by nature, the generator matrix  $G$  is thus dense [24]. The process of multiplying  $I$  by  $G$  can be computationally costly if the length of  $I$  is large, which is the case in the DVB-S2 system.

In order to improve the efficiency of encoding there have been two general approaches taken in the literature. The first being to improve the structure of LDPC codes, LDPC codes can be formed through random generation of bits making up the  $H$  matrix, the variable node in parity check matrix. This approach leads to a high level of encoding/decoding complexity, dense generator matrices. In [24] it has been shown that an informed selection of bits making up  $H$  can

reduce the complexity of both encoding and decoding. In [24] four methods for generating well-structured LDPC codes are presented, which describe algorithms defining the placement of binary ‘1’s in either the matrix  $H$  or the arrangement of nodes in a bipartite graph. The second approach to improving encoder efficiency is to transform the encoding algorithm by use of the specialized structures developed in [24]. The sum-product encoder algorithm given in [25] is a highly efficient technique however it requires a  $H$  matrix where all the parity bits are found in the upper triangle, requiring several matrix permutations. Another method described in [25] is iterative matrix inversion which operates based on the Jacobi principle. The combination of approaches has produced algorithms which outperform traditional matrix multiplication in terms of efficiency.

The LDPC encoder presented in the standard is based on some of the principles discussed above however given the large and sparse nature of the  $H$  matrix in the DVB-S2 system, a specialized algorithm is developed in the standard. It utilizes the indices of the ‘1’ bits in  $H$  rather than forming the complete  $H$  matrix. The purpose of the encoding algorithm is to generate the  $n_{ldpc} - k_{ldpc}$  parity bits to be added to the message. The standard provides a system for calculating the position and value of the parity bits using LUTs directly from the information bits. The DVB-S2 system is rate adaptive hence the amount of parity bits generated varies according to the transmission mode currently selected. The standard thus defines 10 unique LUTs to match the 10 modes, for both the large and short length scenarios, which can be selected.

### **Parameters**

$p$ -Represents the parity bit array of length  $n_{ldpc} - k_{ldpc}$ .

$i$  -Represents the information bit array of length  $k_{ldpc}$ , the output of the BCH Encoder.

$LUT$ -The look up table corresponding to the given code rate

$q$ -Constant value defined in the standard

### **LDPC Encoder Algorithm** [20]

1. Initialize the parity bit array  $p$  to ‘0’.
2. For  $j = 0$  to  $k_{ldpc} - 1$
3.     if ( $j$  is a multiple of 360 )
4.     then
5.         for  $m = 0$  to (number of values in the line of the  $LUT$ )
6.          $b$  =value from  $LUT(m)$

```

7.            $p_b = p_b \oplus i_j$ 
8.           end
9.           Change to next line in LUT
10.        end
11.        else
12.            for  $m = 0$  to (number of values in the line of the LUT)
13.                 $b = \text{value from } LUT(m)$ 
14.                 $z = (b + j \bmod 360 \times q) \bmod (n_{ldpc} - k_{ldpc})$ 
15.                 $p_z = p_z \oplus i_j$ 
16.            end
17.        end
18.    end
19.    for  $c = 1$  to  $(n_{ldpc} - k_{ldpc}) - 1$ 
20.         $p_c = p_c \oplus p_{c-1}$ 
21.    end
22.    Append  $p$  to  $i$  forming the LDPC codeword.

```

The LDPC encoder module in a similar manner to the BCH module requires information from the adaptive module in order to define the value of  $k_{ldpc}$  as well as select the appropriate *LUT* and value of constant  $q$ , see Table 2.3, used during the encoding process.

**Table 2.3-Table of values of q [6]**

Code Rate	q
1/4	135
1/3	120
2/5	108
1/2	90
3/5	72
2/3	60
3/4	45
4/5	36
5/6	30
8/9	20
9/10	18

The parity bit array represented by  $p$  must be initialized to '0'. Once the process of initialization has been completed, the next step involves traversing the information array  $i$ . The information is bit accumulated using two different techniques dependent on whether the current bit index of  $i$  is a multiple of 360. The process of accumulation is a method of generating values for the parity array stored in  $p$ . If the index is divisible by 360, the accumulation process targets specific bits identified by their index. These indices are stored in the *LUT* associated to the indicated given mode. Assuming the current code rate was given as  $\frac{1}{4}$  and the current bit index is 0. The module

will scroll along the first line of the *LUT*, and accumulate  $i_0$  with every parity bit given by the indices in the *LUT*. Using the *LUT* given by Table 2-4, the first 3 accumulators for  $i_0$  are given in (2.1).

$$\begin{aligned}
 p_{1140} &= p_{1140} \oplus i_0 \\
 p_{23606} &= p_{23606} \oplus i_0 \\
 p_{36098} &= p_{36098} \oplus i_0
 \end{aligned} \tag{2.1}$$

The module traverses the entire length of the *LUT* line before returning to algorithm line 3. If the current bit is not a multiple of 360 the following process is implemented. The bits which are not multiple of 360 do not have their accumulation indices found in the *LUT*. The required indices must be calculated from those given in the *LUT*. The line in the *LUT* is traversed and each value is stored in the variable  $b$ .

The value is used as follows given equation (2.2) [11].

$$z = (b + j \bmod 360 \times q) \bmod (n_{ldpc} - k_{ldpc}) \tag{2.2}$$

Where  $z$  is the desired index, the accumulation at index  $z$  then proceeds. The value of  $j$  represents the global loop index while  $q$  is a constant defined in Table 2.3 dependent on the transmission mode. After all of the information bits have been traversed, the next step in is a sequential accumulation of all the parity bits, which involves adding adjacent parity bits together. Finally the parity bit array  $p$  is appended to  $i$  forming the completed FECFRAME.



**Table 2.4-Look up table for code rate 1/2 copied from [11]**

23606 36098 1140 28859 18148 18510 6226 540 42014 20879 23802 47088	36046 32914 11836
16419 24928 16609 17248 7693 24997 42587 16858 34921 21042 37024 20692	7304 39782 33721
1874 40094 18704 14474 14004 11519 13106 28826 38669 22363 30255 31105	16905 29962 12980
22254 40564 22645 22532 6134 9176 39998 23892 8937 15608 16854 31009	11171 23709 22460
8037 40401 13550 19526 41902 28782 13304 32796 24679 27140 45980 10021	34541 9937 44500
40540 44498 13911 22435 32701 18405 39929 25521 12497 9851 39223 34823	14035 47316 8815
15233 45333 5041 44979 45710 42150 19416 1892 23121 15860 8832 10308	15057 45482 24461
10468 44296 3611 1480 37581 32254 13817 6883 32892 40258 46538 11940	30518 36877 879
6705 21634 28150 43757 895 6547 20970 28914 30117 25736 41734 11392	7583 13364 24332
22002 5739 27210 27828 34192 37992 10915 6998 3824 42130 4494 35739	448 27056 4682
8515 1191 13642 30950 25943 12673 16726 34261 31828 3340 8747 39225	12083 31378 21670
18979 17058 43130 4246 4793 44030 19454 29511 47929 15174 24333 19354	1159 18031 2221
16694 8381 29642 46516 32224 26344 9405 18292 12437 27316 35466 41992	17028 38715 9350
15642 5871 46489 26723 23396 7257 8974 3156 37420 44823 35423 13541	17343 24530 29574
42858 32008 41282 38773 26570 2702 27260 46974 1469 20887 27426 38553	46128 31039 32818
22152 24261 8297	20373 36967 18345
19347 9978 27802	46685 20622 32806
34991 6354 33561	
29782 30875 29523	
9278 48512 14349	
38061 4165 43878	
8548 33172 34410	
22535 28811 23950	
20439 4027 24186	
38618 8187 30947	
35538 43880 21459	
7091 45616 15063	
5505 9315 21908	

## 2.5 Literature survey of FEC decoders

The DVB-S2 FEC encoder structure and algorithms have been presented in great detail in the preceding sections, continuing with the description of the DVB-S2 physical layer model, the definition of a receiver structure is required. The DVB workgroup defines only the transmission system at the physical layer. This has led to several different receiver structures being developed and presented in the literature.

The aim of the literature survey is firstly to gain an understanding of the decoding approaches and algorithms available in the literature for BCH and LDPC code in order to select an appropriate decoding structure for the DVB-S2 FEC. The requirements for a suitable structure are: compatibility with decoding the concatenated BCH-LDPC code, the decoder must provide best possible error correcting performance, referred to as performance in the section, compared with those presented and finally the decoder must be of realizable complexity. The complexity of the decoder must be considered as the goal is to produce a realistically implementable decoding system. The second reason is that the processing power available to implement the decoder in software, is limited. These metrics will be considered when examining the decoding options presented as follows.

The literature survey will be divided into three sections BCH, LDPC and concatenated decoders. The motivation of the decomposition is to gain a complete understanding of the possible solutions available for the BCH and LDPC module independently before considering solutions specialized to decode the concatenated code.

A second broad differentiation made in the process of the review is the separation of algorithms into hard and soft decision variants. Hard decision decoding implements an algorithm which at its basis selects the decoded codeword out of the set of all possible codewords based on Hamming distance, where the minimum value is selected. Soft decision decoding utilizes soft information, generated during the process of decoding; this is used to calculate the Euclidean distance of the potential codewords. The minimum codeword is then selected as the decoded codeword. The subsequent sections form a review of decoding techniques available for application to the DVB-S2 FEC, for LDPC and BCH codes.

### 2.5.1 LDPC decoding

LDPC codes were originally presented by Gallager in his doctoral thesis [26] in 1963. In the succeeding years there have been a broad range of approaches set forth to decode and improve the performance of LDPC decoding.

Gallager presented two algorithms for LDPC decoding, which take different decoding approaches. The first is a hard decision algorithm, assuming transmission over a binary symmetric channel (BSC), the algorithm uses the parity check equations given by the LDPC  $H$  matrix to determine whether to flip the values of the bits in the received sequence. The algorithm flips the value of the bits until all the parity check equations are satisfied; it is thus known as the bit flipping (BF) algorithm.

There have been many variations made to the BF technique including weighted BF (WBF) [27] and modified weighted BF (MWBF) in [27] and [28], where the improvement is based on flipping the appropriate bits only once a given threshold is achieved. The performance of the decoders are dependent on the threshold value if the value is too high the incorrect bits are not flipped, if they are too low the correct bits may be incorrectly flipped. These decoders are shown to better performance, in scenarios where the threshold is suitably defined, beyond that of the BF algorithm. Reliability ratio-based-weighted BF (RRWBF) [29] builds on the MWBF technique by using all the bit node information to calculate the metric which determines whether the bit should be flipped. The algorithm determines a reliability ratio using the input value of the bit nodes. It has shown to produce a coding gain of 1dB over the traditional BF algorithm. The computational cost required to determine the bit flipping metric increases the complexity of the RRWBF decoder thus a implementation efficient RRWBF (IERRWBF) is provided in [30]. The IERRWBF maintains the error correcting performance while reducing the complexity using parallelization and reducing the number of computations using LUTs.

In [31] the candidate based BF (CBBF) decoder is discussed; the approach is based on the correlation between the columns of  $H$ . The correlation is used together with the parity check equations to determine the correct bits to flip. The BF technique has previously only been presented in hard decision form however in [32] both a hard and soft iterative decoders are presented. The hard decision decoder differs from Gallager's BF technique on the basis that only a single bit is flipped every iteration. The metric determining whether the bit is flipped is based on the syndrome weight of vectors which contain more than two errors. The soft decision algorithm is a slightly modified version of the hard decision as it takes into account channel reliability information when calculating the bit flipping metric. An issue with flipping a bit in an iterative manner is that the decoder may be caught in a loop, where the same bit is flipped and then flipped back in subsequent iterations. To counteract this, a loop detection technique is applied to both algorithms to break any cycles. The hard and soft decision algorithms together with the CBBF are shown to provide better performance than BF, however the soft decision decoder and CBBF come at the cost of greater complexity.

There have been several other hard decision algorithms presented for LDPC decoding such as the majority logic (MLG) decoder given in [33] [34] which uses a majority voting technique to determine the value of a selected bit. The concept behind MLG is based on the parity check relationships in a similar manner to BF. The majority voting technique is advanced in [35] using reliability or channel values and an iterative structure to improve the decision of the majority vote, which shows significant improvement in performance over traditional MLG.

As is the case with most hard decision algorithms it provides a lower degree of complexity easing the process of implementation, however they suffer in terms of performance relative to their soft decision counterparts. The second algorithm presented by Gallager was a probabilistic iterative decoder; initialized using the channel transition probabilities. The scheme uses the check and variable node structure, to calculate the probability of a bit being '0' or '1'. The algorithm is called Belief Propagation, also known as the sum product algorithm (SPA) [27] [36] [37] [38] [39] and is a form of message passing decoding. The name comes from the term "beliefs" which is the term given to the probabilities of the given bit being a '0' or '1' based on values of the bits which are related to it described by the Tanner graph. The concept of propagation is based on the manner in which the "beliefs" are updated; the process is iterative and propagates as a "belief" is based on the "belief" of other related nodes. The algorithm has shown to reach near ML decoding performance as well as approach the Shannon limit.

The BP algorithm was presented by Gallager in 1963 however it was only popularized when LDPC codes were rediscovered 30 years later, the main issue with their lack of popularity at the time of conception was due to a lack of technology required for efficient implementation of the

decoder. BP decoding has since become the basis for majority of the decoding algorithms presented in the literature. There have been several variations made to BP such as the message passing schedules technique given in [40]. The Tanner graphs of specific LDPC codes are analyzed and improved message passing schedules are derived; when applied to BP the improved schedules provide better performance and in given cases at a lower complexity when compared to BP. Another variation given in [41] focuses on reducing the complexity for short LDPC codes, containing a large degree of short cycles by modifying the reliability of the messages passed however providing a lower error correcting performance.

The modifications given above focus on reducing the complexity of the decoding algorithm while maintaining similar levels of error correcting performance relative to BP. The approach is taken in the development of the uniformly most powerful (UMP) BP based algorithm given in [42] [43] [44] which simplifies processing at the check nodes. This degrades the performance of the decoder however in [45] a normalization approach is presented. The normalization approach improves the performance of UMP based schemes, however still below that of the BP decoding.

The min-sum (MS) algorithm [46] like UMP is another algorithm which looks to balance complexity and performance. The MS algorithm makes an approximation in the process of updating the check nodes. This reduces the complexity of decoding by decreasing the number of multiplications required to calculate the probability associated with each bit. The MS algorithm is modified in [47] where a predetermined offset, known as offset MS (OMS), is added to the check node update calculation, improving the decoding of the MS algorithm. The offset adjusts the error of the approximation and is calculated by analysis of the iterative information produced by the decoder. The decrease in error of approximation leads to a reduction in the number of errors produced. The concept is extended in [48] where the calculation of the offset is determined in an iterative manner dependent on the soft information produced in previous iterations. This is shown to improve performance at the cost of greater complexity than MS and OMS.

The forced convergence (FC) method [49] is another modification of BP which differs from the approach taken by MS. The approximation is made with regards to individual nodes; the assumption is that most variable nodes will converge to the correct value within several iterations of decoding. The update of the converged variable nodes will thus be halted reducing the number of calculation required to decode. The properties in identifying the converged variable nodes is key and determines the performance of the system, which is in the best case similar to BP, these are defined together with several improvements in [50].

The structure of the LDPC code is important in determining the decoding performance. A large portion of the decoding algorithms are iterative and operate on the transfer of information between bit and check nodes. The structure of the bit and check nodes can thus be arranged to

improve decoding. The main detriment to iterative decoding is the formation of cycles in the Tanner graph as it is shown to skew the shared soft information reducing the effectiveness of message passing decoding. The problem has been considered in [24] [51] [52] [53] which provide various algorithms for improving the structure of LDPC  $H$  matrices, by reducing the number of short cycles in the Tanner graph of  $H$ . The decoding of the improved construction parity check matrices outperform similarly generated matrices using traditional techniques.

There has also been other approaches taken to solve the problem of short cycles in  $H$  matrices, rather than removing short cycles at construction, a cyclic lifting technique is presented in [54]. Cyclic lifting is the process of “lifting” short cycles from the LDPC Tanner graph while maintaining the basic code properties such as degree distribution. The effect of short cycles is also shown to play a significant role in producing the error floor problem hence the removal of cycles improves the performance in the error floor region. The short cycles in LDPC codes can be identified by simulation using a message passing decoder, for a specific  $H$ . The algorithm presented in [55] proceeds to identify the short cycles, termed trapping sets, using a sampling simulation technique. Knowledge of dominant short cycles, short cycles which are prominent in error events, allow the decoder to switch to a default scenario when the decoder is trapped in a cycle. The process reduces the effect of short cycles on performance however at the cost of high complexity as it requires a large amount of storage and preprocessing. In [56] the method of identifying error sets is taken to next level, where the concept focuses on the early identification of non-decodable blocks, reducing the decoding power wasted on non-decodable blocks, effectively reducing the complexity of the system.

The concept of short cycles as has been discussed is shown to reduce decoding performance however instead of removing them, an algorithm is developed in [57] which modifies BP to take advantage of short cycles. The algorithm is shown to improve the performance with regard to the algorithms mentioned which remove or identify short cycles. The assumption is that it requires a great number of short cycles to outperform the other algorithms, which is not the case given traditional LDPC decoding.

The transfer of soft information has been discussed as being the key component in providing BP performance. Two techniques have been presented which attempt to analyze the soft information transferred in the BP decoder, density evolution (DE) [58] and extrinsic information transfer (EXIT) charts [59] [60]. DE and EXIT chart analysis are used in the literature to analyze the extrinsic information produced by message passing decoders. The information has shown to be a valuable tool in improving the performance of decoding systems. In [61] DE is applied to the MS and BP decoding structures, illustrating the differences in information produced by both systems. This allowed for an offset value to be determined which reduces the information difference

between MS and BP, allowing MS closer to BP error performance. A similar approach is given in [62] which scales the transferred soft information, based on DE information, in the case of MS decoding, a maximum scaling factor is calculated which provides maximum coding gain for a given code. In [47] scaling factors are produced for offset based BP and normalized BP which are reduced complexity variations of BP in the same vein as MS decoding.

The EXIT chart technique measures similar information to DE however where DE is numerical EXIT charts are graphical. The curve fitting approach to improving performance are provided in [63] and [64], where the approach is based on reducing the gap between the bit node and check node information curves, achieved by varying the code parameters. The performance of the analyzed codes is shown to improve using the curve fitting approach.

The final approach to be applied to LDPC decoding systems are the hybrid decision decoding schemes as presented in [65] [66] [67]. The characteristic algorithm in this field is the two-stage algorithm, which is a combination of two iterative decoding algorithms. The first stage is a soft decision decoder followed by a hard decision decoder. If the soft decision decoder fails the decoding is transferred to the hard decision decoder and vice versa until the codeword is correctly decoded. In [68] an algorithm is presented which makes use of BP as the first stage with a small number of iterations, after all of the iterations have completed a hard decision is made based on the LLR ratios, resulting in a binary codeword. The results of which is passed to the second stage being an IERRWBF decoder, schemes for reducing the complexity of the hard decision stage are also presented. There are also variations such as those given in [67] which reverse the stages where the first stage consists of the hard decoder and the second stage consists of the soft decoder. This scheme has shown to produce similar performance to BP with a much reduced complexity, for a similar number of iterations.

A similar algorithm is presented in [69] by Fossorier, combining reliability based decoding specifically OSD, as the second stage, with BP. The Fossorier decoder outperforms BP in terms of performance for given code lengths, however at the cost of much greater complexity per iteration. The OSD algorithm is also combined with adaptive BP (ABP) in [70]. ABP is a variation of BP which adapts the  $H$  matrix of the code based on reliability information. The aim is to reduce the effect of unreliable bits on the decoding. The combination to form ABP-OSD in [71] has shown to outperform reliability based decoders of similar length. The reliability based OSD algorithm is presented again in concatenation with a BF mechanism in [72], to form the BF-OSD decoder. The BF can be one of a number of variants [27] [28] [29] [30] mentioned earlier in the section, the BF techniques are generally hard decision and are of low complexity. The combined decoder is thus of lower complexity than the preceding concatenated schemes.

The BF scheme sums the BF metric values which act as input into the OSD module. The scheme provides comparable performance to BP with a much reduced complexity.

The LDPC decoding mechanisms presented range over a broad spectrum of approaches. The DE and EXIT chart approaches mentioned in the course of the review cannot be considered as they improve decoding performance however do not define a specific decoder structure. They are techniques which can be applied to any message passing soft decoder. The same reasoning can be applied to the  $H$  construction and modification algorithms which can be applied to improve performance once a decoding structure has been defined. The BF technique presented by Gallager has shown to provide adequate LDPC decoding performance with low complexity. The modifications to BF such as RRWBF are shown to make significant coding gains making it attractive for selection. The performance however of the BF variants are limited when compared to the soft decision BP decoder. This has a much greater complexity due to the calculations required to determine the “beliefs”. The general trend in the soft decision decoders examined in the review has aimed at reducing the complexity of the BP decoder while attempting to maintain the decoding performance. This has been achieved to varying levels of success by MS, UMP, ABP and FC together with their alternatives. The dual soft decision concatenated structures such as the Fosserier and ABP-OSD decoders are shown to improve the coding gain above that of BP, with an increase in complexity. The soft-hard decoder concatenations provide BP like performance at lower complexity. Taking into account the metrics considered for a suitable decoding structure it is apparent that selected LDPC decoder will be based on BP, as it provides the best available performance whilst the complexity is still manageable in terms of software and hardware implementation.

### 2.5.2 BCH decoding

The BCH error correcting code has gained great popularity in communications in recent years, the justification being the availability of simple algebraic techniques for BCH decoding. This has allowed development of low cost and complexity receivers which maintain reasonable decoding performance; several of these structures will be examined as a suitable implementation for the DVB-S2 FEC decoder.

The conventional BCH decoding algorithm consists of three steps [73], syndrome calculation, derivation of the error locator polynomial and finally identification of the errors in the codeword using the error locator polynomial. An implementation of which is depicted in Figure 2.11.

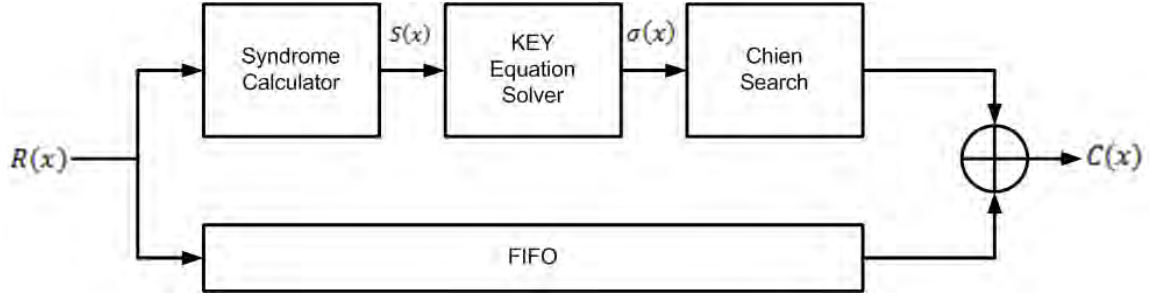


Figure 2.11-BCH decoding process [52]

The input into the BCH decoder given Figure 2.11 is  $R(x)$ , which is the binary input into the BCH decoder. The first stage in BCH decoding is syndrome calculation, the purpose being to form the syndrome polynomial given in (2.3).

$$S(x) = S_1 + S_2x^1 + \dots + S_{2t}x^{2t-1} \quad (2.3)$$

Given that  $t$  denotes the error correcting capability of the BCH code. Where  $S_j$  is determined as per the relationship given in (2.4) where  $j \in [1, 2t]$ .

$$S_j = R(\alpha^j) = \sum_{i=1}^v (\alpha^j)^{e_i} = \sum_{i=1}^v (\beta_{e_i})^j \quad (2.4)$$

$\alpha$  is the primitive element of the BCH code, the number of errors present in the codeword  $R(x)$  is given by  $v$ . The error locator terms are given by  $\beta_{e_i}$  where  $e_i$  is the  $i$ th error location. The calculation of which can be facilitated using a process of division using the primitive elements.

The syndrome polynomial  $S(x)$  is required in order to develop the error locator polynomial  $\sigma(x)$  given in (2.5), which makes up second stage of the decoding process. The Key Equation solver is responsible for determining the relationship between the syndrome and error locator polynomial.

$$\begin{aligned} \sigma(x) &= (1 + x\beta_{e_1})(1 + x\beta_{e_2}) \dots (1 + x\beta_v) \\ &= 1 + \sigma_1x^1 + \sigma_2x^2 + \sigma_3x^3 \dots \sigma_vx^v \end{aligned} \quad (2.5)$$

The complexity of determining  $\sigma(x)$  is due to the system of equations defined by the syndromes being under constrained. There is thus a range of possible solutions, ideally in decoding the aim is to determine the solution which contains the minimum amount of errors. There have been several presentations in the literature which aid in the computation of the  $\sigma(x)$ .



The Berlekamp Massey algorithm (BMA) [74], is the combined work of Berlekamp and Massey. It is the most popular technique implemented in industry and forms the  $\sigma(x)$  in an iterative manner. A concern with the BMA is the throughput of the decoder, the iterative nature of the algorithm creates a bottleneck when implemented [75]. There have been several enhancements constructed in order to resolve the issue. An approach being to transform the BMA in order to reduce the complexity such as inversion-less BMA (RiBMA) given in [76] and the further simplified inversion less BMA (SiBMA) [77]. These are BMA schemes which have been parallelized and simplified for VLSI implementation. The reduced complexity implementations shows improved throughput in comparison to traditional BMA. The complexity of the BMA has also been reduced using fast Fourier transforms (FFT) in [78] an issue with this system is that the reduction occurs in terms of computational complexity. The use of FFT however has led to an increase in storage complexity due to the storage of the associated LUTs.

The modified Euclidean algorithm [79] [80] is an alternative technique for determining the key equation. The algorithm applies a series of mathematical techniques in order to develop the series of polynomials required to find the key equation; at a complexity similar to BMA.

The third stage in the process of BCH decoding is a Chien search which determines the roots of  $\sigma(x)$ . The roots are the locations of the errors in the codeword; the final task involves flipping the bits of the positions in error, implemented in Figure 2.11 in the form of the XOR gate.

As with the LDPC decoders previously surveyed and with most practical decoding structures in general, the soft decision algorithms provide improved levels of error performance over the hard counterparts [81]. There have been several soft decision algorithms presented for application in BCH decoders such as the generalized minimum distance (GMD) algorithm [82] [83] developed by Forney. The premise is the generation of a set of candidate codewords using algebraic methods. GMD decoders select the least reliable bits of the received codeword, which are sent to a candidate codeword generator. The generator creates a series of test patterns dependent on the input bits, the test patterns are added to  $R(x)$  to form variations of the binary received codeword  $R(x)$ . The candidate codewords are then decoded using a hard decision BCH decoding algorithm. The result of which is a refined set of codewords, these codewords undergo a process of selection in the decision making unit such that the most likely codeword is selected. The process is depicted in Figure 2.12.

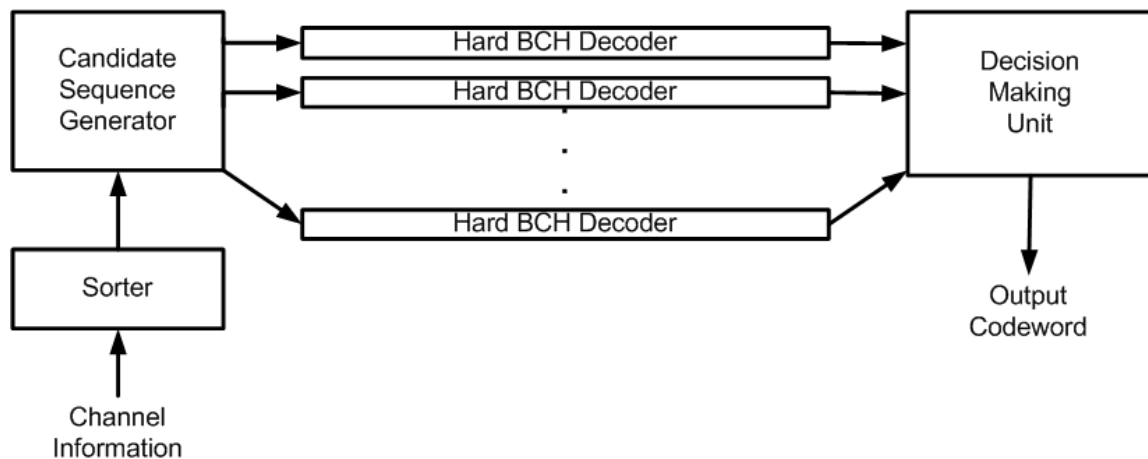


Figure 2.12-GMD decoder structure [84]

The drawback of such a soft decision system is the multiplicative increase in the amount of hardware required. There are several other soft decision algorithms which produce a set of candidate codewords such as those produced by Chase in [85], Chase provided three algorithms for determining the selection of bits to be used in constructing the set of test patterns. This plays an important role in determining the set of candidate codewords. The Chase schemes vary in their approach of determining the number of least reliable bits to select, thus varying the amount of test patterns generated [86].

There have been many adaptations made to the Chase algorithms mostly aimed at reducing the amount of test patterns produced while maintaining the decoding performance, such as the dynamic scheme presented in [87]. The scheme divides the original set of candidate codewords into two subsets and selects one of the subsets to progress with during decoding. The basis for the selection is based on the reliability information from the channel. The scheme given in [88] defines a threshold which is used to reduce the number of test patterns generated by the Chase algorithm. The threshold is based on reliability information; the assumption is that the number of unreliable bits selected is fixed by the algorithm. There are cases where the reliability value of a selected least reliable bit may be low relative to the other bits in the codeword but in general can be termed reliable. The threshold excludes those bits, where any bit above the threshold is not considered unreliable, thus reducing the number of test patterns generated by the Chase algorithm.

The sliding encoding window (SEW) [89] algorithm is a technique which focuses on the cyclic properties of the BCH code to generate candidate codewords. The purpose is to improve codeword diversity. It has shown to be most effective when combined with the Chase algorithm or BMA such as that presented in [90] which provides improved decoding performance when compared to regular Chase decoding.

In [91] [92] the Koetter-Vardy (KV) approach is adapted for Chase decoding; the KV algorithm is a soft decision algorithm originally developed for decoding Reed-Solomon codes. The algorithm converts the input channel reliability information, into a matrix of reliability values associated to each codeword bit. The KV algorithm is made up of three stages: matrix formation, polynomial interpolation and factorization. The algorithm is computationally complex due to the matrix permutations and is increased with the addition of Chase decoding. The Chase decoder generates a set of TPs which are permuted into their associated matrices using the KV approach, after which the process of interpolation and factorization is undertaken. The result of which is improved decoding performance relative to the traditional Chase and KV algorithms.

In [93] a variation to the soft decision decoders mentioned above is presented which improves decoding performance while reducing the complexity. The decoder compensates for an additional error beyond that given by the least reliable set improving the decoding performance. The reduction on complexity is achieved by removing the Chien search from the algebraic decoder, the module is replaced with a lower complexity module capable of finding the errors using the least reliable values called the compensation error magnitude solver.

All of the above mentioned techniques utilize soft information in the generation of the sets of test patterns and candidate codewords; however there have been presentations which make use of soft information in the probability propagation phase to improve decoding. A suboptimum MAP decoder with a SISO Hamming decoder has been presented in [94], there have also been applications of BP like algorithms to BCH decoding such as SPA implemented in [95] and ABP in [96]. The propagation comes at great cost in complexity but with much improved error correcting performance. In order to reduce the complexity due to soft decision propagation several decoders have chosen to focus only on a portion of the codeword. In [97] an algorithm is presented which examines the use of error magnitudes in selecting least reliable bits, the use of the error magnitudes produces a much lower complexity system than selected hard decision decoders. The soft decoder operates only when the errors occur in a designated range of locations; it is thus highly dependent on the reliability information input into the decoder, which is channel dependent.

The algorithm presented in [98] analyses soft decision decoders but focuses on improving the structure of the code using the method known as extended parity check matrix(EPCM) into which the original parity check matrix is permuted. The utilization of the EPCM is shown to produce improved performance in low rate system.

There have been several approaches discussed above which can be selected to decode the BCH codewords. The hard decision algebraic decoders such as BMA are shown to be low complexity and provide reasonable decoding performance. The performance is extended when it is combined

with a reliability based decoder such as the GMD or the Chase algorithm. The system requires greater complexity however the trend in the presented work has been to modify the Chase algorithm in order to reduce said complexity. The soft decision reliability based schemes are prime candidates for the selection as they provide suitable decoding performance at a reasonable complexity.

### 2.5.3 Concatenated decoding

In the preceding sections a literature survey of BCH and LDPC decoding structures has been conducted on an individual basis, the target being the selection of algorithms in the design of a DVB-S2 FEC decoder. There are however several systems available which provide a complete scheme for decoding the DVB-S2 FEC, decoding both the BCH and LDPC codes. These have been presented in both literature and industry. In general the decoders developed by industry focus on low complexity implementations and are concatenations of the popular decoding techniques developed above.

In [99] a BCH encoder/decoder structure is implemented which utilizes BMA decoding, together with a BP decoder implemented in [100] to decode LDPC codes, forming a BMA-BP decoding structure. There are many other such combinations of FPGAs available on the market designed to handle the specific constraints of the DVB-S2 system. Instead of BMA, RiBMA or SiBMA systems are implemented in a similar vein BP is generally replaced with MS or ABP. It is important to note that regardless of the variations to BMA BCH decoding or BP LDPC [101] [102] [103] [104] decoding, the concatenated decoders operate independently of each other.

There have been several presentations in the literature such as that given in [105] which presents a compromise between decoding performance and complexity. The scheme implements a BMA decoder together with a fixed offset MS (FOMS) algorithm, which is a variation of the MS algorithm. FOMS introduces a constant offset; reducing the errors induced by the MS approximation. In [106] a similar scheme is presented which implements a low complexity BP decoder similar to MS, the BCH decoding is implemented using a BMA algorithm however the Chien search circuitry is reformed in a manner that improves the efficiency of the system.

A concatenated iterative decoding scheme is presented in [13] which facilitates the transfer of soft information between the BCH and LDPC decoder's in order to improve the resultant error correcting performance. The decoding system consists of a Chase and BP decoder for BCH and LDPC codes respectively. The concatenated system benefits from the sharing of soft information between the BP and Chase decoder which is shown to improve the decoding performance over similar independently operational decoders. The algorithm is iterative in nature and implements

BP decoding for a fixed number of iterations before switching to a single pass Chase decoder. The soft information derived from the BP decoding is transferred to aid in the BCH decoding. If decoding is still unsuccessful the conditioned soft information is transferred back to the BP decoder, until either a codeword is successfully decoded or a fixed number of iterations are achieved. The performance of the BP-Chase decoder outperforms the constituent decoders the coding gain can be attributed to the soft information transfer however at higher complexity.

The literature review undertaken above has presented several alternative decoding structures which can be selected for decoding the DVB-S2 FEC. In order to select a viable solution the decoder structure considered must be able to decode the concatenated BCH-LDPC code. The metrics used to measure potential options are moderate complexity and best possible performance. In the review of the LDPC decoder it was shown that the BP decoder which is an iterative message passing algorithm met the requirements above. In the case of the BCH codeword the BMA algorithm was combined with reliability based decoders systems to provide coding gain. The concatenated systems presented in the review focused on low complexity implementations however a concatenated BP-Chase decoder was examined. The BP-Chase is a concatenation of the decoders which meet the selection criteria. The algorithm presented in [13] is shown to produce error correcting performance over and above BP and Chase decoders. The BP-Chase system will thus be selected as the receiver system to be used in the course of the dissertation. The system meets the metrics for selection as well as has potential for improvements; which will aid in producing a novel decoding algorithm.

## **2.6 Conclusion**

In the preceding sections the DVB-S2 FEC structure has been discussed and detailed with consummate detail. The components that make up the DVB-S2 protocol are analyzed in brief, whilst highlighting their relevance to the FEC structure. The FEC structure is then decomposed into the BCH and LDPC encoding systems each of which is examined. A literary review of the DVB-S2 structure is then undertaken the result of which is the selection of the concatenated iterative BP-Chase decoder given in [13]. The concatenated iterative decoder will act as the base for the FEC receiver the implementation of which will be discussed in greater detail in the subsequent chapter.

# Chapter 3

## PHYSICAL LAYER IMPLEMENTATION

### 3.1 Introduction

This chapter aims to construct and implement a DVB-S2 physical layer (PL) system model in order to generate error correction based performance results in both an AWGN and satellite channel. In order to fulfill one of the original aims of the dissertations as well as building a platform from which the system can be extended. In the process of examining the DVB-S2 protocol so far the PL has been outlined in Chapter 1 and detailed in Chapter 2. The next stage involves adapting the models previously presented in order to create a complete system which can be realized in order to achieve the above mentioned aim, which is the basis for the work in this chapter.

A complete PL system model requires a transmission and reception system as well as a channel through which the transmitted signals can propagate; the basic model of which is depicted in Figure 3.1 below. The PL transmission system has been fixed in the DVB-S2 protocol and the implementation details and algorithms of which are presented in Chapter 2, depicted in Figure 1.2 and Figure 2.1. The DVB-S2 PL model discussed previously is made up of several functional blocks which allow the protocol to be used for a variety of applications. They however do not all play a role in providing error correction control, they do not add to the performance of the protocol. The construction of the model to be used in the chapter focuses on the decoding performance and hence the transmission model is condensed in Section 3.1, in order to simplify the analysis of the error control coding. The only module considered is the FEC (BCH and LDPC) as it is the major contributor in provision of error control. The link layer system modules are not considered as the encapsulated data does not affect the error correcting performance at the PL, which is the focus of the dissertation. The same can be said of the Mode & Stream Adaptation module which is responsible only for administrating input into the PL.

The PL model defined thus far includes a defined transmission model however a channel is required through which the signal can propagate. The literature available regarding DVB-S2 PL models provide results mainly in AWGN channels [12] [13] [20] [107]. In recent years there have been several campaigns undertaken which aimed to model the satellite channel. In order to determine the model which will be implemented, Section 3.2 presents a survey of the literature to

develop the concept of satellite channel modeling as well as examining the models which have been developed. A model will then be selected and discussed in regard to its implementation in the PL model.

The reception system of the PL model is not specified by the DVB-S2 protocol, to select an appropriate model a literary survey was undertaken in Chapter 2. The result of which was the selection of the Chase-BP decoder developed in [13], due to its improved error performance. The Chase-BP decoder will be presented in detail in Section 3.3, focusing on providing the constituent and concatenated decoding algorithms as well as the details for the integration of the decoder in the PL model. In Section 3.5 the results of the implementation of the PL system model are provided and discussed, finally a conclusion highlighting the outcomes of the chapter is given in Section 3.6.

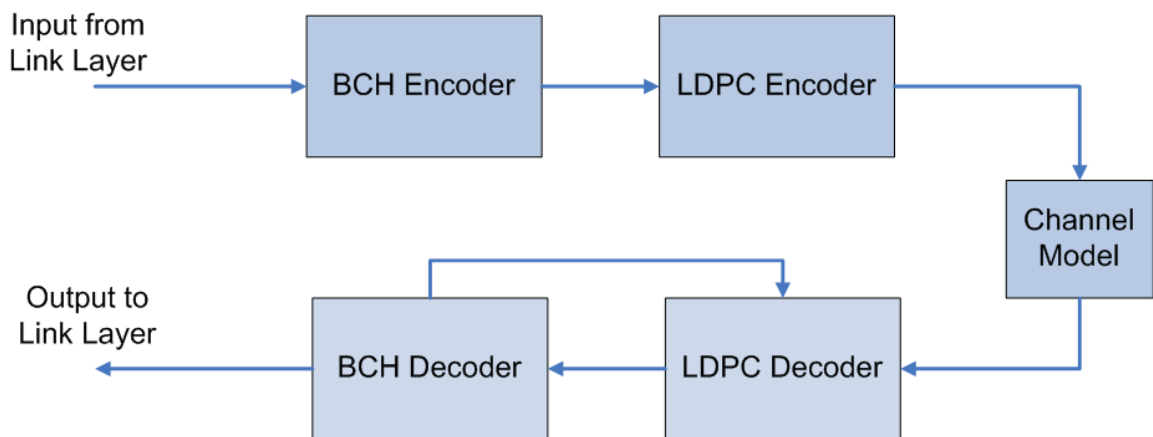


Figure 3.1-FEC system model

### 3.2 Transmission model

The focus of this section is the provision of the integration and implementation details of the transmission model in the PL system model. The simplified transmission model as depicted in Figure 3.1 is made up of the DVB-S2 FEC module which forms the main contributor of the error correcting capability of the system.

The FEC module presented in Chapter 2 consists of the BCH and LDPC encoders, the algorithms for which have been presented in detail in Section 2.3 and 2.4 respectively. The purpose of the transmission model is to apply the FEC encoding algorithms to the input data in order to detect and correct a given number of errors at the receiver, essentially providing a defense against corruption over a channel. The transmission scheme achieves this by applying channel coding

(BCH and LDPC) to the input information. The input information into the transmission model is in the form of binary data. The transmission model then proceeds to encode binary information blocks of length  $k_{bch}$  to a BCH codeword of length  $n_{bch}$  using the BCH encoding algorithm. The BCH codeword represented by  $B(x)$  in Figure 3.2 is then concatenated with the LDPC scheme.  $B(x)$  of length  $k_{ldpc}$  is encoded using the LDPC encoding algorithm to a LDPC codeword of length  $n_{ldpc}$ . The output of the transmission model is a binary LDPC codeword, which encompasses the BCH codeword; the last operation of the LDPC Encoder is to map the binary codeword to  $\mp 1$  for transmission across the channel.

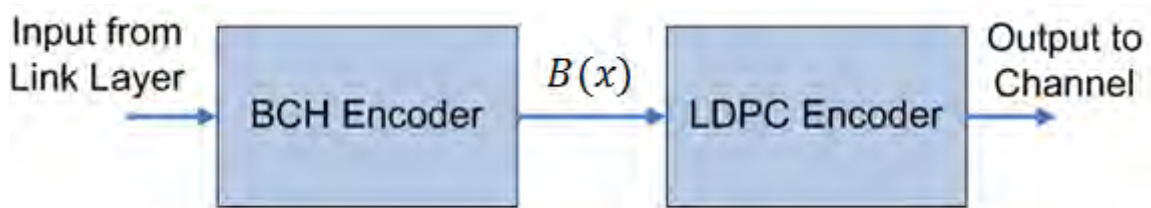


Figure 3.2-Transmission model

The transmission model has been described in detail in the above section with reference to algorithms given by the DVB-S2 standard, presented in previous chapters. The subsequent stage of constructing the PL model requires the selection and analysis of the channel model as follows.

### 3.3 Channel model

The aim of this section is to select and define a channel model, which will act as a more accurate analog for a satellite system, in the PL model. In the literature the AWGN channel has been used as a model for satellite channels however in recent years there have been several projects initiated mainly by the European Space Agency (ESA) [108] through various intellectual bodies, for the measurement and modeling of satellite channel models, concentrating mainly on the Land-Mobile satellite(LMS) channel.

The drive for research into satellite channel modeling can be attributed to several reasons. One of those being infrastructure reuse, such as fixed television satellites reaching their end-of-life which renders them incapable of providing their original function in a fixed receiver scenario. Mobile devices are not restricted in this manner as they are capable of tracking and acquisition [109] and are thus capable of reusing the satellite infrastructure. The growth and distribution of



mobile systems worldwide has spurred the development of a variety of mobile centric applications and environments [110] hence the drive to model the LMS channel is to provide better prediction of the performance of mobile services rendered in a satellite medium.

To improve the understanding of satellite channels a brief description of the terms and modeling techniques are provided. A literature survey is then undertaken to allow for the selection of a channel model which will be implemented. The selected channel will then be developed, concentrating on its integration into the PL model. The implications of the link budget in a satellite system are also produced.

### 3.3.1 **Satellite channel modeling**

A satellite channel model is a representation of the environment through which signals propagate in a satellite system; an accurate channel model takes into account the variety of disturbances experienced by a transmitted signal such as shadowing and reflection.

The generation of satellite channel models can be understood as the formation of the channel characteristics in terms of the statistical distributions and state diagrams. The modeling is based on experimentation and measurement campaigns which measure the characteristics of a received signal. The measurement campaign focuses in general on the signal from a single satellite and measures results in a range of environments and elevation angles.

The LMS channel will be the focus of the dissertation in this section. The selection of the LMS channel is appropriate in terms of the DVB-S2 protocol as there are several applications in DVB-S2 such as DSNG lend themselves to a mobile scenario [111]. In general DVB-S2 operates with stationary receivers however the disturbance measured in high density environments, such as urban areas, are similar to those experienced by both mobile and stationary receivers [111]. The LMS channel model effectively describes the propagation of signals between a mobile terrestrial transmitter/receiver and a satellite. The LMS channel has been assigned several bands in the microwave spectrum such as L and S range, models have also been generated in Ku and Ka the traditional satellite bands, in order to reuse existing satellite infrastructure as well as to avoid problems due to the saturation of the L and S band [112].

A signal propagating through the LMS channel experiences three different types of effects based on the propagation of the signal through the different layers of the atmosphere [2], these are ionospheric, tropospheric and regional or local. The ionospheric and tropospheric effects are caused by the disturbances experienced by the signal in the Ionosphere and Troposphere respectively such as geomagnetic storms or lightning [113], the effects of which are generally not

considered in modeling as they are negligible below 25GHz. These do not affect the S, L and Ku bands [114] as they fall beneath 25GHz. Local effects are those caused by buildings or interacting radio waves within the region of the receiver.

The local effects are the main focus of modeling as they play a dynamic role in affecting the received signal [110]. It is important to note that the variation of the environment and elevation angle of the mobile receiver becomes paramount in determining the characteristics of the received signal as it varies the nature of the local effects. In an urban environment for instance there is a greater degree of blockages due to passing objects and buildings than in the rural equivalent, directly affecting the nature of the channel.

The LMS channel received signal can be generally modeled by three components, the line of sight(LOS) component, the diffuse wave or shadowed components comprising the multipath signal and the component due to specular reflection. Shadowing is a form of fading which is caused by obstacles in the path of the receiver and is common in terms of mobile scenarios, especially in high density environments. In terms of the literature the shadowed component is assumed to have the greatest influence [109] [110] [115] [116] upon the received signal and the channel models aim to accurately define the depth and duration of this effect.

The LMS channel is generally represented as a sequence of states, each of which describes a different level of interference or disturbance upon the received signal; which is generally represented by a Markov chain [109] [110] [115] [117] [118]. A Markov chain is a discrete time random process where the system exists in a single state at any given time and switches between states randomly. The changes between the states or transitions are defined to be random but are conditioned by statistical probabilities known as transitional probabilities [119]. The transitional properties  $P$  given in Figure 3.3 represent the probability of transitioning to a particular state, In Figure 3.3 two states are defined the “Good” and “Bad” state, when the system is in the “Good” state there are two possible choices upon transition, the system will either stay in the “Good” state defined by the probability  $P_{GG}$  or switch to the “Bad” state, the probability of which is given by  $P_{GB}$ . The states comprising the Markov chain are used to describe the state of the channel or the state of shadowing in the channel. This creates a method for efficient shifting between the states as would be experienced by a mobile receiver.

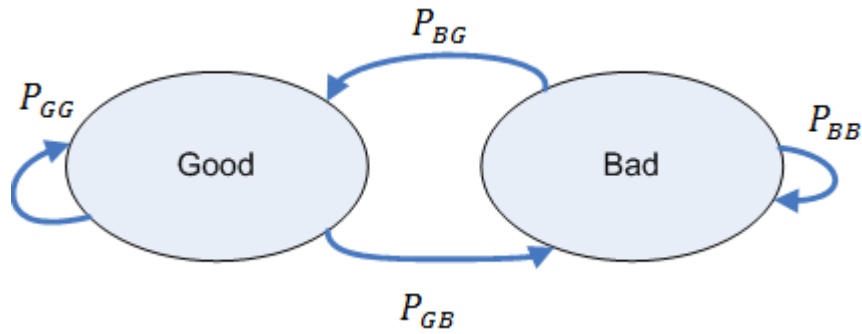


Figure 3.3-Two state Markov chain

In the process of modeling the shadowing in a LMS channel, a statistical distribution such as the Rayleigh, Rice or Suzuki distribution is selected. The statistical distribution is then adjusted, by defining specific parameters of the distribution, in order to obtain the closest fit to the level of shadowing indicated during the measurement campaign. The states forming the Markov chain are each linked to a unique set of parameters, the statistical distribution are functions of these parameters allowing different levels of shadowing to be produced in each state. The basic concept of the LMS channel models have been considered; the next stage analyses the models presented in the literature in order to select one to be implemented in the PL model.

### 3.3.2 Literature survey of LMS channel models

The narrowband LMS channel has been analyzed and modeled in great detail due to the growth of the mobile sector in communications, the results of the modeling will be considered in the following literature review. The modeling of the LMS channel is generally represented in the form of a Markov chain; in the literature these can be divided broadly into either two state or three state models.

The two state Markov channel presented in [120] and depicted in Figure 3.3 above, consists of a “Good” and “Bad” state, where the “Good” state refers to LOS conditions or an interval during which there is high received signal power and the “Bad” state is the converse, state in which shadowing occurs. In [120] the multipath component, effect of reflection, in both the “Good” and “Bad” states is represented in the form of a Rayleigh distribution. In the LOS state or “Good” state, the directly received signal adds a constant amplitude to the output, transforming the Rayleigh distribution into a Rician process  $p_{Rice}$  given by (3.1), where  $c$  represents the ratio between the direct signal and the multipath power,  $I_0$  is the modified Bessel function of order zero and  $S$  is the instantaneous received power.

$$p_{Rice}(S) = ce^{-c(S+1)}I_0(2c\sqrt{S}) \quad (3.1)$$

In the “Bad” state it is assumed that no LOS signal occurs hence the effect is a pure Rayleigh distribution ( $p_{Rayl}$ ) with a mean power  $S_0$  in (3.2).

$$p_{Rayl}(S|S_0) = \frac{1}{S_0} \exp(-S/S_0) \quad (3.2)$$

The nature of  $S_0$  is time varying and is given by log normal distribution in (3.3), where  $\mu$  is the mean power level decrease and  $\sigma^2$  is the variance due to shadowing. The values of which are given in [120] for varying environments and elevation angles. The model is called the Lutz model and provides a fairly accurate method for determining the local effects on the signal.

$$p_{LN}(S_0) = \frac{10}{\sqrt{2\pi\sigma} \ln 10} \cdot \frac{1}{S_0} \exp\left[-\frac{(10 \log S_0 - \mu)^2}{2\sigma^2}\right] \quad (3.3)$$

The computation of the transitional probabilities  $P$  given in Figure 3.2 is another important aspect to consider; in the Lutz model [120]. The Lutz distribution given by  $p_{LN}$  is determined by the duration of existing in a single state, calculated using the receivers transmission rate ( $R$ ) and velocity ( $v$ ), determined during measurement, using (3.4).

$$D_g = \frac{1}{P_{GB}} = \frac{R}{v} D_b(m) \quad (3.4)$$

The duration in bits is given by  $D_g$  and  $D_b$  for the good and bad states respectively and  $m$  is the distance in meters.

The two state model has been further developed in [115] and [116]. In [115] the Lutz model is applied to a measurement campaign undertaken more recently, which considers several more environments and elevation angles. In [116] the concept of the two states is advanced to the point where each state can take on more than one set of parameters in a given environment and elevation angle using a threshold factor to select which parameters to utilize. The level of

shadowing in each state is given by the Loo model, which is a combination of a Rice distribution given in (3.1) and log normal distribution given in (3.3). The Loo model [121] assumes the received signal varies as per the Rician model over shorter shadowing periods and like a log normal distribution over longer periods.

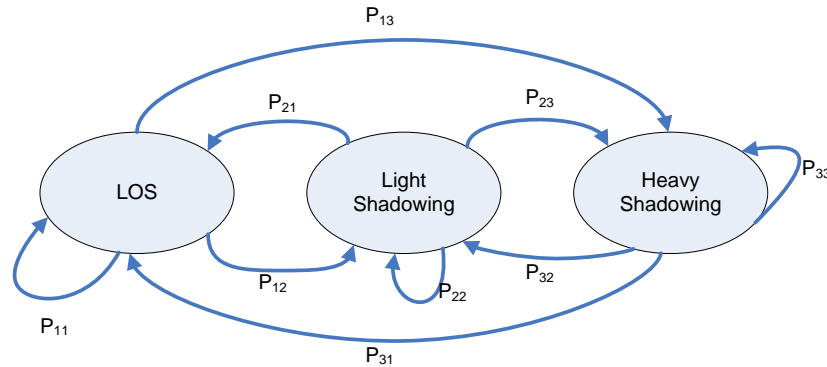


**Figure 3.4-Three state channel model**

The three state Markov model as seen in Figure 3.4 consists of LOS, Light Shadowing and Heavy Shadowing states, the improved number of states allows for a more realistic interpretation of the channel. Presented in [108] and [110] the three state model measures S and L band characteristics respectively, implementing a Loo model in a similar manner as that discussed in [116] above. Similarly in [118] the 3 state approach is undertaken across the L,S and Ka bands, the campaign unlike those previously discussed presents a wideband LMS channel, employing a combination of Loo, Rician, Rayleigh and log normal distributions to provide the level of shadowing in each state.

There have also been variations to the 3 state model given in Figure 3.4, instead of differentiating between the level of shadowing in [109] and [115] a model for the Ku band is presented consisting of LOS, Shadowed and Blocked. In [115] the LOS state is modeled using a Rice distribution see (3.1), while the shadowed state is given by a combination of log normal and Rayleigh distribution (3.2) and (3.3); the Blocked state is described as being approximately -20dB below the LOS and is not modeled. In [109] all three states are characterized by the Rice distribution given in (3.1).

The transition probabilities in the three state model are determined using the equations given in (3.5) and (3.6). The state probability  $P_k$  is given by the ratio of the number of samples in state  $k(N_k)$  given environment  $j$  ( $Env_j$ ) to the total number of samples ( $N_f$ ) taken in environment  $j$ .

$$P_k(Env_j) = \frac{N_k}{N_f} \quad (3.5)$$

$$P_{i,j}(Env_j) = \frac{M_{i,j}}{M_i} \quad (3.6)$$

The transitional probabilities are determined in a similar manner, where  $M_{i,j}$  are the number of transitions experienced between state  $i$  and  $j$  in a given environment and  $M_i$  is the total number of state frames corresponding to state  $i$ , essentially the number of frames transmitted when in that particular state.

It is important to understand that three state models are considered to be more accurate representations of the satellite systems as they allow for a greater degree of flexibility in terms of the level of shadowing produced. In many case the choice between the formation of a two or three state model is based on the application scenario of the model, the level of shadowing may not always be paramount, and on the accuracy and quantity of measurement results obtained. A second aspect to consider when identifying a suitable system for the PL system model is the availability of the complete set of parameters required to generate the shadowing in each state, in several presentations the entire range of measurements are not always available due to implementation issues. The complexity of the method of implementing the channel must also be considered due to hardware implementation restrictions. Considering these factors the channel presented in [109] was selected. The measurement campaign provided a complete set of result and was carried more recently then the other systems discussed. The method for generating the shadowing is also simple to implement, the details of which will be provided as follows.

### 3.3.3 Implementation

The LMS channel model selected [109] was supported by the ESA and the measurements were obtained in the Ku band in South Germany. The implementation details of the channel model will be discussed in terms of incorporation into the physical layer model.

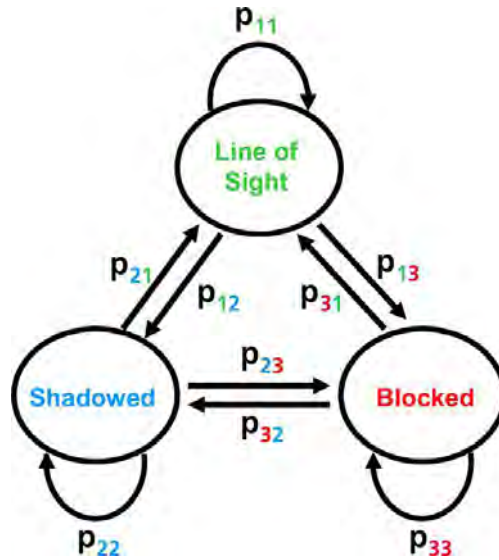


Figure 3.5-Ku band LMS channel model [109]

The channel model is made up of three states LOS, Shadowed and Blocked; each of which is modeled using a Rician distribution given in (3.7).

$$p_R(r) = \frac{r}{\sigma^2} e^{-\frac{r^2+z^2}{2\sigma^2}} I_0\left(\frac{r \cdot z}{\sigma^2}\right) \quad (3.7)$$

The values of the parameters required to generate the Rician random variable  $p_R$  are provided in Table 3.1 below.

Table 3.1 Ka band LMS channel parameters [109]

Environment	State Transition Matrix	S	Rice sigma	Rice z	Rice Factor	Mean
Highway	0.9862 0.0138 0.0000	0.8922	0.0947	0.9892	17dB	0dB
	0.1499 0.8378 0.0123	0.0823	0.3010	0.3510	-1.6dB	-9dB
	0.0008 0.0396 0.9596	0.0255	0.0505	0.0000	0dB	-23dB
Rural	0.9795 0.0204 0.0001	0.7844	0.0916	0.9976	17dB	0dB
	0.1007 0.8277 0.0716	0.1555	0.2464	0.4020	1.2dB	-8dB
	0.0010 0.1813 0.8177	0.0600	0.0993	0.0000	0dB	-17dB
Suburban	0.9796 0.0204 0.0000	0.7831	0.0829	0.9994	18dB	0dB
	0.0929 0.8571 0.0500	0.1715	0.2289	0.4393	2.6dB	-7dB
	0.0015 0.1876 0.8109	0.0454	0.1054	0.0000	0dB	-17dB
Urban	0.9902 0.0098 0.0001	0.6025	0.0926	0.9936	17dB	0dB

	0.0714	0.8756	0.0529	0.0825	0.1900	0.4132	-3.7dB	-7dB
	0.0000	0.0140	0.9860	0.3150	0.0610	0.0000	0dB	-21Db

The measurements were taken in four environments Highway, Rural, Suburban and Urban. The transition probabilities  $P$  (shown as the transitional probabilities in Figure 3.5) are given by the state transition matrix and  $S$  represent the state probabilities. The values of Rice sigma ( $\sigma$ ) and Rice  $z$  ( $z$ ) are used in order to generate the value  $p_R$  which is the value of the shadowing in the form of a probability.

In terms of replicating the channel described in [109], all of the parameters have been provided, the channel can transition effectively between states as well as generate differing levels of fading in each state according to (3.7). The channel will transition only between the states and is assumed to exist in a single environment, for the purpose of the implementation the environment considered is the Highway, the top row of Table 3.1 is utilized.

It is important to consider how the shadowing will affect the PL system; the input into the channel model is in the form of bits of length  $n_{ldpc}$ , the values of which are  $\pm 1$ . The channel model then proceeds to generate a value  $p_R$ , which is considered as a form of fading. The equation of the implementation is given in (3.8) where  $r$  is the output of the channel model.

The fading component is multiplied with both the link budget constant  $k_{lb}$  and the input bit value given by  $d$ , which is  $\pm 1$ . The link budget constant will be defined in the following section, the result of the multiplication is then added to  $n$  which is the noise generated assuming an AWGN channel.

$$r = p_R k_{lb} d + n \quad (3.8)$$

The details required for the implementation of the channel model have been given; the system replicates the LMS channel by implementing a form of shadowing based on a Rician distribution, resulting in the output given in (3.8). The following section discusses the power costs associated with transmission in a satellite channel by analyzing the link budget.

### 3.3.4 Link budget



The link budget is an important part of satellite communications; a large amount of power is required when transmitting in a satellite channel, due mainly to the large distances over which communication takes place as well as the effects of shadowing.

In order to calculate an accurate analog in a LMS channel these losses must be taken into account, in (3.8) the constant  $k_{lb}$  was defined, which acts as a scalar constant in terms of the received bit energy. The aim of the section is to calculate the value of  $k_{lb}$  given the link budget values provided in Table 3.2.

$$P_r = P_T G_T G_R L_A \quad (3.9)$$

In order to calculate  $k_{lb}$ , it is important to understand equation (3.9) which defines the received signal power ( $P_r$ ) in terms of the transmitter power ( $P_T$ ), the gain at the transmitter  $G_T$ , the gain at the receiver  $G_R$  and  $L_A$  in (3.10) which is a summation of losses such as those due to shadowing ( $L_o$ ) and free space loss ( $L_s$ ).

$$L_A = L_s + L_o \text{ (dB)} \quad (3.10)$$

$$P_r = k_{lb} \frac{P_T G_R G_T}{L_A} \quad (3.11)$$

The value of the link budget  $k_{lb}$  can be calculated by reordering (3.9) to form the equation given in (3.11). The values of the parameters are given in Table 3.2 below, the resultant being -137.8dB which is within the range of the received antenna gain. The value of  $k_{lb}$  is very small as was expected due to the heavy free space loss in satellite systems. In terms of the implementation  $k_{lb}$  acts as a constant scaling factor, this shifts the performance curves by 137.8dB. In the presentation of the simulation results the value of  $k_{lb}$  will not be taken into account, simply to allow for easier relative comparison of results in the AWGN and satellite channels relative to each other

**Table 3.2-Link budget values [109]**

Satellite EIRP (dBW)	50
Free Space Loss (dB)	205.3

Additional Loss(dB)	1.5
Receiver Antenna Gain(dBi)	19
Received Power at LNB Input (dBW)	-137.8
Receiver Antenna Noise Temp. (K)	80
LNB Noise Figure (dB)	0.9
C/N <sub>0</sub> at LNB Output (dBHz)	69.13
Noise Equivalent Bandwidth (kHz)	5
Carrier to Noise Ratio CNR (dB)	32.14

The three state LMS channel model selected above is important in providing a better analog for predicting the effects of traversing a satellite channel. Several types of models have been investigated however the accuracy and detail given in [109] matched the requirements for implementation in the PL system. The channel model will provide a more accurate representation than that of the AWGN channel however for ease of relative analysis will only take into account shadowing losses and not those due to free space loss.

### 3.4 Receiver model

The aim of this section is to present the implementation of the receiver system in the PL model, focusing on the process of integration. In previous sections of this chapter the transmission and channel models have been discussed, the final component to be integrated is the receiver model. In Chapter 2 of the dissertation a literature survey was carried out in order to select a decoding structure suitable for use in the DVB-S2 physical model. The decoder must be capable of decoding the FEC codeword defined in the DVB-S2 protocol, taking this into account the outcome of the survey was the selection of the concatenated iterative BP-Chase decoder produced in [13]. The decoder implements a concatenated decoding structure switching between BP and Chase decoder to correctly decode the FEC codeword. The BP-Chase decoder has shown to provide improved error correcting performance over its constituent decoders. The input into the receiver system is in the form of a vector of energy values of length  $n_{ldpc}$ , the output of the system is the corrected binary FEC codeword.

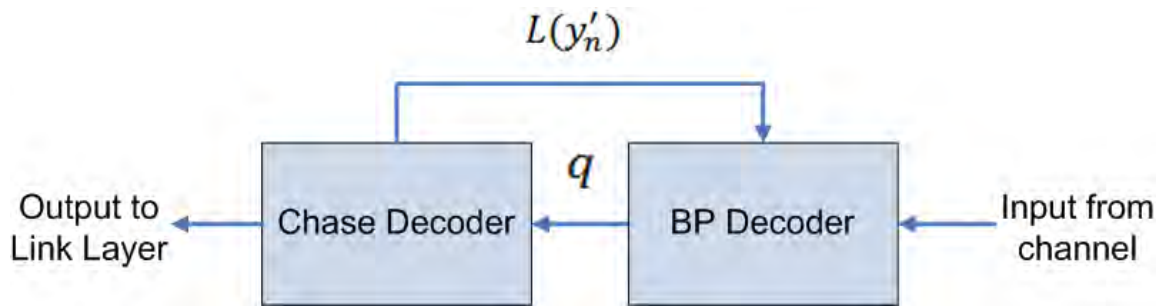


Figure 3.6-Receiver model

The distinct difference between the iterative concatenated BP-Chase decoder, to be referred to as the BP-Chase decoder for the remainder of the dissertation, and the individual component decoders is the transfer of soft information between the BP and Chase decoders, represented by  $q$  and  $L(y'_n)$  given Figure 3.6. The passing of the soft information increases the complexity of the decoding however it improves the decoding performance as the process of decoding conditions the soft information improving the ability of the individual components to successfully decode the codeword. A single iteration of the BP-Chase decoder, implements the iterative BP decoder after which a single pass of the Chase decoder occurs.

In order to clearly detail the implementation of the BP-Chase decoder, the BP and Chase decoding components will be discussed individually in Section 3.4.1 and 3.4.2 respectively. The concatenation and soft information transfer will then be discussed in Section 3.4.3.

### 3.4.1 Belief propagation

Belief propagation is the message passing decoding technique originally described by Gallager in his thesis [26] in 1969 will be discussed together with several variants in Chapter 2. The algorithm is an iterative decoding scheme and involves the passing of messages or “beliefs” between the variable and check nodes in the Tanner graph, see Figure 2.10, which is used to graphically represent a LDPC code. The BP algorithm [26] [45] [122] [123] [124] [125] will be presented as follows.

There are two basic variations of the algorithm, the probability domain and the log domain algorithms. The difference being the log domain decoder utilizes the ratio of the probabilities implemented in the probability domain technique. The motive for implementing log likelihood ratios (LLR) instead of operating with the probabilities is the reduced complexity, the probability domain algorithm requires multiplications which are more complex than the associated additions in the log domain. The log domain decoder is the algorithm which will be implemented.

The BP decoder as previously mentioned operates iteratively with messages, in the form of LLRs, passed between the connected bit and check nodes and vice versa in a single iteration. In order to fully describe the BP algorithm the following definitions are required, the LDPC code has a parity check matrix  $H_{mn}$ , where  $n$  is the number of columns in  $H$ , which is equivalent to the number of bit nodes and code length; while  $m$  is the number of rows of  $H$  and equivalent to the number of check nodes. The set  $N(m)$  are the bits which participate in check  $m$  and  $M(n)$  are the checks which bit  $n$  participates in. A very important definition in the algorithm is the set given by  $\frac{N(m)}{n}$  and  $\frac{M(n)}{m}$  which is the set of  $N(m)$  and  $M(n)$  excluding bit  $n$  and  $m$  respectively.

The transmitted signal is a binary codeword modulated using BPSK before transmission across the channel. The channel is in the form of the LMS channel model presented in Section 3.3 with zero mean, variance given by  $\frac{N_0}{2}$  where  $N_0$  is the noise power and the shadowing factor  $p_R$ . The result of the transmission of the signal through the noisy channel is the input into the decoder  $y_n$ . A second consideration must be of the parameter  $I_{max}$  which represents the maximum amount of iterations the BP decoder can complete before the decoder halts. The value of  $I_{max}$  determines the level of error correcting performance, a greater number of iterations improves the conditioning of the passed messages, improving the error correcting capability however at the cost of increased complexity.

The BP algorithm will be described in several stages the Initialization, Check Node Update, Bit Node Update and Decision phase.

### **Parameters**

- $F_n$  - LLR of bit  $n$  which is derived from the input into the decoder,  $y_n$ .
- $L_{mn}$  - LLR of bit  $n$  which is transmitted from check node  $m$  to bit node  $n$ , the value of which is derived from  $z_{mn}$ .
- $z_{mn}$  - LLR of bit  $n$  which is transmitted from bit node  $m$  to check node  $n$ , the value of which is derived from  $L_{mn}$ .
- $z_n$  - *a posteriori* LLR of bit  $n$  derived from the *a priori* information  $F_n$  and  $L_{mn}$ .

### **BP Algorithm** [13],[45],[103]

#### Initialization:

Set  $F_n = (\frac{4}{N_0})y_n$  and  $z_{mn} = F_n$  for all  $m$  and  $n$ .

### Iterative Processing:

Iterate while  $i_t \leq I_{max}$ , where  $i_t$  the current number of iterations is less than the given maximum number of iterations. The  $L_{mn}$  message is sent between a bit node and check node along an edge, while  $z_{mn}$  is sent from the check node to the bit node.

#### 1) Check Node Update

For all check nodes  $m$  connected to bit nodes  $n$  calculate the update message  $L_{mn}$  using (3.12) and (3.13).

$$T_{mn} = \prod_{n' \in \frac{N(m)}{n}} \frac{1 - \exp(z_{mn'})}{1 + \exp(z_{mn'})} \quad (3.12)$$

$$L_{mn} = \ln \frac{1 - T_{mn}}{1 + T_{mn}} \quad (3.13)$$

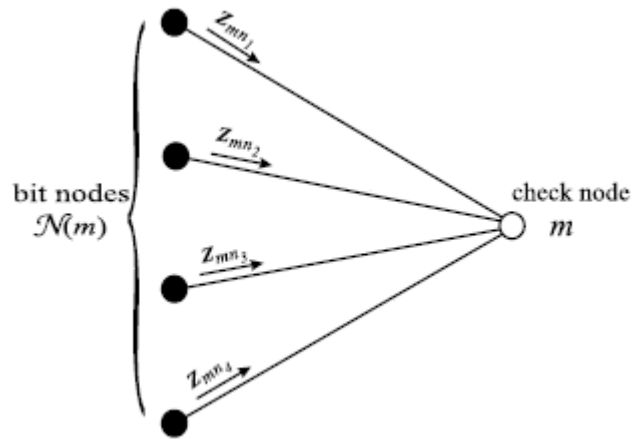


Figure 3.7-Process of updating the check nodes [122]

The calculated value of  $L_{mn}$  signifies the value of the messages or beliefs received from the edges connected to the given bit nodes as seen in Figure 3.7.

#### 2) Bit Node Update

For all bit nodes  $n$  connected to check nodes  $n$  calculate the update message  $z_{mn}$ .

$$z_{mn} = F_n + \sum_{m' \in \frac{M(n)}{m}} L_{m'n} \quad (3.14)$$

For all  $n$  update  $z_n$ .

$$z_n = F_n + \sum_{m \in \frac{M(n)}{m}} L_{mn} \quad (3.15)$$

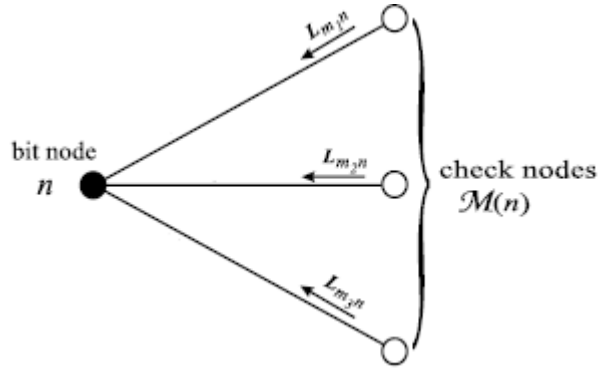


Figure 3.8-Process of update in bit nodes [122]

The message  $z_{mn}$  is defined by the messages or beliefs received from the edges connected to the check nodes seen in Figure 3.8.

### 3) Decision Phase

Form the vector  $\hat{c}_n$  such that  $\hat{c}_n = 0$  if  $z_n < 0$  and  $\hat{c}_n = 1$  if  $z_n > 0$ .

If the formed codeword  $\hat{c}$  is a valid codeword,  $H\hat{c} = 0$ , the algorithm terminates and the output of the decoder is  $\hat{c}$ . If  $\hat{c}$  is not a valid codeword then the algorithm iterates while  $i_t \leq I_{max}$ , return to the Check Node update phase.

The BP decoder receives as input from the channel  $y_n$  and through the iterative process described above either fails or provides a valid codeword given by  $\hat{c}_n$ . The next section considered is the Chase decoder which forms the second component of the BP-Chase decoder.

### 3.4.2 Chase decoder

The Chase decoder as was previously mentioned in Chapter 2 is a soft decision block decoder which utilizes reliability information to improve decoding performance. The Chase decoder forms the second component of the BP-Chase decoder and the algorithm will be presented in the following section.

The Chase algorithms were originally presented by Chase in 1972, in [85] Chase presented three algorithms which can be used in conjunction with an algebraic decoder to provide improved decoding performance, when compared to sole algebraic decoding. The implementation of the Chase algorithms' provide maximum likelihood decoding performance in AWGN and Rayleigh channels at high SNR's [126]. The process of Chase decoding consists essentially of three stages, the definition of a most likely (ML) sequence of bits based on input from the channel, the formation of a set of test patterns using one of the three Chase algorithms; which are added to the ML sequence to form a set of candidate codewords, the third step sends the candidate codewords to an algebraic decoder and a selection process is applied to select the codeword which will be the output of the decoder.

- 1) Define the ML sequence.
- 2) Generate and add the test patterns to the ML sequence
- 3) Decode candidate codewords and select the output codeword.

As has been previously mentioned Chase presented three algorithms or methods for generating a set of test patterns to be utilized in the second stage of the decoding process. The algorithms vary in terms of the complexity, where the most complex Chase 1 generates the largest amount of test patterns (TP). The algorithms are based on the channel measurement decoding technique, which operates on the principle of Hamming distance  $d_h$ , is a property of a linear block codes. The Chase algorithm forms a sphere of potential codewords in  $GF(2)$  where the radius of the sphere is given in terms of  $d_h$ , dependent on the Chase algorithm used. The Chase algorithm also requires reliability information from the channel given by a vector  $\alpha_i$  which is of codeword length.

The channel measurement technique is depicted in Figure 3.9 where  $X_A$  and  $X_B$  represent possible codewords and  $Y$  is the binary representation of the reliability information  $\alpha_i$ . The codewords  $X_A$ ,  $X_B$  and  $Y$  are surrounded by a sphere of radius  $\left\lfloor \frac{d_h-1}{2} \right\rfloor$ , which is a function of the hamming distance. The technique takes advantage of the algebraic decoder which provides a unique error pattern when the codeword spheres overlap. In the case of Figure 3.9 the  $X_A$  and  $Y$  codeword spheres overlap, given the single case of overlap  $X_A$  is selected as the output codeword. The approach aims to develop a set of error patterns and select the codeword based on

the concept of analog weight. This is implemented by effectively changing the radius of the sphere of  $Y$ , varying the amount of TPs generated.

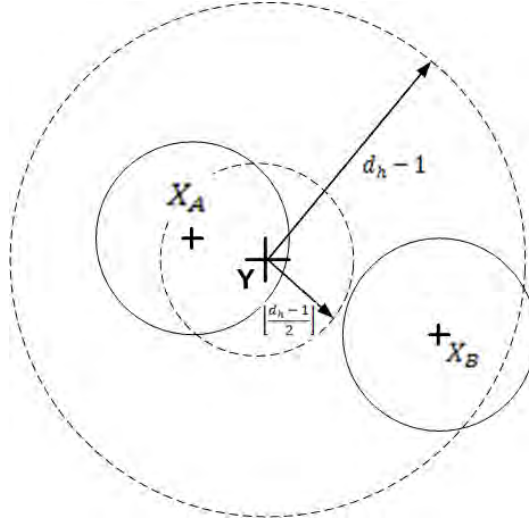


**Figure 3.9-Depiction of channel measurement decoding technique**

The Chase 1 algorithm generates test patterns such that all codewords within a hamming distance of  $d_h - 1$  or less of  $Y$ . Let the set of test patterns generated by the Chase 1 algorithm be given by  $S_T$  for a given  $Y$  it is possible to generate a TP such that  $d_H(X, Y \oplus T) \leq (d_h - 1)$  if  $d_H(X, Y) \leq (d_h - 1)$  where  $X$  is added to the potential candidate codewords. The actual implementation of the Chase algorithm is dependent on the value of  $d_h$ , based on whether it is even or odd. The set of test patterns  $S_T$  is defined as the set of all binary vectors of length  $n$  and hamming distance given by (3.16).

$$d_h = t + (i - 1)(2t + 1) \quad i \in [1, M] \quad (3.16)$$

If  $d_h$  is even the value of  $M$  is given by  $\left\lceil \frac{d_h}{(2t+1)} \right\rceil$  else  $\left\lceil \frac{(d_h-1)}{(2t+1)} \right\rceil$ . The Chase 1 algorithm as has been previously discussed is the most complex form presented by Chase as it considers a greater sphere of possible codewords. The Chase 2 and 3 algorithms are simplifications of Chase 1 developed in an effort to compromise between decoding performance and complexity.

The Chase 2 algorithm [85] defines the set  $S_T$  as all the binary vectors of length  $n$  which contain no particular number of binary '1's in  $p$  least reliable bit(LRB) positions and the remainder of the elements are binary '0's. The LRB positions are obtained by selecting the  $p$  lowest values in the



input vector  $\alpha_i$ . The determination of the value of  $p$  is given in (3.17), the value of which determines the complexity of the algorithm, the amount of TPs generated is  $2^p$ .

$$p = \begin{cases} n - t & \text{if } 0 \leq t \leq \left(\frac{d_h}{4}\right) - 1 \\ \left\lfloor \frac{(d_h - 1)}{2} \right\rfloor & \text{if } d_h \text{ is odd and } t = \left\lfloor \frac{(d_h - 1)}{2} \right\rfloor \\ \min \left\{ (n - t), \left\lfloor \frac{(t + 1)d_h}{4(t + 1) - d_h} \right\rfloor \right\} & \text{otherwise} \end{cases} \quad (3.17)$$

The Chase 3 algorithm is the least complex of those presented in [85], the algorithm takes the same approach given by Chase 2. The difference being that the Chase 3 algorithm has  $p$  binary “1”s in the  $p$  least reliable positions. If  $d_h$  is even the value of  $p$  is given by  $p = 1, 3, \dots, (d - 1)$  else if  $d_h$  is even  $i = 0, 2, 4, \dots, (d - 1)$ . The significance of the Chase 3 algorithm requires the generation of  $\left\lfloor \frac{d_h}{2} + 1 \right\rfloor$  TPs, the growth in terms of complexity of the algorithm is linear with increase in  $d_h$ .

The description of the Chase algorithms given above describes the generation of TPs which forms the second stage of the Chase decoder. All three stages of the decoding process will be given as follows.

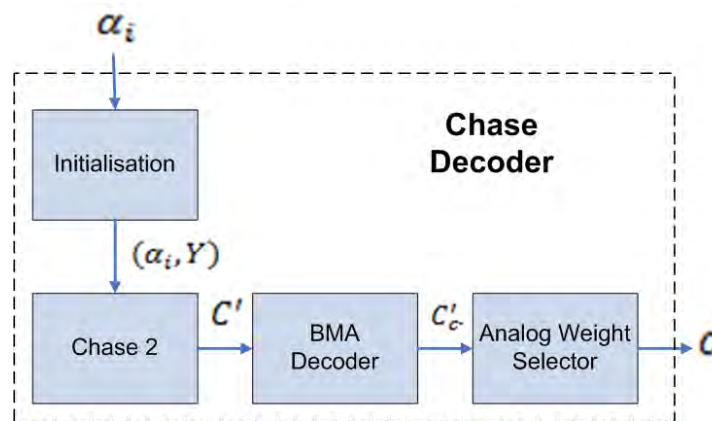


Figure 3.10-Chase decoder structure

**Chase Decoder** [18] [85] [126]

The Chase Decoder algorithm to be implemented as seen in Figure 3.10 consists of four functional blocks pertaining to the different stages of decoding, where the BMA decoder and Analog weight selector make up stage 3 of the decoding process.

In the process of defining the Chase decoder algorithm several assumptions are required. The input into the Chase decoder is the resultant of a binary BCH codeword modulated using BPSK and transmitted over an AWGN channel. The resultant signal is represented by  $\alpha_i$  of codeword length  $n$  is known as reliability. The Chase decoding algorithm has been developed for iterative processing [127] however given the description of the BP-Chase decoder in [13], only a single pass algorithm is implemented. The Chase decoder algorithm presented below will thus not take into account the iterative component. The BP-Chase decoder utilizes the Chase 2 algorithm in the stage of generating TPs and thus the value of  $p$  is based on (3.17). In the same manner in which  $I_{max}$  determines the performance and complexity in BP; the value of  $p$  is to Chase decoder by increasing the value of  $p$  the potential codeword space is increased, effectively checking a larger number of alternatives at the cost of greater complexity.

### Initialization

Form the ML sequence  $Y$ , where  $Y = \left( \frac{(1 - \text{sgn}(\alpha_i))}{2} \right) \quad \forall i \in [1, n]$ .

The first step involves choosing the most likely sequence of bits which make up the codeword based on the channel conditions. The channel measurement information can be defined by  $\alpha_i$ ; a hard decision is taken based on  $\alpha_i$ , in order to produce the most likely sequence of bits given by  $Y$ .

### Chase 2

- 1) Form the reliability information vector  $L_i$  from  $\alpha_i$ , where  $L_i = \{|\alpha_i|\}$ .
- 2) Determine the set of indices of the LRBs, the LRBs are the  $p$  minimum values of  $L_i$ .
- 3) Construct the  $2^p$  TPs using the Chase 2 algorithm, where  $T$  represents the set of  $p$ -dimensional vectors, consisting of all combination of  $p$  variables in  $GF(2)$ .
- 4) Construct the set of candidate codewords  $C'$  where the set consists of  $2^p$  elements, where  $C'_{(j)}(k) = Y_{(j)} \oplus t_j(k) \quad \forall j \in [1, p], \forall k \in [1, 2^p]$ .

The Chase 2 module is responsible for the construction of the set of candidate codewords by adding each TP of set  $T$ , represented individually by  $t_j$  to the ML codeword  $Y$ . The binary addition adds only the  $p$  bits which make up the minimum values of  $L_i$ .

#### BMA Decoder

- 1) Syndrome Calculator
- 2) Key Equation Solver
- 3) Chien Search

The algebraic decoder selected for implementation was the BMA discussed in Section 2.5.2, the algorithms of which will not be presented to maintain clarity in the definition of the Chase decoder. The generalized BCH decoding structure consists of three basic steps given above and where the BMA is used to solve for the error locator polynomial in step 2. The algebraic decoder operates on the set of candidate codewords  $C'$ , firstly verifying if the codewords contained in the candidate codeword set are valid, if so the algebraic decoder proceeds to correct detected errors. The output of the decoder is the set of valid error corrected codewords given by  $C'_c$ .

#### Analog Weight Selector

- 1) Calculate the set of analog weights  $m$  from the input  $C'_c$  which is the set of valid corrected codewords. Where  $m(k) = -\sum_{j=1}^n (Y_{(j)} \oplus c_j(k)) L_j$ .
- 2) Select the output codeword  $C$ , if  $(k) = \max_{j \in [1, 2^p]} \{m(j)\}$  then  $C = c(k)$ .

The analog weight selector determines the closest match to the ML codeword while taking into account the measure of reliability given to the designated bit. The analog weight is effectively a scheme which measures the distances between the spheres pictured in Figure 3.9 above, factoring in the channel reliability. In step 2 the codeword with the minimum analog weight is selected as the output of the decoder, given by  $C$ .

The Chase Decoding algorithm has thus been defined; the BP-Chase decoder will be presented as follow, highlighting the sharing of soft information between the constituent decoders.

### **3.4.3 BP-Chase decoder**

In the previous sections the BP and Chase decoders have been defined building towards the BP-Chase decoder. The concatenated iterative BP-Chase decoder presented in [13] by Shi et al; the

decoder improves upon the performance of the constituent decoders by sharing soft information. It passes the conditioned soft information, improving the input into the constituent decoders. The following section will focus on the generation and transfer of soft information between the BP and Chase decoders as well as the utilization within the decoders; the process of switching between the decoders is also considered.

The BP-Chase algorithm consists of three steps and operates upon the assumptions made in the previous decoder. The structure of the decoder is given in Figure 3.6; the input into the decoder is the resultant of a FEC codeword modulated using BPSK and transmitted over an AWGN channel given in  $y_n$ . The notation employed in the definition of the constituent decoders will be used to define the BP-Chase decoder algorithm below.

**Iterative Algorithm** [13]

- 1) The LDPC decoder receives the input from the channel in the form of a vector of codeword length given by  $y_n$  and performs BP decoding, the algorithm works iteratively until either  $H\hat{c}_n = 0$  making  $\hat{c}_n$  a valid codeword or the maximum number of iterations given by  $I_{max}$  is reached. If a valid codeword is obtained the iterative concatenated algorithm terminates and the output of BP-Chase decoder is  $\hat{c}_n$ . If the maximum number of iterations is reached the algorithm proceeds to step 2. The last act of the BP decoder is to transfer the soft information which will be used by the Chase Decoder in the form of the *a posteriori* LLR  $z_n$
  
- 2) The BCH decoder runs the Chase algorithm for a single iteration using the transferred soft information  $z_n$  from the LDPC decoder to replace the channel information  $\alpha_i$ , altering the equations in the Initialization and Chase 2 phases of the Chase Decoder Algorithm in Section 3.4.2. Decoding then commences with the normal process. Once a codeword  $C$  has been selected the algorithm either terminates if the analog weight  $m$  of  $C$  is equal to zero. If  $m$  is not equal to zero the algorithm proceeds to step 3. The BCH decoder forms the soft information to be transferred to the BP module. The soft information is derived using the formula given by equation (3.18).

$$L(y'_j) = \frac{2}{\sigma^2} \times \left[ \max_{c(k) \in C'_c, y'_j=0} \{m(i)\} - \max_{c(k) \in C'_c, y'_j=1} \{m(i)\} \right] \quad (3.18)$$

The soft information transferred to the LDPC decoder  $L(y'_j)$  is based on the analog weights assigned to the codewords in the corrected candidate codeword set  $C'_c$  where  $c$  is the index of

the bit in the set of codewords  $C'$ . The soft information for each bit  $y'_j$  is based on the variance of the channel given by  $\sigma^2$  as well as the difference between the maximum analog weight given by the set of codewords in  $C'_c$  with  $y'_j = 0$  ( $\max_{c(k) \in C'_c, y'_j=0} \{m(i)\}$ ) and set of codewords in  $C'_c$  with  $y'_j = 1$  ( $\max_{c(k) \in C'_c, y'_j=1} \{m(i)\}$ ), if either of the sets are empty, default soft outputs are employed.

- 3) If  $i_c$ , the number of concatenated iterations, the number of times that switching occurs from the BP to Chase decoder, is less than  $I_{cMax}$ , the maximum number of concatenated iterations allowed, then proceed with BP decoding. The BP decoder uses the received soft information from the Chase decoder to replace the value of  $F_n$  (determined from the received channel) in equations (3.15) and (3.16) given in Section 3.4.1. If  $Hy_n = 0$  then the codeword is considered valid and the algorithm terminates, otherwise go back to step 2. If  $i_c$  is greater than or equal to  $I_{cMax}$ , halt the decoding process.

An important metric to highlight is the value of  $I_{cMax}$  which determines how many iterations the BP-Chase decoder implements. In the same manner which  $p$  and  $I_{max}$  are important in determining error correcting performance in the Chase and BP decoders respectively. The value of  $I_{cMax}$  is a compromise between the level of performance due to improved conditioning and level of complexity.

The algorithm presented above describes the BP-Chase decoder which forms the reception system in the PL system model. The preceding sections have defined the constituent decoders as well as providing the concatenated decoding implementation information. The reception system receives a FEC codeword which has propagated over the channel as input and after a degree of processing produces a binary FEC codeword as output. The definition of the reception system completes the construction of the PL model, from which performance results can be obtained, which will be presented as follows.

### 3.5 Simulation results

This section aims to present and discuss results generated by the PL model implementation, constructed throughout the course of the chapter. The results presented are in the form of error performance curves in both the AWGN and a LMS channel. The LMS channel was selected and implemented in order to provide a more realistic representation of the disturbances experienced by a signal propagating through a satellite system. The result of which are more accurate

measures of performance for the receiver system. This forms one of the original contributions of the dissertation. The performance results generated in both channels will be compared and discussed as follows.

In order to generate simulation results for the PL system model, depicted in Figure 3.1, the algorithms detailed in the preceding sections were implemented in software, using the C++ programming language. There is an issue which is important to note in terms of high level software implementations. They provide a great degree of flexibility in terms of allowing modification to the implementation. They however require a greater amount of processing power as they utilize high level instructions. The available processing power for experimentation is fixed, so the complexity of the implementation is bounded.

There are several factors which contribute to the complexity; the DVB-S2 defines very large block lengths which require a greater number of computations to decode. The DVB-S2 FEC provides powerful decoding performance thus for comprehensive analysis of the decoder it must be simulated to low bit error rates, which require a larger amount of simulated transmissions. The final issue is the decoding structure, which is iterative in nature and requires a great deal of computation. In order to compensate for this issue the codes used to generate results will be of medium length and the lower end of the DVB-S2 defined length. It has been previously discussed that as the LDPC code increases in terms of block length so does the performance; what we aim to gauge from testing medium length codes is to identify trends which can be applied to longer length codes. The medium length codes provide lower performance however the aim of the chapter is to produce results as well as provide comparative analysis, rather than simulate longer block codes; it was preferred to provide more comprehensive performance results.

Prior to generating the PL system results in a satellite channel, the PL system requires validation in the AWGN channel. The error performance metric which will be used in analyzing the results is bit error rate (BER), a ratio of the number of received bits in error versus the total number of bits transmitted. This will be measured against SNR ( $\frac{E_b}{N_0}$ ), the depiction of which are the performance curves.

The results generated using the PL system model are validated using the performance curves presented in Figure 3.11. In this case an LDPC (3, 6) code of length (1416, 1134) is concatenated with a BCH (63, 51) code, the result of which is a 0.648 code rate. The BP-Chase decoder was initialized with the value of  $p$  set to 3 for the Chase inner decoder, the BP inner decoder initialized  $I_{max}$  to 10 and the overall  $I_{CMax}$  of the BP-Chase decoder is set to 5. The result of

which is given in Figure 3.11, importantly the performance curves match the results produced in [13], showing little variation from that given in the literature.

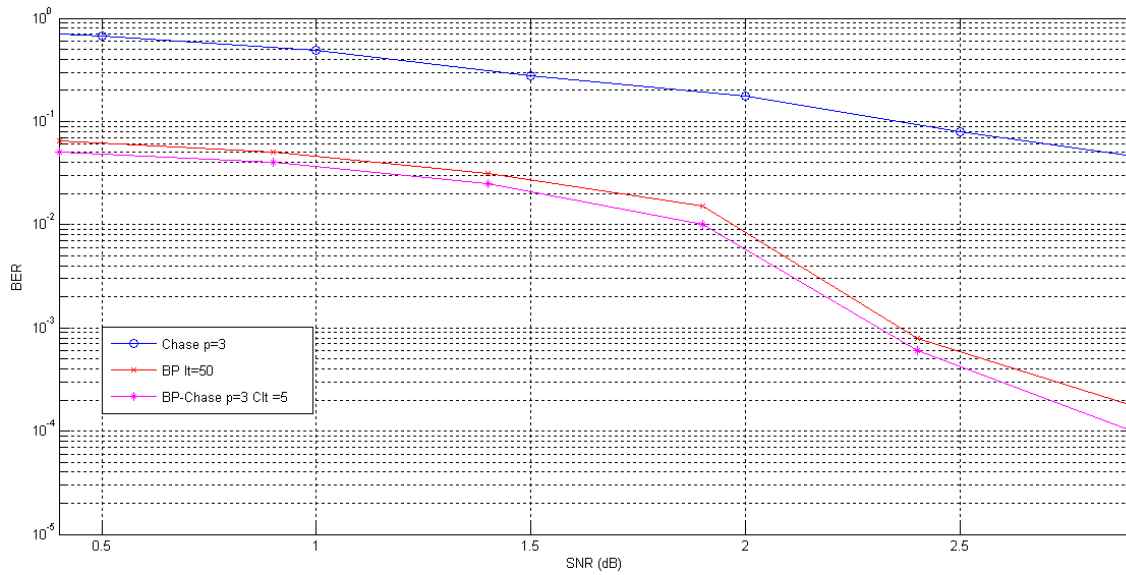


**Figure 3.11- BER performance of PL decoding system over AWGN channel**

The second important result given in Figure 3.11 are the presentation of the BP and Chase decoder simulation for similar codes to that utilized by the BP-Chase decoder. The BP decoder uses a (3, 6) code of length (1412, 916) with the  $I_{max}$  equal to 50, the Chase decoder uses a (63, 51) BCH codeword with  $p$  set to 2. The significance of these results is that they validate the selection of the BP-Chase decoder system. In Chapter 2 the motivation for the selection was provision of improved performance over its constituent decoders. The results produced show a noted improvement over the BP and Chase decoder at low SNR while maintaining an improved level of performance as the SNR increases beyond 2dB. The difference in performance can be attributed to the transfer of soft information between the constituent decoders and is quantified to a coding gain of 0.13dB at a BER of  $10^{-3}$  over BP.

The benefit of which is further exhibited in Figure 3.12 which provides the BER performance of the BP-Chase decoder together with its constituents for half rate codes. In Figure 3.12 a BCH(15,7) code is concatenated with a (3,6) LDPC code of length (540,270), where the inner Chase decoder has  $p$  set to 2, the inner BP decoder has  $I_{max}$  equal to 10 and the concatenated system has  $I_{cMax}$  set to 5. The constituent decoders operate on the identical BCH and LDPC codes respectively, the parameters of which are  $p$  equals 2 and  $I_{max}$  equal to 50. Figure 3.12 allows for a direct comparison of the performance of concatenated and constituent decoders as they all operate on the identical code, with identical decoding parameters. The BP-Chase decoder similarly shows improved performance over the independent BP and Chase decoders. At a BER

of  $10^{-3}$  the BP-Chase decoder provides coding gain of 0.2dB over BP and a visibly improved performance over the Chase system.

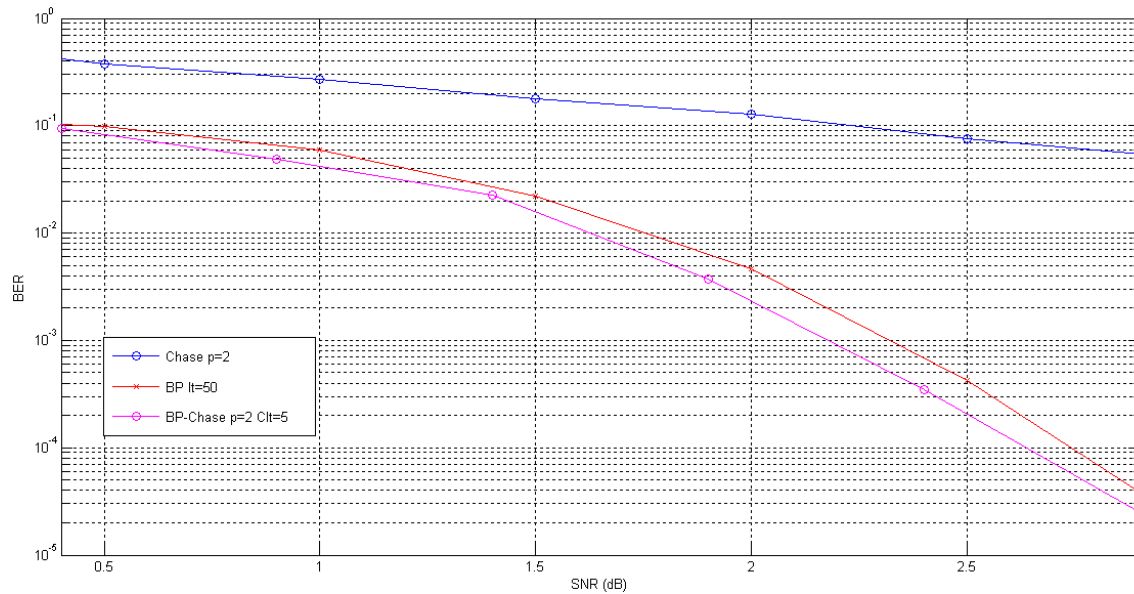


**Figure 3.12-BER performance of half rate codes in PL decoding system over AWGN**

Another important conclusion which can be confirmed is the assumption made previously that the BP decoder performance is the core provider of error correcting performance in DVB-S2. The BP decoder is shown to vastly outperform the Chase decoder in both Figure 3.11 and 3.12.

The results depicted above allow for the validation of the simulated output of the constructed system model, as it is shown to match results given in the literature. They also confirm the selection for the receiver system, as the BP-Chase decoder is shown to provide improved decoding performance at two different code rates and lengths.

The satellite channel to be implemented is the Ku band LMS model produced in [109] described in Section 3.3. The assumptions made in the implementation are that the Highway environment is selected. The reason for which is twofold, the Highway environment describes the best case performance of the LMS channel in terms of level of shadowing. The environment is low density hence there is a smaller number of blockages. DVB-S2 although present in high density environments are generally stationary and positioned in order to reduce the number of blockages. They experience a much lower level of shadowing than mobile terminals.



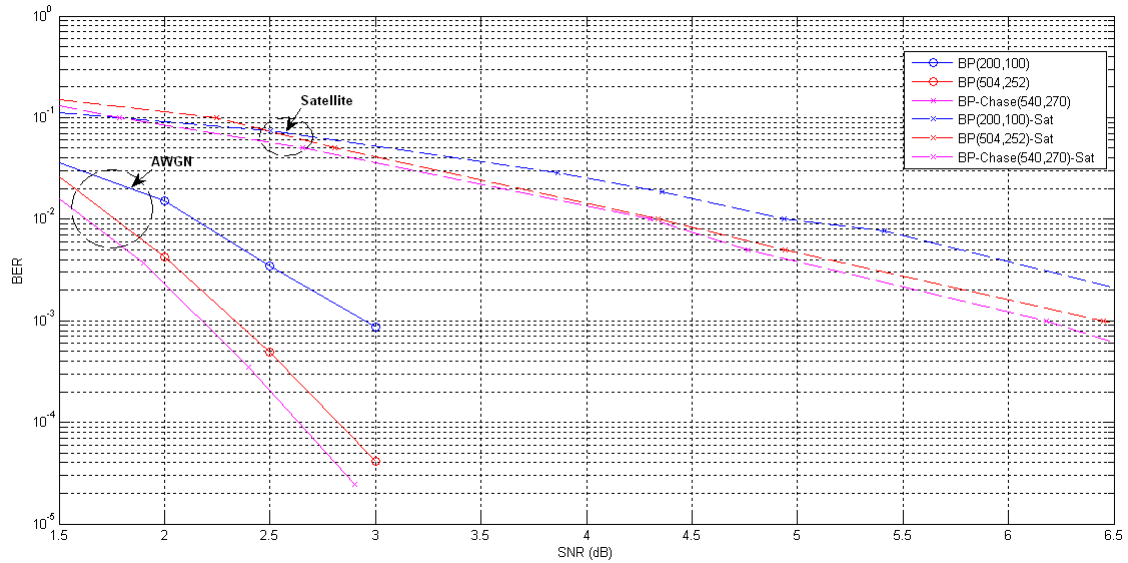


**Figure 3.13-PL system BER results over AWGN and satellite channel**

Figure 3.13 and 3.14 depict performance results in both AWGN and the satellite channel for BP and the BP-Chase decoder. In Figure 3.13 three different medium length codes are presented, BP decoding results are presented for LDPC codes of length (200,100) and (504,252) with  $I_{max}$  set to 50. BP-Chase decoder results are also given for the (540,270) length concatenated scheme described in Figure 3.12. The difference between the results produced is notable. A trend which can be observed is that the satellite channel shifts the performance of the decoders, across all decoders and code lengths. This can be attributed to the effect of shadowing on the transmission and can be quantified at a BER of  $10^{-3}$  producing a reduction in coding performance of 3.9dB for the BP-Chase decoder; similar declines in performance are experienced by the BP decoders.

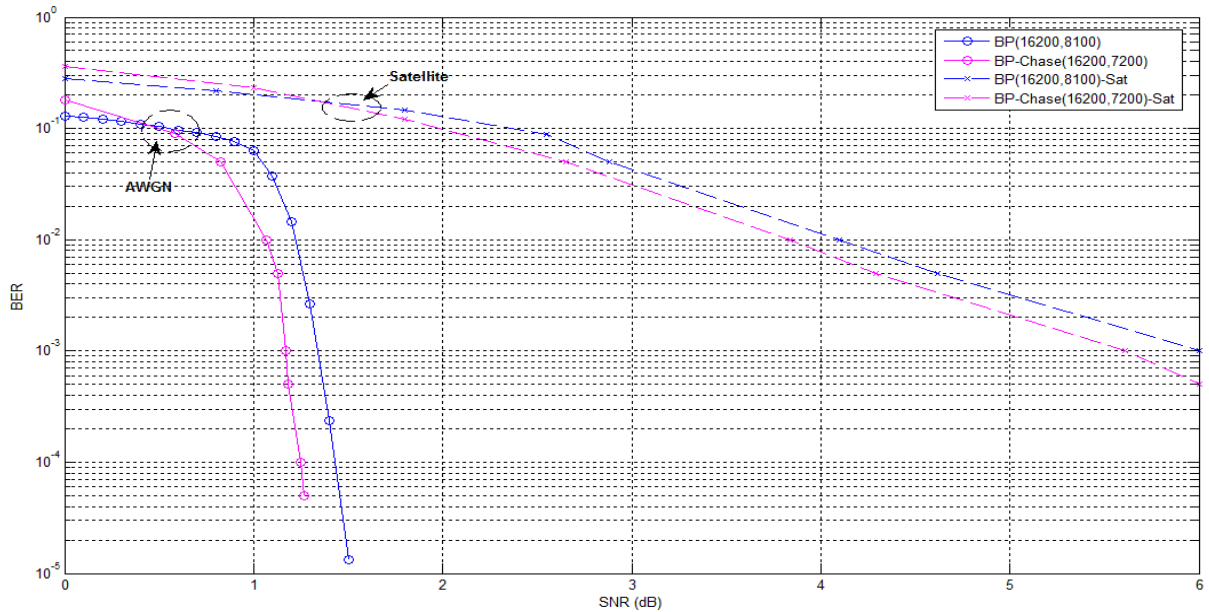


Figure 3.14-PL system BER results for large code lengths over AWGN and satellite channel

The loss due to shadowing is further reiterated in Figure 3.14 which depicts the performance of a DVB-S2 short length code in both channels. The LDPC code utilized by the BP decoder is of length (16200, 8100) given in Figure 3.14. The resulting performance endorses the theory behind LDPC codes, as it shows that the longer length code has much improved decoding performance for a fixed distance. The BP-Chase decoder implements a concatenated BCH-LDPC code of equivalent length defined in the standard [11]. The results given in Figure 3.14 match those of Figure 3.11 and 3.12 in that the concatenated system provides improved decoding performance of 0.2dB at a BER of  $10^{-3}$ . The trend in Figure 3.13 is also maintained where the performance of the decoders of higher block length are shifted in the satellite channel. The shift is similar to that of the medium length codes; at a BER of  $10^{-3}$  the performance of the BP-Chase decoder is shifted by 4.2dB, which again can be attributed to the level of shadowing.

The conclusions that can be drawn with regard to the results is that the affect of shadowing in a satellite channel plays a significant role in reducing error correcting performance. The AWGN channel was discussed to be an inaccurate model for a satellite system as it does not accurately model the effects of shadowing. The LMS model implemented, which was in fact the best case environment, is shown to reduce the decoding performance by approximately 4dB across all the decoders simulated. This can be attributed to the blockages and disturbances expected in the LMS channel. The loss is solely that of the effect of shadowing as the free space loss is not taken into account, which would further negatively affect the performance shifting the curve a further  $k_{lb}$  dB. The outcome of implementing the satellite channel in the PL model has shown to reduce

the decoding performance of the system; the shifted performance results make up the first original contribution of the dissertation.

### **3.6 Conclusion**

The preceding chapter has focused on the definition, construction and implementation of the PL system model. The model composes the transmission, channel and reception systems each of which were discussed and detailed in terms of their implementation requirements. A LMS channel model was selected in order to provide a more accurate representation of a satellite channel. The results of which were presented, validating the receiver system decoding structure in an AWGN channel as well as providing results in a satellite medium; fulfilling one of the objectives of the dissertation. The results in the satellite channel show a shift in the performance curve of approximately 4dB, depicted in several cases, to the detriment of performance.

The construction and validation of the PL system model, including the implemented satellite channel, acts as a base for attempting further improvement. The subsequent chapter will attempt to build on the PL model performance results, by improving the BP-Chase decoder.

# Chapter 4

## ADVANCED CONCATENATED DECODER

### 4.1 Introduction

The aim of the chapter is to construct and define an improved error correcting receiver structure, which will be integrated into the PL system model. The novel decoding structure forms the second original contribution of the dissertation. The novel decoder attempts to expand upon the receiver structure given in [13], implemented in Chapter 3, to advance the error correcting performance.

Throughout the course of the dissertation the PL has been modeled and implemented. In Chapter 2 the literature was reviewed with regard to the receiver system, the result of which was the selection of the BP-Chase decoder. The performance of the implemented receiver structure was presented in Section 3.5 and is shown to match that given in the literature thus validating the receiver implementation.

The BER curves specifically those of Figure 3.12 show that the BP-Chase decoder outperforms its constituent BP and Chase decoders. At a BER of  $6 \times 10^{-2}$  a coding gain of 0.2dB and 2.2dB is achieved with regard to BP and Chase respectively, for equivalent decoding parameters. The gains in error correcting performance can be credited to the sharing of soft information between the constituent decoders, the details of which are provided in [13].

The main motivation for selecting the BP-Chase decoder was that it allowed for improved soft decoding performance of a concatenated BCH-LDPC code, which forms the DVB-S2 FEC. In the process of producing a novel decoder, the structure of the BP-Chase decoder will be preserved firstly to retain the ability to decode concatenated BCH-LDPC codes; allowing the system to remain relevant to DVB-S2. It is also important to maintain the gains made by soft information sharing. The methodology is to improve the performance of the constituent BP and Chase decoders in order to improve the overall performance of the concatenated decoder.

The development of the novel decoder requires the selection of a decoding scheme or schemes which enhance the constituent decoder performance. This requires a review of the literature expanding upon the survey carried out in Chapter 2 and will be presented in Section 4.2. The selected decoding algorithm will then be detailed in Section 4.3. In Section 4.4 the novel decoding structure will be presented, focusing on the integration of the chosen decoding

algorithms into the PL system. The simulation results are given in section 4.5 and to conclude the outcomes of the chapter are given in Section 4.6.

## 4.2 Constituent decoder development

The system model depicted in Figure 3.1, has been constructed and implemented throughout the course of Chapter 3. The result of which was observed in Figure 3.11 and Figure 3.12, showing the improved decoding performance of the BP-Chase decoder over its constituent BP and Chase decoders. The improvements are attributed to the soft information transfer in the concatenated system which allows conditioning of soft information between the inner decoders, improving error detection and correction [13]. The concatenated iterative decoder is depicted in Figure 3.6 and indicates the transfer of soft information  $q$  from the BP to Chase decoder's and  $L(y'_n)$  from the Chase to BP decoder's; the formation and transfer of which is described in Section 3.4.3.

One of the aims of the dissertation, given in Chapter 1, is to produce a decoding structure which improves performance of the constructed DVB-S2 PL. The methodology used to construct the improved decoder, is to maintain the BP-Chase decoder structure and improve the constituent BP and Chase decoders. The assumption being examined is that by attempting to improve the constituent decoders a reciprocal increase in gain will be achieved in the performance of the concatenated decoder.

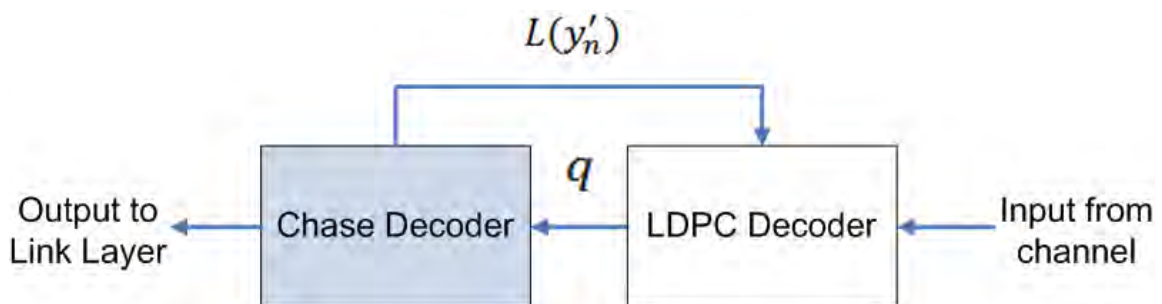


Figure 4.1-Construction of improved system model

The DVB-S2 FEC provides error correcting performance by concatenating BCH and LDPC channel codes [11]. The majority of the error correcting performance in the FEC is provided in the form of large length LDPC codes; concatenated with low length BCH codes. The core benefit of the concatenation is that the BCH code negates the error floor problem inherent with iterative

LDPC decoding. The potential performance improvement experienced by the concatenated decoder, related to improving the BCH decoder module is thus logically minimal. The BCH codes are not as powerful when compared to the LDPC codes utilized in DVB-S2. The difference is marked when considering the results of Figure 3.11 and 3.12 illustrating a gain by BP over Chase of 1.7dB at a BER of  $6 \times 10^{-2}$ . The focus of the improvement will thus be centered on the decoding the LDPC module. The objective being to replace the LDPC Decoder block in Figure 4.1, while utilizing the soft information at the input and generating soft information at the output. The following review will thus examine possible improvements to the BP decoders presented in the literature.

#### 4.2.1 Literature review of improved BP decoders

The goal of the literature review is to analyze and select a suitable LDPC decoding algorithm for implementation within the BP-Chase structure presented in Chapter 3, see Figure 4.1. The core components defining suitability are that the algorithm must provide improved performance when compared to BP. The algorithm must also be able to adequately integrate into the decoding structure presented in Figure 4.1, generating and utilizing soft information.

In Chapter 2 a broad review of the LDPC decoding landscape was considered, for the most part discussing the modifications made to the soft information BP or SPA. The BP algorithm originally presented by Gallager in [26] and further expanded upon in [27] [36] [37] [38] [39], attempt to reduce the complexity of BP while retaining the error correcting performance. This has been seen in algorithms such as MS and UMP decoding [42] [44] [45]. There have also been hybrid models presented in [65] [66] [67] [68] which combine soft decision BP with a variety of hard decision decoders in order to reduce the complexity of the system. This however only maintains the error correcting performance it does not improve it, which does not achieve the goals of the review.

In the literature reviewed only the Fossorier algorithm [69] provides superior performance to BP. Fossorier presents a concatenated decoding structure using both SPA and OSD (Ordered statistics decoding) to decode LDPC codes. The Fossorier technique is shown to elevate traditional LDPC decoding to achieve ML decoding performance whereas SPA only provides suboptimum performance. It operates on the principle of soft information conditioning in the same manner as the BP-Chase decoder; the soft information generated by the BP decoding phase is used to aid the OSD. In order to understand the operation of the BP-OSD decoder a description of OSD as well as the algorithm is presented.

OSD is a reliability based decoding scheme presented by Fossorier and Lin in [128]. OSD operates in a very similar manner to the Chase algorithms, analyzed in Chapter 3. The algorithm forms a sequence of test patterns given input reliability or channel measurement information. OSD in the same manner as the Chase algorithm can be defined for different levels of complexity. OSD- $i$  is the OSD algorithm, where the value of  $i$  determines the dimension of the codeword space. The greater values of  $i$  generate greater numbers of candidate codewords, the complexity of OSD grows with  $i$ .

OSD operates on the principle of reordering of the input codeword, utilizing the input reliability information. The algorithm applies a series of permutations based on the generator matrix  $G$  of the input code, in order to generate a set of bits known as the most reliable basis (MRB) are obtained. The MRB is used to generate the set of candidate codewords, the method of which varies as per the flavor of the OSD, dependent on the value of  $i$ . The output of OSD is a single codeword which is selected based on the analog weight. The algorithm can be divided into three basic steps.

- Construction of MRB
- Reorder and re-encode
- Codeword Selection

In order to fully define the hard output OSD algorithm given in [128] several assumptions and definitions are required. The block code utilized is a  $(N, K)$  binary linear block code, the  $K$  most reliable independent positions (MRIP) form the MRB. The input into the OSD is an encoded binary codeword, modulated using BPSK and transmitted over an AWGN channel, given by  $y_{osd}$ . The hard decision of which gives the binary sequence  $y$ . The second input into the decoder is the generator of the linear block code  $G$ , the permutations applied to the input vectors are given by  $\lambda$ .

### **OSD- $i$ Algorithm** [69],[122]

#### Construction of MRB

- 1) Order the received reliabilities given by  $\alpha = |y_{osd}|$  in decreasing order, the shifted ordering defining the permutation  $\lambda_1$ .
- 2) Apply  $\lambda_1$  to  $y$  and the columns of  $G$ , to obtain  $y_1$  and  $G_1$  respectively.
- 3) Perform Gaussian elimination on  $G_1$  starting from the left and moving towards the right, where all dependent columns are permuted after the last independent column, to obtain the matrix  $G_2$  and the permutation  $\lambda_2$ .

- 4) Apply permutation  $\lambda_2$  to  $y_1$  to obtain  $y_2$ .

The construction of the MRB ( $y_2$ ) is computation intensive due to the application of the permutations. The MRB consists of the  $K$  positions, of the set of columns in  $G_2$ .

#### Reorder and re-encode

- 1) For  $0 \leq l \leq i$  make all changes of  $l$  of the  $K$  MRB positions of  $y_2$ .
- 2) For all changes to  $y_2$  re-encode the  $K$  bits using  $G_2$ , to form the candidate codeword set  $C$ .

Form the sphere of candidate codewords based on the value of  $i$  and the MRB positions of  $y_2$ . The  $l$  changes are made to the MRB which is essentially forms a new information vector which is re-encoded with  $G_2$  to form the candidate codeword set  $C$ .

#### Codeword Selection

- 1) Calculate the decoding cost of each candidate codeword  $D(y, c) = \sum_{j=1; c_j \neq y_j} |y_j|$  where the function  $D$  represents the discrepancy between the received binary input  $y$  and the candidate codeword given by  $c$ .
- 2) The candidate codeword of lowest cost is selected as the output given by  $C_o$ .

There have been several variations to OSD given in the literature which will be mentioned. In [130] a strategy is presented which utilizes a supercode of the overall block code to generate the MRB, however this leads to an exponential increase in the complexity of the algorithm with regards to the code length. The opposite approach is taken in [131] which reduces the amount of reliable information sets taken into account when generating the MRB, the result of which is a reduction in error correcting capability. The failing of the algorithms [130] [131] mentioned above is that they only partially take into account the bits which are not considered in the set of MRIPs, an issue which affects the performance as the code length increases, as the number of unselected bits increase. The Fossorier BP-OSD algorithm [69] solves this issue allowing it to provide improved decoding for longer length codes.



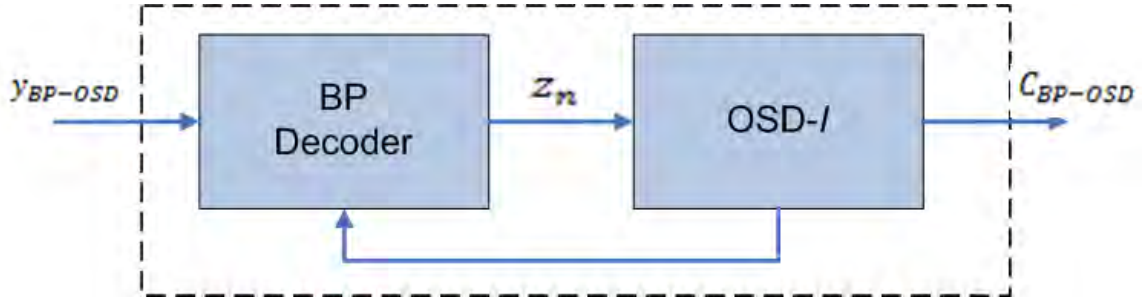


Figure 4.2-BP-OSD decoder

The Fossorier BP-OSD is a concatenated decoder consisting of a BP decoder followed by an OSD, depicted in Figure 4.2, the BP decoding system has been described in detail in Chapter 3 and the OSD algorithm has been given above. The focus of the presented algorithm centers on the soft information transfer between the decoders. The notation for both the BP and OSD algorithms will be reused in the discussion of the concatenated structure. The assumptions made in the previous decoder definitions are sustained where the input into the decoder is given by  $y_{BP-OSD}$ , which is the resultant of a LDPC encoded codeword modulated using BPSK and transmitted over an AWGN channel.

**BP-OSD Algorithm** [69]

- 1) Perform BP decoding for a single iteration, incrementing  $i_t$ , if the formed codeword  $\hat{c}$  is valid  $H\hat{c} = 0$  then halt BP-OSD decoding and output  $C_{BP-OSD} = \hat{c}$ . If the codeword is invalid halt BP decoding and transmit  $z_n$  the *a posteriori* LLR to the OSD module.
- 2) Perform OSD- $i$  decoding for a single pass, using  $z_n$  to replace  $\alpha$ , if the formed codeword  $C_o$  is valid  $HC_o = 0$  then halt BP-OSD decoding and the output  $C_{BP-OSD} = C_o$ . If the codeword is not valid check if  $i_t \leq I_{max}$ , while this is true return to Step 1, if false output  $C_{BP-OSD} = C_o$  and halt.

In [69] the value of  $i$  is set to either 0 or 1 to reduce the complexity of the decoding system; Fossorier also presented several modifications to the stopping conditions of the concatenated decoder. In [69] several options are examined for selecting a valid codeword other than using syndrome calculation. The benefit of which is a reduction in the complexity of the algorithm as the number of iterations are reduced. This comes at the cost of reduced decoding performance, thus will not be considered.

The BP-OSD algorithm has generated a great deal of interest; in the literature and several schemes have been presented building on the improvements made by Fossorier to LDPC decoding. One of the disputes with iterative decoding of LPDC codes is the LLR oscillation problem posed in [132]. The LLR oscillation problem puts into question the credibility of utilizing LLRs as a measure of reliability. The problem details the fluctuation in the value of LLR mainly in the last iteration of message passing decoding, which inflates the value of the LLR. This makes it unreliable and little is gained if only the last iteration is used to generate the MRB. In [133] a technique is introduced to circumnavigate the oscillation problem which accumulates the LLR in order to generate a more reliable metric from which the MRB can be constructed. The equation of which is given in (4.1), where  $r_n$  represents the reliability value used to construct the MRB and  $e$  is attenuation scaling factor.

$$r_n = \left| \sum_{k=0}^K e^{K-k} - z_n^k \right|, n \in [1, N] \quad (4.1)$$

The accumulation method is shown to achieve performance improvements with a minimal increase in the complexity due to the accumulated  $r_n$  metric. A similar technique was considered in [134] however the approach limits the LLRs used to construct the MRB in OSD. The limiting of the LLR information does not take into account the last iteration in order to reduce the impact of the oscillation error on the OSD decoder. The limitation method is shown to also provide improved performance. There are several other techniques to consider such as the cascaded approach adopted in [72], instead of BP-OSD the system implemented is a BF-OSD concatenation. The BF algorithm previously discussed in Chapter 2 is an iterative technique which has generated a great deal of interest in LDPC decoding literature. In a similar manner to BP the BF technique, of which there are variants, [27] [28] [29] [30] generate soft information which is fed to the OSD decoder to be used as a reliability metric. The main gain in terms of the BF-OSD concatenation is the reduction of complexity when compared to the BP-OSD scheme and provides similar decoding performance. The systems mentioned previously transferred information between the constituent decoders every BP iteration however in [14] the BP decoder iterates for a fixed number of iterations before transferring reliability information. This allows for a greater level of conditioning before transfer to the OSD module. The proposed system is shown to improve upon the Fossorier concatenated system in terms of error correcting performance, solving the error floor problem inherent to iterative LDPC decoding as well as reducing the complexity of the system as OSD is not run on every iteration.

The purpose of the literature review substantiates the selection of an algorithm which provides improved decoding performance over traditional BP decoding. Achieved while utilizing and generating the required soft information to integrate with the BP-Chase decoder presented in [13]. The Fossorier decoder given in [69] fulfills the requirements at the cost of greater complexity; the algorithm however has been improved in terms of error correcting performance at a lower complexity by Yang et al in [14]. The Yang decoder improves the performance while maintaining the benefits of Fossorier concatenation. The concatenated BP and OSD developed by Yang [14] will be referred to as BP-OSD for the remainder of the dissertation. It will be implemented in the PL system model in order to develop a novel decoder.

### 4.3 BP-OSD

The BP-OSD algorithm was selected as the outcome of the literature review to improve BP decoders. The BP-OSD decoder operates using the BP and OSD decoders arranged as depicted in Figure 4.3. The OSD decoder is divided into several sub-blocks the variation from the Fossorier decoder will be shown as follows.

In order to define the BP-OSD require the assumptions made in defining BP and OSD are maintained; the input to the system is  $y_{BP-OSD}$  and the output is the LDPC codeword  $C_{BP-OSD}$ .

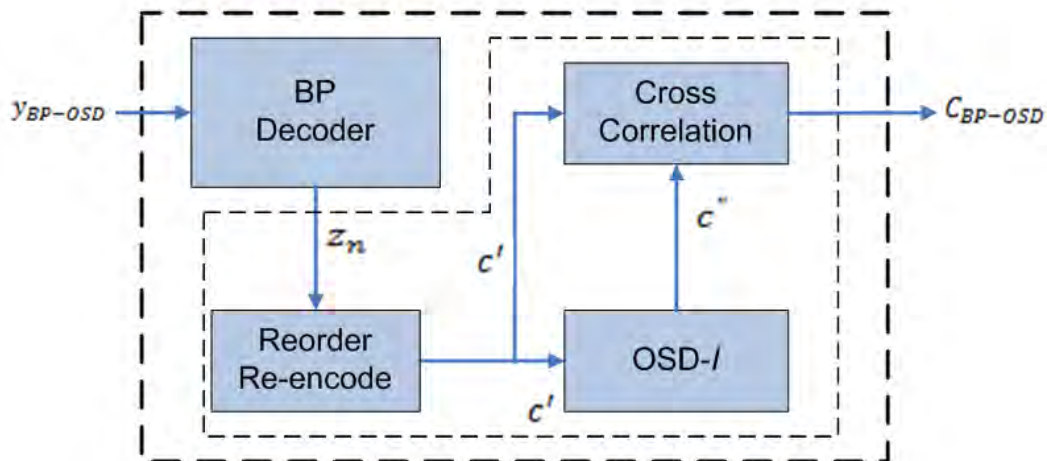


Figure 4.3- Yang BP-OSD mode [14] |

#### BP-OSD Algorithm [14]

- 1) The system proceeds with BP decoding using  $y_{BP-OSD}$  as input, as defined in Chapter 3 until either a valid codeword is obtained when  $H\hat{c} = 0$  at which point the decoder halts and  $C_{BP-OSD} = \hat{c}$  is the output of the decoding system. If the maximum number of iterations is reached  $i_t > I_{max}$  then the BP decoder halts and  $z_n$  is output to the OSD decoder.
- 2) The OSD algorithm is divided into three functional blocks, the Reorder Re-encode block is the first component which handles the permutations required to construct the MRB, using the value of  $z_n$  as the input, as well as the process of re-encoding the MRB to produce the codeword  $c'$ .

The codeword  $c'$  is then sent to the OSD- $i$  functional block which handles the reordering of  $c'$  to generate the list of candidate codewords  $c''$  using the reordering and re-encoding technique described in the OSD- $i$  algorithm.

The final stage in the OSD process is the cross correlation which calculates the correlation between the codeword  $c'$  and the set of candidate codewords  $c''$  where the cross correlation is given by  $Y(c_k'') = \sum_{j=0}^{n-1} z_n \cdot (1 - c_{k_j}'' \oplus c_j')$ , where  $c_k''$  is a candidate codeword of the set  $c''$ . The codeword which produces the highest cross correlation is the output of the system given by  $C_{BP-OSD}$ .

The Reorder Re-encode block unlike in the OSD- $i$  algorithm creates the MRB and re-encodes to generate only a single codeword  $c'$ , the reordering refers to the permutations in OSD- $i$ . The codeword  $c'$  is used as a basis for both cross correlation and reordering to generate the candidate codeword set. In the second stage of the OSD- $i$  functional block, the reordering and re-encoding technique was applied to generate a complete a set of candidate codewords  $c''$ .

The next stage in development is to build the complete novel decoder by integrating the BP-OSD model into Figure 4.1.

#### 4.4 Novel BP-OSD-Chase decoder

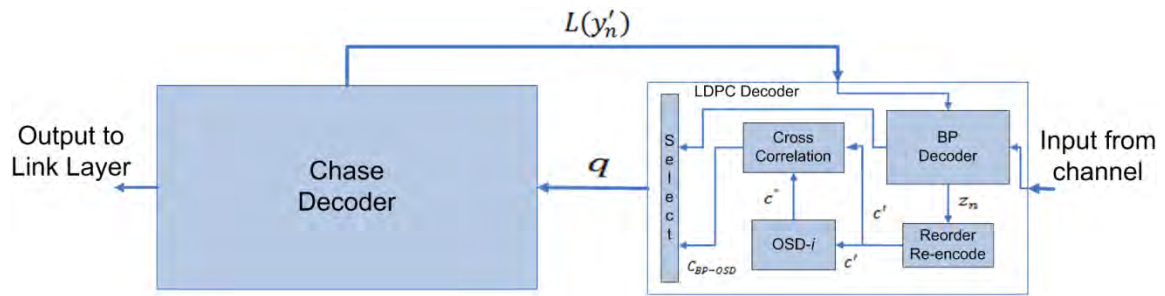


Figure 4.4-Novel BP-OSD-Chase decoder

The following section defines the novel decoding structure which has been developed throughout the course of the chapter. In attempting to improve the decoding structure given in Figure 4.1, the assumption was made that by improving the decoding performance of the constituent LDPC decoder, while maintaining the concatenated structure, a reciprocal increase in the overall concatenated performance can be achieved. The LDPC decoder selected was presented by Yang in [14] and was detailed in Section 4.2.2. The integration of the BP-OSD decoder into the receiver structure given in Figure 4.4 will be discussed as follows.

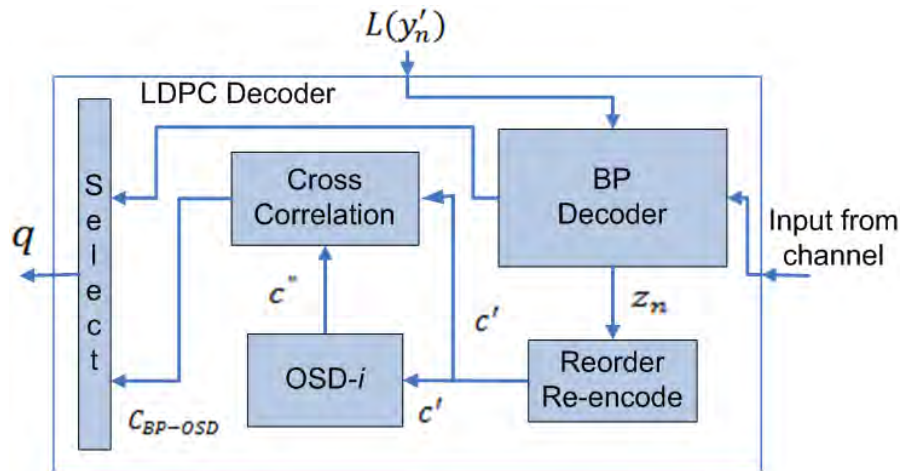


Figure 4.5-Integrated Yang BP-OSD decoder

The BP-OSD module can be seen in greater detail in Figure 4.5, the figure depicts the functional block which replaces the LDPC decoder module in Figure 4.1. In order to understand the integration, the following section will highlight the interactions of the BP-OSD block with the other components in Figure 4.4.

**Input:** The input into the LDPC decoder is fed directly into the BP decoding module and holds to the assumptions made in Section 3.4.3. The second input into the LDPC module is the form of

the soft information  $L(y'_n)$ , which also is fed direct into the BP module to improve the iterative message passing decoding.

**Output:** The output of the decoder is determined by the Select module which handles the administrative duty. If the output codeword defined by the cross correlation is valid  $HC_{BP-OSD} = 0$ , the codeword  $C_{BP-OSD}$  is output and the concatenated decoder halts. If the codeword is not valid the soft information output  $q$  generated by the BP decoder is output to the Chase decoder.

The interactions between the BP-OSD decoder has been fully defined in terms of its integration with the PL system model. The novel decoder has now been fully constructed and is in the form of a BP-OSD-Chase decoder. The BP-OSD is the improved LDPC decoder and the BCH decoding is handled by the Chase decoder. The transfer between the decoders is controlled by the rules defined in [13].

The motivation for the concatenation of the BP-OSD with the BP-Chase structure is to improve the overall decoding performance of the PL receiver system. Improving the decoding performance of the PL system improves the quality of service which DVB-S2 provides. A factor to consider however is the complexity associated with the improved decoder. If the decoder provides optimum performance but is not realizable with regard to implementation or has very low throughput it has little relevance in industry. There are several approaches taken to compute complexity; the difference being the manner which the complexity metric is defined. Implementation complexity defines several metrics such as area, throughput and energy [135]. In [136] [137] the metric chosen are the number of operations which are required to be performed per received bit, which is measured in giga operations per second (GOP). A similar metric is defined by [138] but also takes into account the amount of storage capacity required to operate the system. The complexity of the novel decoder is focused on the computational aspect of the system instead of utilizing GOPs, the metric used are the number of mathematical operations required to decode. The operations considered are real multiplications, real additions and binary additions given in decreasing order of complexity. In most cases of complexity analysis the binary additions are ignored [122] however they will be considered as they form a large proportion of the proposed decoder complexity. The comparison will focus on comparing like metrics rather than comparing additions with multiplications.

In order to develop the BP-OSD-Chase decoder the complexity of the constituent modules will be considered in turn. Given a LDPC code of parameters  $(N, K, j)$  where  $N$  is the block length,  $K$  is the input information length and  $j$  is the number of check sums. Implementing the assumed codeword parameters the complexity of the stages comprising a single iteration of BP are given in Table 4.1.

**Table 4.1 Decoding complexity of a single iteration of BP [37] [42]**

Operation	Number of Computations
$\delta q_{mn}$	$Nj$ additions
$\delta z_{mn}$	$3N(j - 1)$ multiplications
$z_{mn}^x$	$Nj$ additions
$f_n^x \prod_{m'} r_{m'n}^x$	$2N(3j - 4)$ multiplications
$\alpha_{mn}$	$Nj$ additions and $Nj$ divisions
$q_{mn}^x$	$2Nj$ multiplications
$\alpha_n$	$N$ additions and $N$ divisions
$q_n^x$	$2N$ multiplications

The operations can be aggregated to  $11Nj - 9N$  real multiplications and  $N(3j + 1)$  real additions [122], the real divisions will not be considered in order to simplify comparison with the other modules. The complexity in Table-4.1 is given for only a single iteration however in the worst case the complexity is equal to  $(11Nj - 9N)^{I_{max}}$  multiplications and  $(N(3j + 1))^{I_{max}}$  additions where  $I_{max}$  is the maximum number of iterations of BP allowed.

The complexity of OSD as described in Section 4.2.1 is dependent on the value of  $i$  which determines the order of the algorithm implemented; this determines the number of TPs generated. The chief contributor to the complexity of OSD systems are the permutations applied to the  $H$  matrix which requires a large degree of processing. This is endorsed by the information given in Table 4.2 which describes the number of operations required at each stage of OSD decoding.

**Table 4.2-Decoding complexity for OSD order- $i$  reprocessing [128]**

Operations	Real Additions	Binary Additions
<b>Sorting</b>	$N \ln N$	
<b>Gaussian Elimination</b>		$N \min\{K^2, (N - K)^2\}$
<b>Phase-0 reprocessing</b>	$\leq N$	$\leq K(N - K)$
<b>Phase-<math>l</math> reprocessing (<math>1 \leq l \leq i</math>)</b>	$\leq \binom{K}{l} (N - K)$	$\leq \binom{K}{l} l(N - K)$

Maintaining the assumptions made in defining BP complexity, it is apparent that OSD complexity is dominated by the Gaussian elimination term giving  $N \min\{K^2, (N - K)^2\}$  binary additions. The second major contributor is the order- $i$  reprocessing stage which produces  $K^i(N - K)$  real additions [122], dependent on the value of  $i$ .

The final component of the BP-OSD-Chase decoder is the Chase module. The assumptions made in defining the Chase module are that the input is in the form of a square generator matrix of size  $n$ , and the value of  $p$  represents the number of least reliable bits selected as is defined in Section 3.4.2.

**Table 4.3-Decoding complexity of Chase algorithm [139]**

<b>Real Additions</b>	<b>Real Multiplications</b>	<b>Binary Additions</b>
$(n + 4)2^p + (n + 1)2^p + (p + 2)n + 1$	$(n + 1)2^p + 2n + 2$	$(n + 2n)2^p + p2^p + 2^p$

The values given in Table 4.3 are based on a single pass of the Chase-2 decoder which is implemented in the BP-OSD-Chase decoder. The three metrics considered are all dominated by  $p$ . In general the value of  $p$  is low; the value of  $n$  is also generally considerably lower than  $N$ . The BP complexity is thus greater than the Chase decoder, the tradeoff being the decoding performance, which is provided chiefly by the BP decoder.

The BP-OSD-Chase decoder complexity is presented in Table 4.4 the complexity of a single iteration is given, considering the worst case operation. The concatenation of the constituent decoders has led to an expected linear increase in complexity.

**Table 4.4-Decoding complexity of BP-OSD-Chase algorithm**

<b>Real Additions</b>	<b>Real Multiplications</b>	<b>Binary Additions</b>
$(n + 4)2^p + (n + 1)2^p + (p + 2)n + 1$ $+ K^i(N - K) + (N(3j + 1))^{I_{max}}$	$(n + 1)2^p + 2n + 2$ $+ (11Nj - 9N)^{I_{max}}$	$(n + 2n)2^p + p2^p + 2^p$ $+ N \min\{K^2, (N - K)^2\}$

The BP-OSD-Chase is much more complex in comparison to other popular iterative decoders such as UMP-BP and MS [42] as well as the Yang BP-OSD decoder [14]. An important tradeoff to consider when discussing the complexity of the novel decoder is the value of the code parameters used. The values of  $N, K, I_{max}, p$  and to a lesser extent  $n$  play a pivotal role in determining the complexity of the decoder. The tradeoff being performance versus complexity, increasing the value of the code parameters increases both performance and complexity. The decoder can be optimized with regard to the amount of processing power available. Given the above complexity equation the parameters can be selected to provide best possible performance.



The implementation complexity of the system has not been discussed mainly because there is no trivial link between computational complexity, given above, and implementation complexity. The decoder can achieve a high throughput even though it is not suggested by the examining the computational cost or generating a software implementation. A large proportion of the OSD and Chase computations can be parallelized thus improving the throughput. The next stage of the dissertation will present the performance results of the implemented BP-OSD-Chase module. The aim is to verify whether the increase in complexity has translated to an increase in performance.

## 4.5 Simulation results

The following section aims to provide simulation results validating and analyzing the results generated from the Chase-BP-OSD algorithm in the PL system model in both an AWGN and LMS channel. The performance results given are generated for medium length codes given the complexity of the BP-OSD-Chase system. This is due to the constraints in terms of processing power but is in line with the aim of the chapter which is to provide relative performance gains. In order to fully understand the nature of the decoder the decoding parameters will also be varied to determine the nature the decoding effectiveness at different complexities.

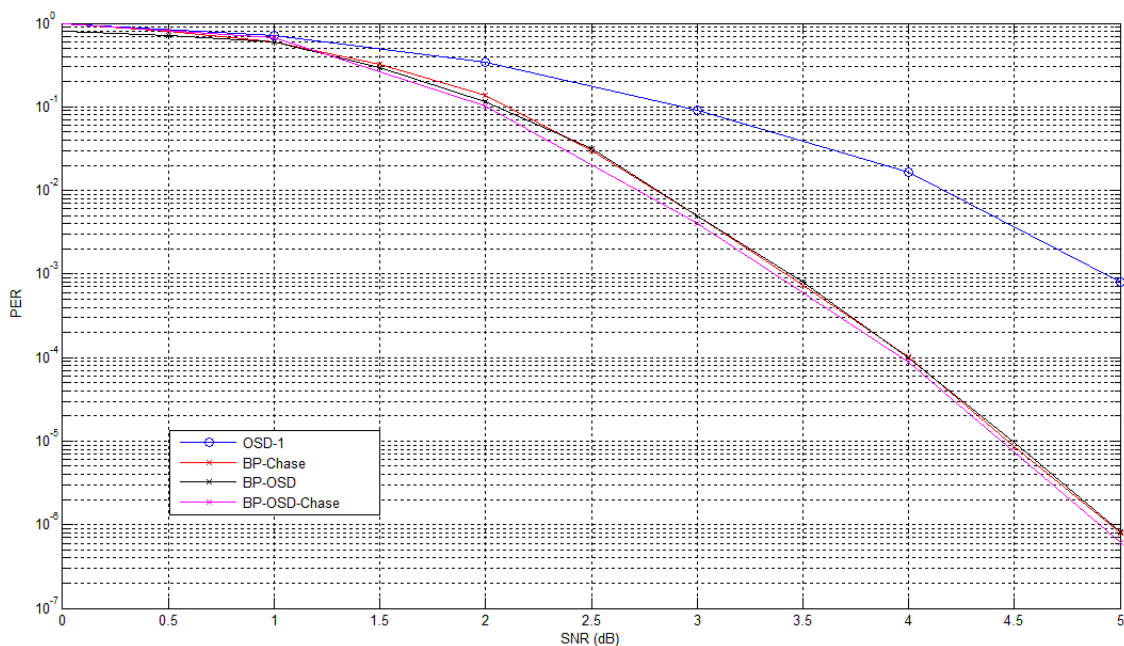


Figure 4.6-PER curves for validation of decoding system

Figure 4.6 depicts the performance of several decoders in terms of packet error rate (PER), where the packet size is equivalent to the block length, versus the SNR in decibels. The results in Figure 4.6 compare the performance of the BP-OSD decoder utilizing a (210,105) LDPC code with parameters(3,6) against the previously implemented BP-Chase decoder and the novel BP-OSD-Chase decoder both utilizing a concatenated (210,105) BCH-LDPC code, constructed from a BCH (15,7,5)code. In order to allow for comparison OSD-1 decoder results are also provided, operating on a (210,105) LDPC code. The performance results for the BP-OSD decoder match similar results presented in [14] validating the implemented model, any variation of which are due to the minimal alteration in code length to allow for comparison with the other concatenated systems.

In comparison with the constituent OSD and BP decoders the BP-OSD decoder is shown to provide superior performance, at a PER of  $10^{-3}$  the BP-OSD decoder provides coding gain of 1.6dB over OSD-1. The performance of the BP-OSD decoder when compared with the BP-Chase system is shown to be very similar, the power of the BP-Chase system in comparison to the performance of BP-OSD system. This validates the selection of BP-OSD as the BP-Chase system was shown to provide performance beyond that of BP in Chapter 3 of approximately 0.2dB.

The BP-OSD and BP-Chase decoders are also shown to solve the error floor problem which afflicts BP decoding performance at 4dB. The BP-OSD and BP-Chase decoders do not experience the issue due to the concatenation with OSD and Chase respectively. The most important conclusion which can be drawn from Figure 4.6 is the improvement of performance when integrating the BP-OSD decoder into the BP-Chase system forming the BP-OSD-Chase decoder. The decoder outperforms both the BP-OSD and BP-Chase decoder, at a PER of  $10^{-2}$  providing coding gain of 0.15dB. This validates the assumption that attempting to improve the error correcting performance of the constituent BP decoder produced coding gain in the concatenated system.

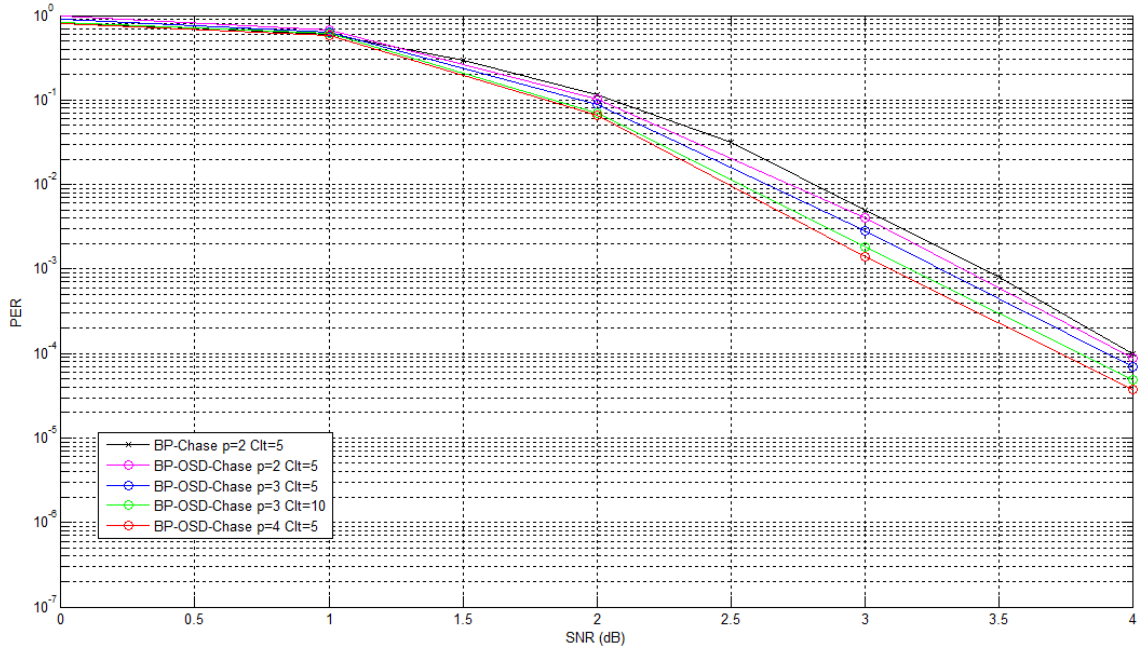


Figure 4.7-Comparison of PER of BP-OSD-Chase for varying decoding parameters for length(210,105)

In Figure 4.7 the performance of the BP-OSD-Chase decoder is further investigated for the (210,105) concatenated BCH-LDPC code. The figure shows several performance results comparing the BP-OSD-Chase for a variety of decoding parameters. The performance of the BP-Chase case with the parameters  $(p, I_{cMax})$  are given with  $p$  equal to 2 and the number of concatenated iterations  $I_{cMax}$  given to be 5; in order to provide a basis of comparison. The BP-OSD-Chase (2,5) results of which have been given in Figure 4.6 above is shown to provide approximately 0.15db coding gain when compared to BP-Chase of equivalent parameters. The BP-OSD-Chase performance results are then provided for the (3,5), (3,10) and (4,5) cases all of which show consistent improvement as the complexity of the system increases in a similar manner as that produced in [13]; where the gains are in the region of 0.25dB, 0.35dB and 0.4dB at a PER of  $10^{-3}$  respectively when compared to the BP-Chase decoder. The performance improvement confirms the assumption made in Section 4.4 that an increase in the decoder complexity will produce a reciprocal increase in performance.

In Figure 4.8 similar gains are achieved by the BP-OSD-Chase decoder of varying parameters utilizing a concatenated BCH-LDPC code of length (496,248), the BCH inner code is of length (15,7,5), when compared to the BP-Chase decoder. At a PER of  $10^{-2}$  the coding gains for the BP-OSD-Chase (2,5),(3,5),(3,10) and (4,5) are 0.15dB,0.2dB,0.36dB and 0.38dB respectively, which is similar to that achieved above.

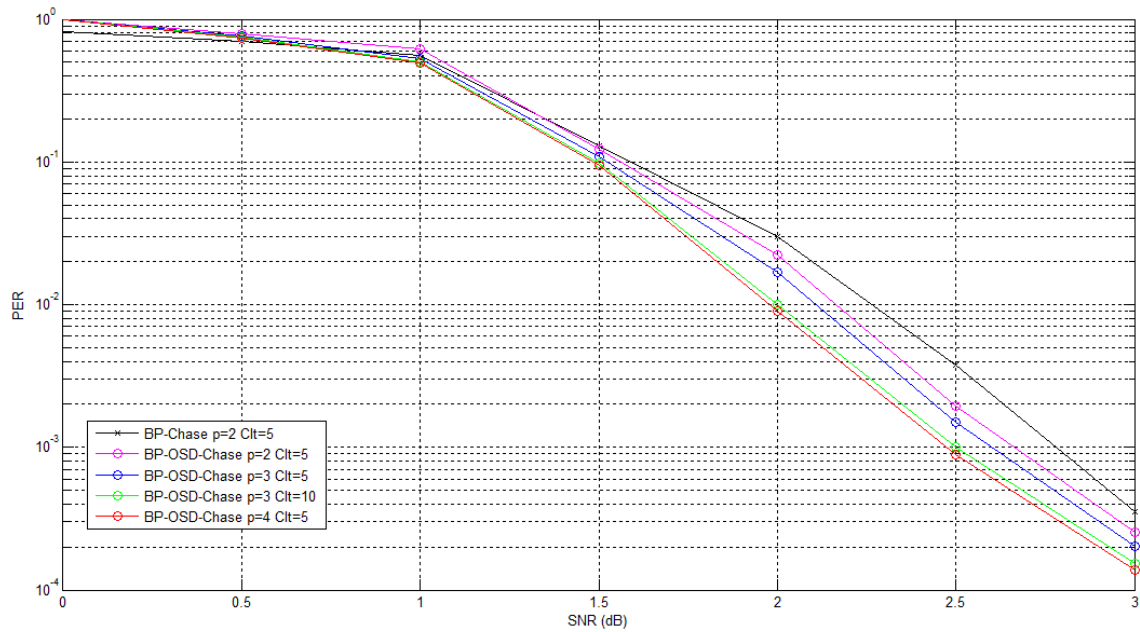


Figure 4.8-Comparison of PER of BP-OSD-Chase for varying decoding parameters for length(496,248)

Figure 4.9 compares the results of the BP-OSD-Chase and BP-Chase decoder in both the AWGN and satellite channel. The results of which are similar to those produced in the Chapter 3 where the effect of shadowing is shown to produce a coding loss of approximately 4dB at a PER of  $10^{-2}$  across both the decoders for both code lengths simulated.

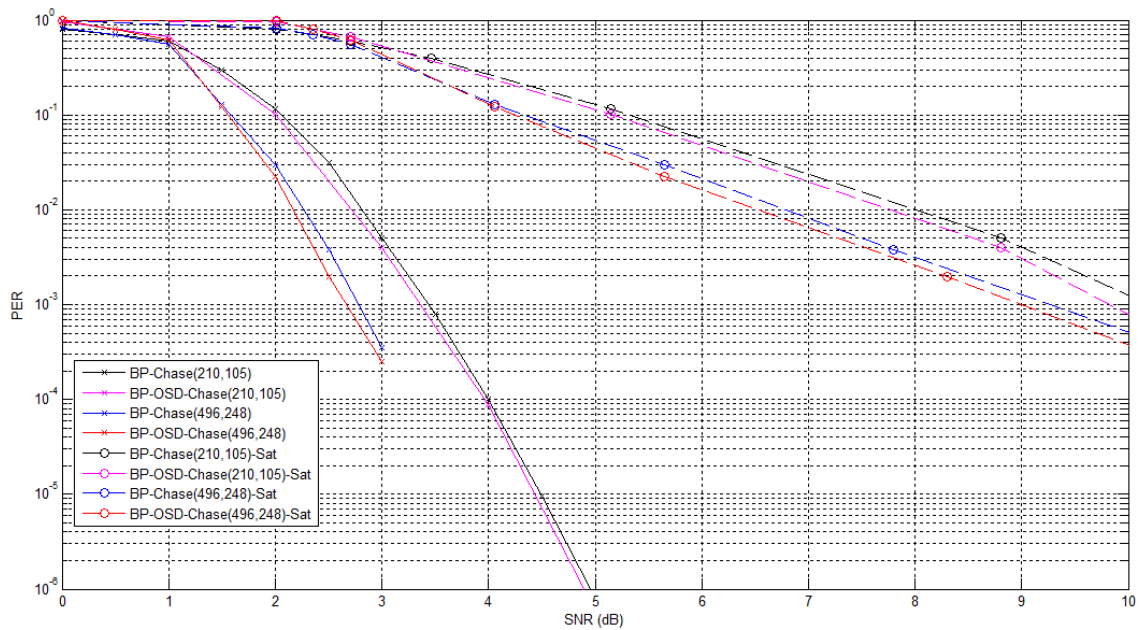


Figure 4.9-Comparison of PER performance of PL system in satellite and AWGN channels

The results presented above confirm that the BP-OSD-Chase decoder, implemented in the DVB-S2 PL model, has produced improved decoding performance when compared to the receiver performance produced in Chapter 3. The second original contribution of the dissertation has thus been achieved. The BP-OSD-Chase decoder is an improvement of the BP-Chase structure and has shown to improve performance at the cost of an increase in complexity. The increase has been quantified in Table 4.2 of Section 4.4 which defines the cost of the additional reliability based decoder. In terms of the DVB-S2 standard the current system improves upon performance but may not be viable for consumer level implementation. Implementations rarely use BP decoders as they are costly to manufacture, this however does not invalidate the work produced. The aim of the dissertation was to achieve a relative increase in performance, which has been achieved. In terms of implementation there are several approaches which can be applied which reduce complexity to manageable levels, such as introducing reduced complexity versions of BP. The aim being to maintain the relative performance gains while reducing the complexity of the constituent models.

## **4.6 Conclusion**

The aim of the chapter was to construct and present a novel decoder which provided improved decoding performance in the PL system model. This was achieved with the methodology focused on retaining the structure of the BP-Chase decoder, presented and implemented in Chapter 3. The intent was to improve the performance of the constituent BP decoder assuming that it would improve the overall decoding performance. The review of the literature presented the BP-OSD decoder originally produced by Fossorier in [69] and improved by Yang et al in [14], the decoder was shown to provide coding gain over traditional BP decoding; the Yang BP-OSD decoder was thus selected for implementation. The details of the decoder were discussed focusing on the implementation within the existing concatenated structure. The result of which was the novel BP-OSD-Chase decoder which was implemented, which when implemented provided a coding gain of around 0.15dB over the BP-Chase decoder however at the cost of greater complexity which was quantified.

# Chapter 5

## CONCLUSION AND FUTURE WORK

### 5.1 Conclusion

The propagation of wireless systems worldwide has gained momentum in recent years; the motivation being the ability to provide services in locations where wired infrastructure is inconvenient. The development and proliferation of mobile devices especially in the form of smart phones has expanded the wireless market to a larger audience. This has increased the demand for improved quality and services. The development of wireless communications has spanned three generations, from traditional voice only to high speed multimedia networks. The goal has been to produce greater transmission speeds as well as improving QoS. Satellite systems play an important role in providing wireless services, the foremost being satellite video broadcasting. The main application of which is to provide television services to a large viewership, over a broad footprint. The DVB-S2 standard has been developed to achieve this, it specifies the PL modules required to achieve given QoS guarantees and transmission rates. The modules are capable of counteracting the issues prevalent with transmission over a satellite channel

The motivation for the dissertation is based on two original contributions; the first is to provide decoding results for the DVB-S2 PL in a LMS channel. The literature provides performance results for DVB-S2 in an AWGN channel. The interest in mobile systems has led to the development of LMS channel models which can be applied to the DVB-S2 sphere of applications. The production of decoding results in a more accurate medium will allow for improved analysis of satellite disturbances on DVB-S2 PL performance. The second original contribution is to produce a novel decoding structure which improves the error correcting performance of the DVB-S2 PL receiver.

The first step to achieve the goals of the dissertation was taken in Chapter 2. The DVB-S2 physical layer transmission was discussed as specified in the standard. The explorative look of the transmission model improves understanding of the requirements for developing an adequate receiver structure. The receiver is not defined by the DVB-S2 standard in order to allow for greater flexibility as per the application. The next stage involved reviewing the literature in terms of BCH and LDPC decoding to select a beneficial pair of decoders to be used as the basis for the receiver. The selected decoders will be used in subsequent chapters; to produce decoding results

in a LMS channel and as a basis for the novel decoder to improve FEC decoding performance. The selected decoding algorithm was the iterative concatenated BP-Chase system presented in [13]. The motivation for the selection is the passing of soft information between the constituent decoders. This allows the concatenated system to provide improved decoding performance over its constituent modules.

In Chapter 3 the focus of the work was on the definition, construction and implementation of the DVB-S2 PL system model. The implementation of the PL model will allow the generation of simulated performance results. It will also be used as a basis for the construction of the novel decoder. The PL system model consists of three components, the transmission, channel model and receiver systems. The transmission scheme is a condensed version of that presented by the standard, focused on the FEC encoding modules, instead of the administrative modules which do not affect decoding performance. The channel model represents the disturbances which a transmitted signal experiences when travelling through a LMS system. The satellite channel model forms a pivotal role in achieving the first original contribution of the dissertation; to produce decoding performance results in a LMS channel. A review of LMS channels presented in the literature was undertaken, considering different satellite bands and Markov representations. The outcome of the review was the selection of a three state Ku band Markov model. The implementation details of which were provided with regard to integration into the PL system model. The receiver system forms the final component of the PL model. The receiver follows the concatenated iterative BP-Chase structure defined in [13]. The constituent Chase and BP decoding structures are discussed after which the concatenated decoder is presented, completing the definition of the PL model. The implementation of the PL system allowed for the generation of simulation results representing the error correcting performance of the system. The results validate the selection of the receiver structure as the BP-Chase decoder is shown to outperform the constituent decoders by 0.2dB over BP at a BER of  $10^{-3}$  in an AWGN channel. Simulation results were also generated using the selected LMS model, achieving the first contribution of the dissertation. The results given in the satellite channel are shown to reduce the performance of the implemented decoders by approximately 4dB over a range of block lengths. The reduction in performance is attributed to the effect of shadowing on the PL system, which is not considered in AWGN channels.

In Chapter 4 the second original contribution of the dissertation is considered. It requires the construction of a novel decoder which will improve upon the performance of the DVB-S2 PL system constructed in Chapter 3. The novel decoder retains the BP-Chase structure in order to maintain the benefits associated with soft information sharing. The aim is to improve the performance of the constituent BP decoder. To select a scheme capable of improving the BP performance; a survey of the literature was provided focusing on the BP-OSD scheme developed

by Fossorier [69]. The criteria for selection were improved decoding performance over BP as well as generating and utilization of the soft information produced by the existing BP-Chase structure. The criteria was met by the Yang BP-OSD decoder in [14] resulting in the presentation of the Yang BP-OSD algorithm. The details of the decoder together with its integration into the PL system model are given, to form the novel BP-OSD-Chase decoder. The simulation results of the PL system show that the BP-OSD-Chase decoder achieves a coding gain of 0.15dB over the BP-Chase decoder. This is at the cost of greater complexity which is quantified with regard to decoding parameters selected. The second contribution of the dissertation has thus been achieved.

## **5.2 Future work**

The following are potential paths along which future research work can take in order to expand upon the research presented in the dissertation:

- 1) The next stage in improving the PL system is to reduce the complexity of the BP-OSD-Chase decoder. There have been several techniques mentioned in the literary reviews. These reduce the decoder complexity while maintaining the decoding performance. The application of these techniques to the decoder may improve throughput and reduce the computational complexity. In the same vein the decoder can be implemented in the form of an FPGA. Potential parallelization techniques can be applied to the hardware implementation in order to reduce the complexity.
- 2) There is also the option of extending the system to incorporate the data link layer by reusing soft information. The soft information will be passed from the PL to the data link layer; to improve the decoding performance of the link layer. There are several presentations given in the literature which define decoders for the DVB-S2 link-layer FEC (LL-FEC) [140]. This is over and above the FEC at the PL, see Figure 2.4. The adopted LL-FEC code is a systematic Reed-Solomon (255,191) code. A RS code is an advanced form of BCH code, which uses parity bit information to perform error correction. The LL-FEC frame as seen in Figure 5.1 consists of 255 columns and a variable number of rows. The first 191 columns in the frame make up the application data table, application datagrams are received from the upper layers of the system



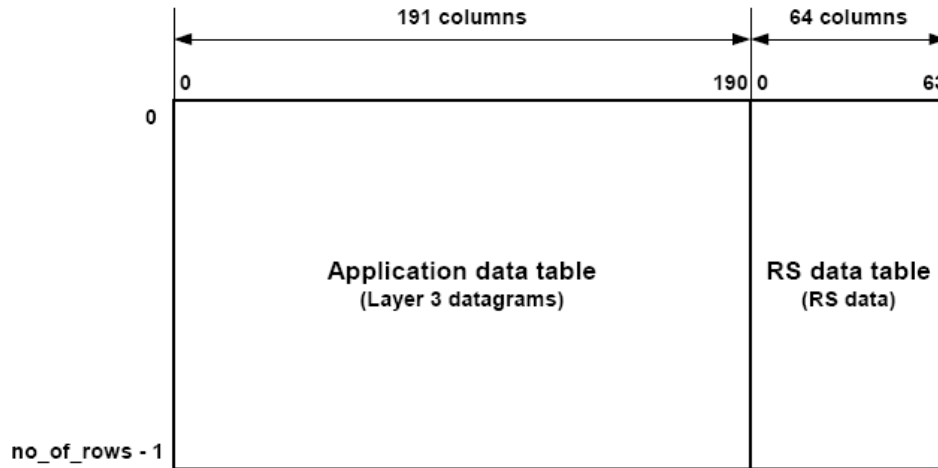


**Figure 5.1-Structure of LL-FEC frame [140]**

The right part of the LL-FEC frame, is called the RS Data Table (RSDT) which consists of 64 columns and contains the FEC parity information. The parity information is used at the receiver to determine if any errors have occurred as well as correct them. The RS (255,191) code can correct up to 64 erasures. If more than 64 erasures are detected in the frame which is determined using a CRC check. It is assumed that the RS (255,191) cannot cope with the received frame and it is discarded. This reduces the performance of the system as the LL-FEC frames are large, variable amount of rows, thus a large portion of data is lost. In terms of digital video broadcasting it reduces the quality of the received video causing distortion. The aim of the future work is to increase the errors correcting ability of the LL-FEC using the soft information generated by the novel BP-OSD-Chase decoder in order to reduce the number of frames dropped by the system.

## REFERENCES

- [1] Qualcomm Incorporated, "Evolution of Wireless Applications and Services," 2007.
- [2] Gbolahan Rilwan Aiyetoro, "Packet Scheduling in Satellite HSDPA Networks," University of KwaZulu-Natal, Durban, Msc Dissertation 2010.
- [3] Michael Charles. (2011, November) Satellite Communication CSC 490:Wireless Networking. Powerpoint Presentation.
- [4] Satcom. (2002) General Principles of Satellite Communications. Lecture.
- [5] DVB, "Digital Video Broadcasting (DVB);A Guideline for the Use of DVB Specifications and Standards," DVB, Report TR 101 200, 2000.
- [6] Hisakau Katoh, "Transmission System for ISDB-S," *Proceedings of the IEEE*, vol. 94, no. 1, January 2006.
- [7] Christophe Selier and Nicolas Chuberre. (2011, December) Eurasip. [Online]. <http://www.eurasip.org/Proceedings/Ext/IST05/papers/223.pdf>
- [8] DVB, "Introduction to the DVB Project," DVB, Fact Sheet May 2011.
- [9] ETSI, "Digital Video Broadcasting (DVB);Framing structure, channel coding and modulation for 11/12 GHz satellite services," Hardware EN 300 421, August 1998.
- [10] ETSI, "Digital Video Broadcasting (DVB);Framing structure, channel coding and modulation for Digital Satellite News Gathering (DSNG) and other contribution applications by satellite," Hardware EN 301 210, March 1999.
- [11] ETSI, "Digital Video Broadcasting(DVB);Second generation framing structure,channel coding and modulation systems for Broadcasting,Interactive services,News Gathering and other broadband satellite applications(DVB-S2)," Hardware EN 302 307, August 2009.
- [12] Alberto Morello and Vittoria Mignone, "DVB-S2:The Second Generation Standard for Satellite Broad-band Services," *Proceedings of the IEEE*, vol. 94, no. 1, pp. 210-227, January 2006.
- [13] Zhiping Shi, Liang Zhou, Hong Wen, and Shaoqian Li, "Iterative Decoding for the Concatenation of LDPC Codes and BCH Codes Based on Chase Algorithm," in *6th International Conference on ITS Telecommunications Proceedings*, 2006, pp. 12-15.
- [14] Li Yang, Martin Tomlinson, and Marcel Ambroze, "Decoding Low-Density Parity-Check Codes with Error-Floor Free over the AWGN Channel," *IEEE*, pp. 192-196, 2010.
- [15] MathDB. (2011, December) MathDB. [Online]. [www.mathdb.org/notes\\_download/elementary/number/ne\\_N6.pdf](http://www.mathdb.org/notes_download/elementary/number/ne_N6.pdf)
- [16] Hank Wallace. (2010, March) Error Detection and Correction Using the BCH Code. [Online]. [www.aqdi.com/bch.pdf](http://www.aqdi.com/bch.pdf)
- [17] PP Kurur, "Lecture 14: BCH Codes," Notes.
- [18] Jonathan Hong and Martin Vetterli, "Simple Algorithms for BCH Decoding," *IEEE Transactions on Communications*, vol. 43, no. 8, pp. 2324-2333, August 1995.
- [19] Junho Cho and Wonyong Sung, "Efficient Software-Based Encoding and Decoding of BCH Codes," *IEEE Transactions on Computers*, vol. 58, no. 7, pp. 878-889, July 2009.
- [20] ETSI, "Digital Video Broadcasting(DVB);Second generation framing structure,channel coding and modulation systems for Broadcasting,Interactive services,News Gathering and other broadband satellite applications(DVB-S2)," EN 302 307, August 2009.
- [21] Bernhard MJ Leiner. (2010, April) LDPC Codes - a brief Tutorial. [Online]. <http://bernh.net/media/download/papers/ldpc.pdf>

- [22] Seok-Bum Ko KC Cinnati Loi, "Improvements on the design and implememntation of DVB-S2 LDPC decoders," *Computers and Electrical Engineering*, June 2011.
- [23] T Richardson, "Error Florrs of LDPC Codes," Flarion Technologies, Bedminster,NJ, Report.
- [24] K Andrews, S Dolinar, D Divsalar, and J Thorpe, "Design of Low-Density Parity-Check (LDPC) Codes for Deep-Space Applications," IPN, Progress 42-159, 2004.
- [25] David Haley, Alex Grant, and John Buetefuer. (2010, April) Iterative Encoding of Low-Density Parity-Check Codes. [Online]. <http://citeseerx.ist.psu.edu/viewdoc/download?doi=10.1.1.96.957&rep=rep1&type=pdf>
- [26] Robert G Gallager, "Low Density Parity Check Codes," MIT, PhD Thesis 1963.
- [27] Y Kou, S Lin, and M Fossorier, "Low density parity check codes based on finite geometries:A rediscovery and more," *IEEE Trans. Info. Theory*, vol. 47, pp. 2711-2736, Nov 2001.
- [28] N Miladinovic and MPC Fossorier, "Improved bit-flipping decoding of low density parity check codes," *IEEE Trans. Inform. Theory*, vol. 51, pp. 1594-1606, Apr 2005.
- [29] F Guo and L Hanzo, "Reliability ratio based weighted bit-flipping decoding for low-density parity-check codes," *Electronics Lett*, vol. 40, pp. 1356-1358, 2004.
- [30] CH Lee and W Wolf, "Implementation-efficient reliability ratio based weighted bit-flipping decoding for LDPC codes," *Electronics Lett*, vol. 41, no. 13, June 2005.
- [31] G Dong, Y Lit, N Xie, T Zhang, and H Liu, "Candidate Bit Based Bit-Flipping Decoding Algorithm for LDPC Codes," in *ISIT*, Seoul, 2009, pp. 2166-2168.
- [32] TMN Ngatched, M Bossert, A Fahrner, and F Takawira, "Two Bit-Flipping Decoding Algorithms for Low-Density Parity-Check Codes," *IEEE Transactions on Communications*, vol. 57, no. 3, pp. 591-596, March 2009.
- [33] S Lin and DJ Costello Jr., *Error Control Coding: Fundamentals and Applications*, 2nd ed. NJ, Englewood Cliffs: Prentice-Hall, 2004.
- [34] P Zarrinkhat and AH Banihashemi, "Threshold values and convergence properties of majority-based algorithms for decoding regular low density parity-check codes," *IEEE Trans. Commun*, vol. 52, pp. 2087-2097, Dec 2004.
- [35] TMN Ngatched, S Alfa Attahiru, and Jun Cai, "An Improvement on the Soft Reliability-Based Iterative Majority-Logic Decoding Algorithm for LDPC Codes," in *IEEE Globecom*, 2010.
- [36] DJC MacKay and RM Neal, "Near Shannon limit performance of low density parity check codes," *Electronic Lett.*, vol. 32, no. 18, 1996.
- [37] David JC MacKay, "Good error-correcting codes based on very sparse," *IEEE Trans. Info. Theory*, vol. 45, pp. 399-432, March 1999.
- [38] RL Urbanke TJ Richardson, "The capacity of low-density parity check codes under message passing decoding," *IEEE Trans. Inform.*, vol. 47, pp. 599-618, February 2001.
- [39] R Tanner, "A recursive approach to low complexity codes," *IEEE Trans.Inform.Theory*, vol. 27, pp. 533-547, September 1981.
- [40] H Xiao and AH Banihashemi, "Graph-based message-passing schedules for decoding LDPC codes," *IEEE Trans. Commun*, vol. 52, pp. 2098-2105, December 2004.
- [41] MR Yazdani, S Hemati, and AH Banihashemi, "Improving belief propagation on graphs with cycles," *IEEE Commun. Lett*, vol. 8, pp. 57-59, January 2004.
- [42] M. Mihaljević, H. Imai M. Fossorier, "Reduced Complexity Iterative Decoding of Low Density Parity Check Codes Based on Belief Propagation," *IEEE Trans. Commun*, vol. 47, pp. 673-680, May 1999.

- [43] S Papaharalabos and PT Mathiopoulos, "Simplified sum-product algorithm for decoding LDPC codes with optimal performance," *ELECTRONICS LETTERS*, vol. 45, no. 2, January 2009.
- [44] AJ Felstrom and KS Zigangirov, "Time-Varying Periodic Convolutional Codes with Low-Density Parity-Check Matrix," *IEEE Trans. Inform.Theory*, vol. 45, pp. 2181-2191, September 1999.
- [45] MPC Fossorier and J Chen, "Decoding Low-Density Parity Check Codes with Normalized APP-Based Algorithm," Department of Electrical Engineering, University of Hawaii, Honolulu, Paper 2001.
- [46] K Bhattad, V Rathi, and R Urbanke, "Degree Optimization and Stability Condition for the Min-Sum Decoder," in *ITW*, Lake Tahoe, California, 2007, pp. 190-195.
- [47] J Chen and MPC Fossorier, "Density evolution for two improved BP-based decoding algorithm of LDPC codes," *IEEE Communication Letters*, vol. 6, no. 5, pp. 208-210, May 2002.
- [48] Li Wu and M Zhang M Xu, "A Modified Offset Min-Sum Decoding Algorithm for LDPC Codes," pp. 19-22, 2010.
- [49] E Zimmermann, P Pattisapu, PK Bora, and G Fettwei, "Reduced Complexity LDPC Decoding Using Forced Convergence," in *7th International Symposium on Wireless Personal Multimedia Communication*, 2004.
- [50] R Aoyama and Y Kaji, "Improvement of the Forced-Convergence Decoding for LDPC Codes," in *International Symposium on Information Theory and its Applications*, Auckland, 2008.
- [51] FA Newagy, YA Fahmy, and MMS El-Soudani, "Novel Construction of Short Length LDPC Codes for Simple Decoding," *Journal of Theoretical and Applied Information Technology*, pp. 64-69, 2007.
- [52] S Anggraeni and VJeoti, "Novel Code-Construction of High Rate (3, k) Regular LDPC Codes," Universiti Teknologi PETRONAS, Perak,.
- [53] SJ Johnson and SR Weller, "High-Rate LDPC Codes from Unital Designs," The University of Newcastle, Callaghan,.
- [54] R Asvadi, AH Banihashemi, and M Ahmadian-Attari, "Lowering the Error Floor of LDPC Codes Using Cyclic Liftings," *IEEE Transactions on Information Theory*, vol. 57, no. 4, pp. 2213-2224, April 2011.
- [55] E Cavus and B Daneshrad, "A Performance Improvement and Error Floor Avoidance Technique for Belief Propagation Decoding of LDPC Codes," in *IEEE 16th International Symposium on Personal, Indoor and Mobile Radio Communications*, 2005, pp. 2386-2390.
- [56] T Mohsenin, H Shirani-mehr, and B Baas, "Low Power LDPC Decoder with Efficient Stopping Scheme for Undecodable Blocks," *IEEE*, pp. 1780-1783, 2011.
- [57] K Chung and J Heo, "Improved Belief Propagation (BP) Decoding for LDPC Codes with a large number of short cycles," *IEEE*, no. 1464-1466, 2006.
- [58] TJ Richardson and RL Urbanke, "The capacity of low-density parity check codes under message passing decoding," *IEEE Trans. Information*, vol. 47, pp. 599-618, Feb 2001.
- [59] S ten Brink, "Convergence Behavior of Iteratively Decoded Parallel Concatenated Codes," *IEEE Transactions on Communications*, vol. 49, no. 10, pp. 1727-1737, October 2001.
- [60] J Hagenauer, "The EXIT Chart-Introduction to Extrinsic Information Transfer in Iterative Processing," Institute of Communications Engineering (LNT), Munich,.
- [61] A Anastasopoulos, "A comparison between the sum-product and the min-sum iterative detection algorithms based on density evolution," *IEEE*, pp. 1021-1025, 2001.

- [62] J Heo and KM Chugg, "Optimization of Scaling Soft Information in Iterative Decoding Via Density Evolution Methods," *IEEE Transactions on Communications*, vol. 53, no. 6, pp. 957-961, June 2005.
- [63] S ten Brink, G Kramer, and A Ashikhmin, "Design of Low-Density Parity-Check Codes for Modulation and Detection," *IEEE Transactions on Communications*, vol. 52, no. 4, pp. 670-678, April 2004.
- [64] AH Banihashem and H Saeedi, "EXIT Charts of LDPC Codes over BIAWGN Channels with Imperfect Channel Estimation," *IEEE*, pp. 65-68, 2007.
- [65] HR Zeidan and MM Elsabrouty, "Two-stage hybrid decoding for low-density parity check (LDPC) codes," in *Innovations '04*, Dubai, 2007, pp. 18-20.
- [66] P Zarrinkhat and AH Banihashemi, "Hybrid decoding of low-density parity check codes," in *ISTC'03*, Brest, 2003, pp. 503-506.
- [67] Jian Li and Xian-Da Zhang, "Hybrid Iterative Decoding for Low-Density Parity-Check Codes Based on Finite Geometries," *IEEE Comm. Lett.*, vol. 12, no. 1, pp. 29-31, January 2006.
- [68] HR Zeidan and MM Elsabrouty, "Modified Iterative Two-Stage Hybrid Decoding Algorithm for Low-Density Parity-Check (LDPC) Codes," German University in Cairo, Cairo, Paper 2009.
- [69] M. Fossorier, "Iterative reliability-based decoding of low-density parity check code," *IEEE Select. Areas Commun.*, vol. 19, pp. 908-917, May 2001.
- [70] J Jiang and KR Narayanan, "Iterative soft decision decoding of Reed-Solomon codes based on adaptive parity check matrices," *Proc. IEEE Int. Symp. on Inform. Theory*, p. 261, 2004.
- [71] Aditi Kothiyal, Oscar Takeshita, Wenyi Jin, and Marc Fossorier, "Iterative Reliability-Based Decoding of Linear Block Codes with Adaptive Belief Propagation," *IEEE Communications Letters*, vol. 9, no. 12, December 2005.
- [72] G Li, X Zou, and X Wang, "Hybrid Decoding for One Class of Low-density Parity-check Codes," Nanjing University of Posts and Telecommunications, Nanjing, Jiangsu, Paper.
- [73] S Lin and DJ Costello Jr, *Error Control Coding: Fundamentals and Applications*, 2nd ed. NJ, USA: Prentice Hall, 2004.
- [74] ER Berlekamp, *Algebraic Coding Theory*. New York: McGraw-Hill, 1968.
- [75] Junho Cho, Jonghong Kim, and Wonyong Sung, "Error Performance and Decoder Hardware Comparison Between EG-LDPC and BCH Codes," in *SiPS*, 2010, pp. 392-397.
- [76] DV Sarwate and NR Shanbhag, "High-speed architectures for Reed-Solomon decoders," *IEEE Trans. Very Large Scale Integr (VLSI) Syst.*, vol. 9, no. 5, pp. 641-655, October 2001.
- [77] W Liu, J Rho, and W Sung, "Low-power high-throughput BCH error correction VLSI design for multi-level cell NAND flash memories," *Proc. IEEE Workshop on Signal Processing Systems (SIPS)*, pp. 248-253, October 2006.
- [78] S Ding, Z Yang, and C Pan, "Efficient Frequency Domain Decoding of Binary BCH Codes Based on Prime-factor FFT," *IEEE*, pp. 14-17, 2005.
- [79] H Shao, T Truong, H Deutsch, J Yuen, and I Reed, "A VLSI design of a pipeline reed-solomon decoder," *IEEE Trans. Comput.*, vol. 34, no. 5, pp. 393-403, May 1985.
- [80] R Lucas, M Bossert, and M Breitbach, "On Iterative Soft-Decision Decoding of Linear Binary Block Codes and Product Codes," *IEEE Journal on Selected Areas In Communications*, vol. 16, no. 2, pp. 276-296, February 1998.
- [81] WJ Reid III, LL Joiner, and JJ Komo, "Soft Decision Decoding of BCH Codes Using Error Magnitudes," in *ISIT*, Ulm, 1997, p. 303.

- [82] G. D. Forney, "Generalized minimum distance decoding," *IEEE Trans. Inf. Theory*, vol. 12, pp. 125-131, April 1966.
- [83] A Vardy and Y Be'ery, "Maximum-Likelihood Soft Decision Decoding of BCH Codes," *IEEE Transactions on Information Theory*, vol. 40, no. 2, pp. 546-554, March 1994.
- [84] Yi-Min Lin, Chih-Lung Chen, Hsie-Chia Chang, and Chen-Yi Lee, "A 26.9 K 314.5 Mb/s Soft (32400,32208) BCH Decoder Chip for DVB-S2 System," *IEEE Journal of Solid-State Circuits*, vol. 45, no. 11, November 2010.
- [85] D Chase, "A Class of Algorithms for Decoding Block Codes With Channel Measurement Information," *IEEE Transactions on Information Theory*, vol. IT-18, no. 1, January 1972.
- [86] XNN Tendolkar and CRP Hartmann, "Generalization of Chase Algorithms for Soft Decision Decoding of Binary Linear Codes," *IEEE Transactions on Information Theory*, vol. IT-30, no. 5, pp. 714-721, Spetember 1984.
- [87] JH Weber, "Low-Complexity Chase-Like Bounded-Distance Decoding Algorithms," in *GLOBECOM*, 2003, pp. 1608-1612.
- [88] Y Tang and M Lee, "Iterative Chase-2 Algorithm using Threshold for Block Turbo Codes Decoding Design," in *IEEE Intemational Symposium on Microwave, Antenna, Propagation and EMC Technologies for Wireless Communications Proceedings*, 2005, pp. 1154-1157.
- [89] M Lalam, K Amis, and D Leroux, "Sliding Encoding-Window for Reed-Solomon code decoding," in *Turbo Coding*, Munich, 2006.
- [90] K Amis, D Leroux, D Feng and J Yuan M Lalam, "An improved iterative decoding algorithm for block turbo codes," in *ISIT*, Seattle, 2006, pp. 2403-2407.
- [91] H Xia, C Zhong, and JR Cruz, "A Chase-Type Algorithm for Soft-Decision Reed-Solomon Decoding on Rayleigh Fading Channels," in *Globecom*, 2003, pp. 1751-1755.
- [92] R Koetter and A Vardy, "Algebraic soft-decision decoding of Reed-Solomon codes," *IEEE Trans. Inform. Theory*, 2001.
- [93] YM Lin, HC Chang, and CY Lee, "An Improved Soft BCH Decoder with One Extra Error Compensation," *IEEE*, pp. 3941-3944, 2010.
- [94] F. Therattil and A Thangaraj, "A low-complexity soft-decision decoder for extended BCH and RS-like codes," *Proc. IEEE Int. Symp. Inf Theory*, pp. 1320-1324, September 2005.
- [95] H Ogiwara, K Shimamura, and T Shohon, "Sum-Product Decoding of BCH Codes," *IEICE Trans. Fundamentals*, vol. E91-A, no. 10, pp. 2729-2736, October 2008.
- [96] M. Baldi and F. Chiaraluce, "A simple scheme for belief propagation decoding of BCH and RS codes in multimedia transmissions," *Int. J. Digit. Multimedia Broadcasting*, vol. 2008, no. Art. ID 957846, 2008.
- [97] LL Joiner, and JJ Komo WJ Reid III, "Soft decision decoding of BCH codes using error magnitudes," *Proc. IEEE Int. Symp. Inf. Theory*, p. 303, June 1997.
- [98] G Cancellieri and F Chiaraluce M Baldi, "Iterative Soft-Decision Decoding of Binary Cyclic Codes based on Spread Parity-Check Matrices," Ancona,.
- [99] ComBlock, "COM-1209 A Soft High-Speed DVB-S2 BCH Code Decoder & Encoder VHDL Source Code Overview," ComBlock, Maryland, Data Sheet 2009.
- [100] SoftJin, "LDPC Decoder for DVB-S2," SoftJin Technologies, Santa Clara, Data Sheet.
- [101] Frank Kienle, Torben Brack, and Norbert Wehn, "A synthesizable IP Core for DVB-S2 LDPC Code Decoding," University of Kaiserslautern, Kaiserslautern, Paper.
- [102] John Dielissen, Andries Hekstra, and Vincent Berg, "Low cost LDPC decoder for DVB-S2," Philips Research, Eindhoven, Paper 2006.

- [103] Jeong Haeseong and Tae Kim Jong, "Implementation of LDPC Decoder in DVB-S2 Using Min-Sum Algorithm," in *International Conference on Convergence and Hybrid Information Technology 2008*, 2008, pp. 359-362.
- [104] Botao Zhang, Hengzhu Liu, Xucan Chen, Dongpei Liu, and Xiaofei Yi, "Low Complexity DVB-S2 LDPC Decoder," National University of Defense Technology, Changsha, Paper 2009.
- [105] Florent Berthelot, Francois Charot, Charles Wagner, and Christophe Wolinski, "Design methodology for a high performance robust DVB-S2 decoder implementation," in *Euromicro Conference on Digital System Design: Architectures, Methods and Tools*, 2010, pp. 667-674.
- [106] M Gomes et al., "Scalable and Parallel Codec Architectures for the DVB-S2 FEC System," Dep. of Electrical and Computer Engineering, Coimbra, Paper 2008.
- [107] Alberto Morello and Vittoria Mignone, "DVB-S2 - Ready for lift off," EBU, 2004.
- [108] F. P. Fontan, A. A. Villamarín, S. Buonomo, P. Baptista and B. Arbesser M. A. V. Castro, "L-Band Land Mobile Satellite (LMS) Amplitude and Multipath Phase Modeling in Urban Areas," *IEEE Communications Letters*, vol. 3, no. 1, January 1999.
- [109] S Scalise et al., "Measurement Campaign for the Land Mobile Satellite Channel in Ku-Band," in *EMPS*, 2002.
- [110] F Perez-Fontan, M A Vazquez-Castro, S Buonomo, J P Poiares-Baptista, and B Arbesser-Rastburg, "S-Band LMS propagation channel behaviour for different environment degrees of shadowing and elevation angles," *IEEE Transactions on Broadcasting*, vol. 44, no. 1, pp. 40-51, March 1998.
- [111] A Gotta and P Barsocchi, "Experimental video broadcasting in DVB-RCS/S2 with land mobile satellite channel:a reliability issue," *IEEE*, 2008.
- [112] S Scalise, MA Vazquez Castro, A Jahn, and H Ernst, "A Comparison of the Statistical Properties of the Land Mobile Satellite Channel at Ku,Ka and EHF bANDS," *IEEE*, 2008.
- [113] D Anderson and T Fuller-Rowell, "Space Environment Topics: The Ionosphere," Space Environment Center, Boulder, Report 1999.
- [114] IEEE, "521-2002 IEEE Standard Letter Designations for Radar-Frequency Bands," IEEE Aerospace and Electronics Systems Society, Standard 2003.
- [115] S Scalise, H Ernst, and G Harles, "Measurement and Modeling of the Land Mobile Satellite Channel at Ku-Band," *IEEE Transactions on Vehicular Technology*, vol. 57, no. 2, March 2008.
- [116] P Burzigotti, R Prieto-Cerdeira, A Bolea-Alamañac, F Perez-Fontan, and I Sanchez-Lago, "DVB-SH Analysis Using a Multi-State Land Mobile Satellite Channel Model," *IEEE*, pp. 149-155, 2008.
- [117] Wenzhen Li, Choi Look Law, V K Dubey, and JT Ong. (2010, May) Ka-Band Land Mobile Satellite Channel Model Incorporating Weather Effects. [Online]. [http://www.google.co.za/url?sa=t&source=web&cd=4&ved=0CCwQFjAD&url=http%3A%2F%2Fwww3.ntu.edu.sg%2FCentre%2Fpwtc%2Fimages%2Fresearch%2FDownload%2FOJP\\_6.pdf&rct=j&q=satellite+channel+models&ei=EQMJTKmOEsOF4QbLjvmPAQ&usq=AFQjCNHk8hLG9MBuRAXxkL1ybFu09LaQHQ](http://www.google.co.za/url?sa=t&source=web&cd=4&ved=0CCwQFjAD&url=http%3A%2F%2Fwww3.ntu.edu.sg%2FCentre%2Fpwtc%2Fimages%2Fresearch%2FDownload%2FOJP_6.pdf&rct=j&q=satellite+channel+models&ei=EQMJTKmOEsOF4QbLjvmPAQ&usq=AFQjCNHk8hLG9MBuRAXxkL1ybFu09LaQHQ)
- [118] MA Vázquez-Castro and F Pérez-Fontán, "LMS Markov Model and Its Use for Power Control Error Impact Analysis on System Capacity," *IEEE Journal on Selected Areas in Communications*, vol. 20, no. 6, August 2002.
- [119] School of Computer Science, "Chapter 11 Markov Chains," University of Virginia, Virginia, Notes 2006.
- [120] E Lutz, D Cygan, M Dippold, F Dolainsky, and W Papke, "The Land Mobile Satellite Communication Channel-Recording, Statistics and Channel Model," *IEEE*

- Transactions on Vehicular Technology*, vol. 40, no. 2, pp. 375-386, May 1991.
- [121] C Loo and JS Butterworth, "Land Mobile Satellite Channel Measurements and Modeling," *Proceedings of the IEEE*, vol. 86, no. 7, July 1998.
- [122] MPC Fossorier and J Chen, "Decoding Low-Density Parity Check Codes with Normalized APP-Based Algorithm," *IEEE*, pp. 1026-1030, 2001.
- [123] C Spagnoly, E Popovici, and W Marnan, "New Algorithm For LDPC Decoding Over GF(q)," in *ISSC*, Dublin, 2005.
- [124] N Traore, S Kant, and TL Jensen, "Message Passing Algorithm and Linear Programming Decoding for LDPC and Linear Block Codes," Institute of Electronic Systems Signal and Information Processing in Communications, Aalborg, 2007.
- [125] W Ryan, "Introduction to LDPC," University of Arizona, Arizona, Notes 2001.
- [126] CB Vicente and JH Weber, "Dynamic Chase Decoding Algorithm," in *ITW2003*, Paris, 2003.
- [127] SA Hirst, B Honary, and G Markarian, "Fast Chase Algorithm with an Application in Turbo Decoding," *IEEE Transactions on Communications*, vol. 49, no. 10, October 2001.
- [128] M Fossorier and S Lin, "Soft-decision decoding of linear block codes based on ordered statistics," *IEEE Trans. Inform. Theory*, vol. 41, pp. 1379-1396, 1995.
- [129] MPC Fossorier and S Lin, "Soft Decision Decoding of Linear Block Codes based on Ordered Statistics," *IEEE Trans. Inform. Theory*, vol. 41, no. 5, pp. 1379-1396, May 1995.
- [130] HJ Greenberger, "Approximate maximum likelihood decoding of block codes," Jet Propulsion Laboratory, Pasadena, CA, The DSN Progress Report 1979.
- [131] M Fossorier and S Lin, "Reliability-based information set decoding of binary linear codes," *IEICE Trans. Fundam.*, vol. E82-A, October 1999.
- [132] T Ohtsuki and S Gounai, "Decoding algorithms based on oscillation for low-density parity check codes," *IEICE Trans. Fundam.*, vol. E88-A, no. 8, pp. 2216-2226, August 2005.
- [133] C Zhao, E Xu and L Zhang M Jiang, "Reliability-Based Iterative Decoding of LDPC Codes Using Likelihood Accumulation," *IEEE Communications Letters*, vol. 11, no. 8, pp. 677-679, August 2007.
- [134] D Zijian and Q Guolei, "Improved BP-OSD Cascade Decoding Algorithm Using Limited Likelihood Information," in *2nd International Conference on Signal Processing Systems (ICSPS)*, 2010, pp. 23-25.
- [135] F Kienle, N Wehn, and H Meyr, "On Complexity, Energy- and Implementation-Efficiency of Channel Decoders," *IEEE Transactions on Communications*, vol. 59, no. 12, pp. 3301-3310, December 2011.
- [136] C. H. van Berkel, "Multi-core for mobile phones," in *Proc. Design Automation. Test Europe Conf. Exhibition*, 2009, pp. 1260-1265.
- [137] S. C. Eberli, ETH Zurich Integrated Systems Laboratory, Zurich, PhD Dissertation 2009.
- [138] S Galli, "On the fair comparison of FEC schemes," *Proc. IEEE Int. Conf. Commun*, pp. 1-6, 2010.
- [139] C Xu, YC Liang, and WS Leon, "A Low Complexity Decoding Algorithm for Extended Turbo Product Codes," *IEEE Transactions on Wireless Communications*, vol. 7, no. 1, pp. 43-47, January 2008.
- [140] "Digital Video Broadcasting (DVB); DVB specification for data broadcasting," , June 2004.
- [141] Amin Shokrollahi. (2010, March) LDPC Codes: An Introduction. [Online].



[www.ics.uci.edu/~welling/teaching/ICS279/LPCD.pdf](http://www.ics.uci.edu/~welling/teaching/ICS279/LPCD.pdf)

- [142] Alberto Gotta and Paolo Barsocchi, "Experimental video broadcasting in DVB-RCS/S2 with land mobile satellite channel: a reliability issue," in *IWSSC*, 2008.
- [143] Christopher Jones, Esteban Valles, Michael Smith, and John Villasenor. (2010, April) APPROXIMATE-MIN' CONSTRAINT NODE UPDATING FOR LDPC CODE DECODING. [Online]. [http://www.google.co.za/url?sa=t&source=web&cd=1&ved=0CBkQFjAA&url=http%3A%2F%2Fwww.ee.ucla.edu%2F~ipl%2Fapproximage\\_min\\_constraint\\_node.pdf&rct=j&q=APPROXIMATE-MIN%27+CONSTRAINT+NODE+UPDATING+FOR+LDPC+CODE+DECODING&ei=3xgJTOy9KpWW4ga80ICWAQ&usg=AFQjCNG6y](http://www.google.co.za/url?sa=t&source=web&cd=1&ved=0CBkQFjAA&url=http%3A%2F%2Fwww.ee.ucla.edu%2F~ipl%2Fapproximage_min_constraint_node.pdf&rct=j&q=APPROXIMATE-MIN%27+CONSTRAINT+NODE+UPDATING+FOR+LDPC+CODE+DECODING&ei=3xgJTOy9KpWW4ga80ICWAQ&usg=AFQjCNG6y)
- [144] Michael Lunglmayr, Jens Berkmann, and Mario Huemer. (2010, April) Parallelized Optimization of LDPC Decoding Algorithms. [Online]. [http://www.google.co.za/url?sa=t&source=web&cd=10&ved=0CEoQFjAJ&url=http%3A%2F%2Fpara08.idi.ntnu.no%2Fdocs%2Fsubmission\\_54.pdf&rct=j&q=ldpc+decoding+algorithms&ei=dBQJTPmVB9KW4gashYyUAQ&usg=AFQjCNGERJf6gO210kDQQzap7Xy9JqR8Pw](http://www.google.co.za/url?sa=t&source=web&cd=10&ved=0CEoQFjAJ&url=http%3A%2F%2Fpara08.idi.ntnu.no%2Fdocs%2Fsubmission_54.pdf&rct=j&q=ldpc+decoding+algorithms&ei=dBQJTPmVB9KW4gashYyUAQ&usg=AFQjCNGERJf6gO210kDQQzap7Xy9JqR8Pw)
- [145] J S Reeve and K Amarasinghe. (2010, April) A parallel Viterbi decoder for block cyclic and convolution codes. [Online]. <http://www.google.co.za/url?sa=t&source=web&cd=8&ved=0CDsQFjAH&url=http%3A%2F%2Flinkinghub.elsevier.com%2Fretrieve%2Fpii%2FS0165168405001775&rct=j&q=BCH+decoding+using+viterbi&ei=zRoJTOOUPIn74AagnfV-&usg=AFQjCNFvH7mEuJfUbkseeC6ZHUA4iFZSfg>
- [146] Marco Baldi, Giovanni Cancellieri, and Franco Chiaraluce, "Low Complexity Soft-Decision Decoding of BCH and RS Codes based on Belief Propagation," in *Riunione Annuale GTTI 2008 -Sessione su Trasmissione Numerica*, 2008.
- [147] Reinhard Gerndt. (2010) Information Theory-BCH, Reed-Solomon and related codes. [Online]. [public.fh-wolfenbuettel.de/~gerndt/rscode.pdf](http://public.fh-wolfenbuettel.de/~gerndt/rscode.pdf)
- [148] PACT, "IEEE Std 802.16e™ LDPC Decoderon XPP-III," White Paper 2006.
- [149] John Dielissen, Andries Hekstra, and Vincent Berg, "Low cost LDPC decoder for DVB-S2," in *Proceedings of the Design Automation & Test in Europe Conference Vol. 2*, Munich, April 2010.
- [150] J Chen and MPC Fossorier, "Density Evolution for Two Improved BP-Based Decoding Algorithms of LDPC Codes," *IEEE Communications Letters*, vol. 6, no. 5, pp. 208-210, May 2002.
- [151] Ali Abdi, Wing C Lau, Mohamed-Slim Alouin, and Mostafa Kaveh. (2010, May) A New Simple Model for Land Mobile Satellite Channels: First- and Second-Order Statistics. [Online]. <http://www.google.co.za/url?sa=t&source=web&cd=2&ved=0CB8QFjAB&url=http%3A%2F%2Fciteseerx.ist.psu.edu%2Fviewdoc%2Fdownload%3Fdoi%3D10.1.1.89.650%26rep%3Drep1%26type%3Dpdf&rct=j&q=satellite+channel+models&ei=EQMJTKmOEsOF4QbLjvmPAQ&usg=AFQjCNFFL8o3Oel7MGQWU>
- [152] L Arnone, C Gayoso, C Gonzalez, and J Castineira. (2010, April) Sum-Subtract Fixed Point LDPC Decoder.[Online]. [http://www.google.co.za/url?sa=t&source=web&cd=8&ved=0CD0QFjAH&url=http%3A%2F%2Fwww.laar.uns.edu.ar%2Findexes%2Fartic\\_v3701%2Fvol\\_37\\_1\\_pag17.pdf&rct=j&q=ldpc+decoding+algorithms&ei=dBQJTPmVB9KW4gashYyUAQ&usg=AFQjCNFh-FfnJb7UIAQCoPg332gP\\_qVBO](http://www.google.co.za/url?sa=t&source=web&cd=8&ved=0CD0QFjAH&url=http%3A%2F%2Fwww.laar.uns.edu.ar%2Findexes%2Fartic_v3701%2Fvol_37_1_pag17.pdf&rct=j&q=ldpc+decoding+algorithms&ei=dBQJTPmVB9KW4gashYyUAQ&usg=AFQjCNFh-FfnJb7UIAQCoPg332gP_qVBO)
- [153] MPC Fossorier and J Chen, "Near Optimum Universal Belief Propagation Based Decoding of Low-Density Parity Check Codes," *IEEE Transactions on Communications*, vol. 50, no. 3, pp. 406-414, March 2002.

- [154] Y Kou, S Lin, and M Fossorier, "Low density parity check codes based on finite geometries: A rediscovery and more," *IEEE Trans. Info. Theory*, vol. 47, pp. 2711-2736, November 2001.
- [155] J Zhang and MPC Fossorier, "A modified weighted bit-flipping decoding of low-density parity-check codes," *IEEE. Comm. Lett.*, vol. 8, pp. 165-167, 2004.
- [156] Tony Gill and Paul Miller, "Re-inventing the Wheel? Standards, Interoperability and Digital Cultural Content," *D-Lib Magazine*, vol. 8, no. 1, January 2002.
- [157] L Yang, M Tomlinson, and M Ambroze, "Decoding Low-Density Parity-Check Codes with Error-Floor Free over the AWGN channel," *IEEE*, 2010.
- [158] K Andrews, S Dolinar, D Divsalar, and J Thorpe, "Design of Low-Density Parity-Check (LDPC) Codes for Deep-Space Applications," IPN, Progress Report 42-159 2004.